MANGOret: An optimization framework for the long-term investment planning of building multi-energy system and envelope retrofits

Journal Article

Author(s):
Petkov, Ivalin (iD); Mavromatidis, Georgios (iD); Knoeri, Christof; Allan, James; Hoffmann, Volker H.
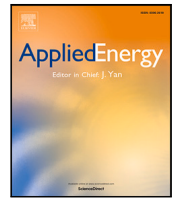
MANGOret: An optimization framework for the long-term investment planning of building multi-energy system and envelope retrofits

Ivalin Petkov [a],*, Georgios Mavromatidis [a], Christof Knoeri [a], James Allan [b], Volker H. Hoffmann [a]

[a] *Group for Sustainability and Technology, ETH Zurich, 8092 Zurich, Switzerland*
[b] *Urban Energy Systems Laboratory, Swiss Federal Laboratories for Materials Science and Technology, Empa, 8600 Dübendorf, Switzerland*

ARTICLE INFO

ABSTRACT

This study presents MANGOret (Multi-stAge eNerGy Optimization — retrofitting), a novel optimization framework and model for the long-term investment planning of existing building retrofits. MANGOret bridges the methodological gaps between energy system modeling and real estate management to present a scalable framework to optimize both energy and non-energy costs while considering building value. With a 2050 horizon, MANGOret is able to harness the strategic value of investment flexibility to optimally phase investments across the multi-objective cost and CO_2 emission decision space considering both operational and embodied emissions.

From the energy perspective, the model generates long-term investment strategies for decentralized multi-energy systems and envelope retrofits. The model considers the interdependent trade-offs between demand- and supply-side measures for a number of technologies across time. Technology scheduling is informed by condition degradation functions from utilizing the Schroeder method. From the real estate management perspective, the framework digitalizes the multi-year investment planning process. The model is supported by series of automated data retrieval and processing steps to consider each contextual building project. Importantly, we develop an archetypal energy demand database to reference demands of various retrofitting packages. By considering all retrofitting-relevant investments, the model incorporates the critical budgeting elements of rental revenues to calculate building value.

We demonstrate the value of the MANGOret framework across various building types and sizes in different Swiss real estate markets. Our results demonstrate relevance for energy engineers and building owners relating to the long-term design, operation, and investment scheduling of existing buildings. We present multiple optimal strategies considering the trade-offs between cost, value, and CO_2 emissions.

Aligning with previous studies, our results show that higher investment costs are necessary to achieve low-CO_2 retrofits relative to minimum cost strategies. Higher costs are, to a large extent, influenced by envelope retrofits and non-energy internal renovations while energy supply systems contribute to a smaller share of the budget. To achieve low-CO_2, retrofits utilize lower embodied emission technology choices and are scheduled early on. Nevertheless, we show that these trade-offs do not necessarily have to be weighed at the extremes of the Pareto front, instead presenting 'minimal regret' solutions which reduce CO_2 at negligible cost increases. Considering both embodied and operational CO_2 emissions over the building life-cycle, our results demonstrate that optimal emission reductions necessitate subsequent reductions in energy consumption. Low-CO_2 retrofitting strategies are typified by reducing energy demands as much as possible in order to self-consume as much renewable energy as possible, typically by solar PV and heat pump coupled systems with grid reliance.

1. Introduction

Meeting ambitious climate goals such as 1.5°C warming above pre-industrial levels requires a drastic reduction of global energy demand alongside low-carbon energy supply transformations [1] — especially in scenarios not heavily relying on negative emission technologies [2].

The building sector presents a critical portion as it accounts for 30% of final energy use and 28% of energy-related CO_2 emissions [3]. For the case of the European building stock, it is estimated that over 90% of existing buildings will remain standing in the required time horizon to meet climate goals – 2050 – and therefore have to be

---

retrofitted in the next decades [4]. Governments have demonstrated the pertinence of increasing the retrofitting rate from the current <1% to around 3%, albeit of sufficient depth [5,6]. Accelerating *deep* retrofits, corresponding to energy savings of greater than 60% [7], encompasses a combination of both Energy Efficiency (EE) measures, particularly of the building envelope, along with Renewable Energy (RE) supply systems.

In developing retrofitting investment strategies, building owners must consider each building's unique context to determine favorable technical, economic, and organizational conditions [8]. A set of studies examining the influence of retrofits on building sector energy demands and emissions take a high-level perspective often employing various scenarios of the rate at which retrofits are conducted [4]. However, they are generally unable to capture the owners' retrofitting investment decision, considering the building stocks' heterogeneous ownership composition which predicates dissimilar retrofitting investment strategies between owner types. For example, the differences in retrofitting investment decisions between private homeowners and real estate owners can vary in economic rationality based on elements such as budgets, risks, logistics, timing, and market aspects [9,10].

An institutionalized set of real estate owners, termed Large-Scale Investors (LSIs), account for a large share of annual building investments and stock ownership, presenting an interesting case to study the diffusion of retrofits due to their leverage in managing investments for large, mixed-use portfolios [9]. For the example of Switzerland, the majority of investments in buildings can be attributed to LSIs (total 72% of investments in 2016, split by 16% public and 56% commercial [11]), albeit their smaller but significant building ownership share (20% of residential and 10% of commercial property [11,12]).[1] These professionalized owners are experiencing increasing regulatory and market pressure to incorporate decarbonization into investment strategies [13–16]. To do so, LSIs require adequate models to evaluate investment strategies for each contextual building retrofitting project over a long-term horizon in an automated and digitized manner [17].

Retrofitting investment decisions in real estate are primarily driven by the Multi-Year Planning (MYP) process at the asset management level to assure adequate financial performance, building quality, along with Environmental, Social and corporate Governance (ESG) considerations [15]. In this formalized process, budgeting is conducted for all interventions, both retrofits and non-energy 'renovations', for each individual asset (e.g. a single building or a group of buildings) with a 5–10 year horizon. Generally, a long-term horizon aligned with building component lifetimes (e.g. 30–50 years) is not considered. MYP is conducted years before 'bottom-up' technical auditing and planning is produced by architects or engineers typically 1–2 years before the project [18], presenting an important early-stage budgeting decision for the potential of energy efficient and renewable *deep retrofits*. Traditionally, MYP is based on Discounted Cash Flow (DCF) models outputting a single economic objective, for example yield, return on investment, and building value, as the basis for the asset retrofitting strategy [19].

Owners typically rely on heuristic approaches when developing asset retrofitting strategies in MYP, limiting their ability to determine the best, or optimal, investment plan depending on their objectives [20]. An additional complexity relates to including a CO_2 objective or another sustainability target into MYP, potentially changing the optimal retrofit investment plan from the solely-economic focused strategies of LSIs. In light of corporate-level emissions targets such as 80% operational CO_2 reduction by 2050, LSIs are presented with a new challenge in aligning asset-level retrofit investment plans. To do so, there is a need for suitable investment planning methodologies capable of capturing the complexities of existing building retrofitting relevant for real estate MYP.

---

[1] Their low ownership share compared to investments is largely due to the large stock of single family homes. LSIs typically own large rental properties in high-value markets.

1.1. Literature review

Existing approaches to evaluate the techno-economic potential of retrofits vary on aspects such as the *where* — the spatial-scale of consideration, *how* — their objectives or goals in conducting the retrofit, *what* — the considered set of technologies, and *when* — scheduling of the retrofits depending on the considered time-horizon. In the following, we review the methodologies in literature which could be used to evaluate the potential of both the demand- and supply-sides of retrofits for existing building investment decisions.

Starting at the highest spatial-scale, a number of methodologies consider techno-economic analyses of retrofits utilizing bottom-up national building stock models (e.g. for the example of the EU [21], Switzerland [22], and Norway [23]) along with agent-based models [24]. Such studies provide valuable insights for urban planners and policymakers to determine how building stock transformations align with long-term climate goals. While such methodologies provide a useful high-level perspective, they lack the required granularity to evaluate the investment decision for contextual existing building retrofitting projects.

In the following, we focus our scope to studies in the energy domain utilizing optimization approaches towards retrofitting evaluation. Next, we review the stream of literature in the real estate management domain relating to decision-making relevant for retrofit investments.

1.1.1. Optimization approaches

A technically-focused set of studies in the energy domain considers the economic and/or environmental potential of retrofits for the *individual* building asset scaled up to the portfolio-level, utilizing mathematical programming approaches such as optimization as the core methodology [25,26]. These retrofitting optimization studies can be generally categorized as focusing on a single building with multiple objectives [27–36], focusing on multiple buildings with a single objective [37–39], along with considering multi-building portfolios within a multi-objective optimization framework [40–49]. Objectives (*how*) are generally categorized as economic, environmental, cultural, and social. These studies analyze a varied set of energy system and energy efficiency technology options, such as: improving lighting, insulating the building envelope, replacing heating distribution and generation systems, along with utilizing RE paired with conversion technologies such as heat pumps. However, few of the optimization model contributions listed here capture the benefits of integrating multiple conversion and storage technologies in the energy system to satisfy the energy demands from various retrofitting packages [32,43,50].

Decentralized multi-energy systems

Meeting such a requirement, Decentralized Multi-Energy Systems (D-MES) integrate multiple technologies with the potential to secure a low-carbon energy system in both existing and new buildings [51]. A D-MES design could be as simple as a natural gas boiler coupled with a hot water storage tank, ranging to a complex design such as an integrated energy hub including RE technologies along with battery or hydrogen storage [52]. To fully consider D-MES optimization for a building retrofit, it is vital to consider the entire technological and temporal decision space relevant to the building.

Primarily, the optimization must consider demand-side measures (most importantly — envelope retrofits) simultaneously with the design and operation of the D-MES. The interdependent demand and supply investment decisions present scheduling trade-offs over the building life-cycle, for example, *what* is best to do – and *when* – about reducing thermal demands through building envelope insulation, in parallel with decisions regarding various options for energy supply and storage systems. For example, both Wu et al. [43] and Schütz et al. [32] presented single-stage multi-objective Mixed Integer Linear Programming (MILP) optimization models considering both energy systems and retrofitting packages for residential buildings, focusing on Swiss and German

cases respectively. While these approaches capture the interdependent investment decision, the models are unable to answer the *when* question due to their limited temporal dimension through modeling a typical representative year.

Importance of a long-term horizon

Recent contributions have shown the importance of considering the entire long-term time horizon of buildings' life-cycles *all at once* in the optimization [31,50,53]. Such *dynamic* (or *multi-stage*) investment strategies involve investment decisions in multiple stages during the building lifetime, allowing the owner to fully harness the value of investment flexibility. Capturing the entire horizon allows for a complete accounting of demand and supply-side investment trade-offs, along with future cost reductions or technological improvements over time. For example, dynamic building D-MES and envelope retrofit investment strategies were recently explored in the novel MILP optimization formulation of the MANGO model in Mavromatidis & Petkov [50]. However, MANGO did not adequately represent the retrofitting investment decision, instead utilizing various scenarios. In a recent work, Richarz et al. [31] proposed a MILP optimization methodology for the scheduling of building modernization measures considering a D-MES for a non-residential building. While considering the interdependence of demand- and supply-side investments, this study is limited in the consideration of future technological improvements and embodied emissions over the planning horizon which could impact scheduling trade-offs. Nevertheless, the aforementioned methodologies for evaluating retrofits in the energy domain have limited consideration for real estate owners' decision-making relevant for MYP.

1.1.2. Real estate decision-making approaches

Real estate LSIs' retrofit decision-making in MYP has a scope beyond just energy-relevant investments [8,19]. Aspects such as non-energy technologies (e.g. interior renovations), cultural heritage, management logistics (e.g. manpower), along with the possible rental revenues and building values after the retrofit [54–57] are also prioritized for each individual asset up to the portfolio-level [58]. As such, another stream of literature has focused on decision-support models relevant for real estate investment planning of for existing buildings. These studies are categorized into six areas for the renovation process: setting sustainability goals, weighting criteria, building diagnosis, generation of design alternatives, estimation of performance, and the evaluation of design alternatives [20,59–61].

Examples of retrofitting decision-support models, such as Gade et al. [62], developed a tool for managers to assign weights to renovated components, followed by a determination of the most profitable renovations for portfolios. Serrano-Jiménez et al. [63] presented a multi-criteria decision support method towards selecting feasible and sustainable housing renovation strategies for two case studies in Sweden. Hirsch et al. [64] developed a framework for decarbonization risks for commercial real estate. Finally, Ayoub et al. [37] developed Science Based Targets for decarbonized investment strategies for UK supermarkets.

Notwithstanding, these decision-support models also present a limited consideration for MYP of existing real estate assets. Primarily, this relates to the latter steps of generating, estimating the performance of, and evaluating retrofit design alternatives on for multiple buildings at once. Here, the merits of optimization approaches provide owners the ability to evaluate and choose among *various* 'ideal' retrofit choices and schedules, considering the interactions of technologies, on a multi-objective basis over a long-term horizon [65–67].

1.2. This paper

We present an opportunity to bridge the gap between the energy optimization and real estate management domains to provide a novel methodology for MYP relevant for investments in existing building retrofits. Taking relevant aspects from both approaches would allow for adequate techno-economic analysis of the retrofit's – *where*, *how*, *what*, *when* – questions relevant for both energy engineers and building owners. Such a model must consider:

- Optimal solutions for *when* to initiate a retrofit and *what* retrofit to do. This is particularly relevant for mismatched component life-cycles which naturally stagger retrofit interventions, presenting a question for optimal retrofit scheduling of a particular component or whether to conduct a deep retrofit.
- All relevant technologies and components – envelope retrofits, energy system, and non-energy – while optimizing the building retrofitting project on both sides of the energy balance (demand and supply).
- A life-cycle costing and (embodied) emissions perspective for associated technologies.
- A long-term time horizon in order to capture interdependencies between technologies and the value of future options to defer, expand, or extend the life of each technology.
- Real-estate relevant aspects as a basis of which to choose from various multi-objective asset investment strategies (*how*). This primarily relates to the impact on rental revenues upon investing in value-added technologies in a building retrofit, with further consideration of how the building value is affected by cost vs. CO_2 trade-offs.
- Aspects related to scalability for considering multiple contextual asset retrofitting strategies (*where*).

With this paper, our objective is to address these methodological and knowledge gaps with the introduction of the novel MANGOret optimization framework. The framework applies the above considerations to give real estate owners the ability to weigh the optimal cost vs. CO_2 trade-offs over the entire long-term multi-objective decision-space for early-stage budgeting before more contextual technical planning is available. To reduce the planning time in creating asset retrofitting strategies, the framework includes a series of automated data retrieval and processing steps.

As a core part of the optimization *framework*, the MANGOret optimization *model* builds upon the MANGO (Multi-stAge eNerGy Optimization) model [50]. In its original MILP formulation, MANGO addressed methodological gaps for the case of multi-stage D-MES investment planning by incorporating a multi-year horizon, inherently demonstrating the value of investment flexibility and dynamic multi-stage D-MES design. The model was applied to a case of multiple interconnected D-MES district configurations. As typical for optimization studies at the district-scale, the district's energy demands were considered as nodes through aggregation of many buildings' demands [68]. However, the MANGO model is not able to consider the techno-economic retrofitting investment decision.

While our approaches in considering energy systems and envelope retrofits can be compared to other MILP models, such as Refs. [31,43], the main novelties of the MANGOret optimization framework are as follows:

- A scalable framework to optimize retrofitting investment strategies of any existing real estate asset considering their contextual nature, demonstrated for a case of several buildings in Switzerland from an LSI portfolio.
- From the energy perspective, the MANGOret model is able to generate optimal multi-stage design solutions and operating strategies for building-level D-MES and envelope retrofits according to economic and environmental objectives over the entire time horizon to 2050, considering existing building components and technologies.
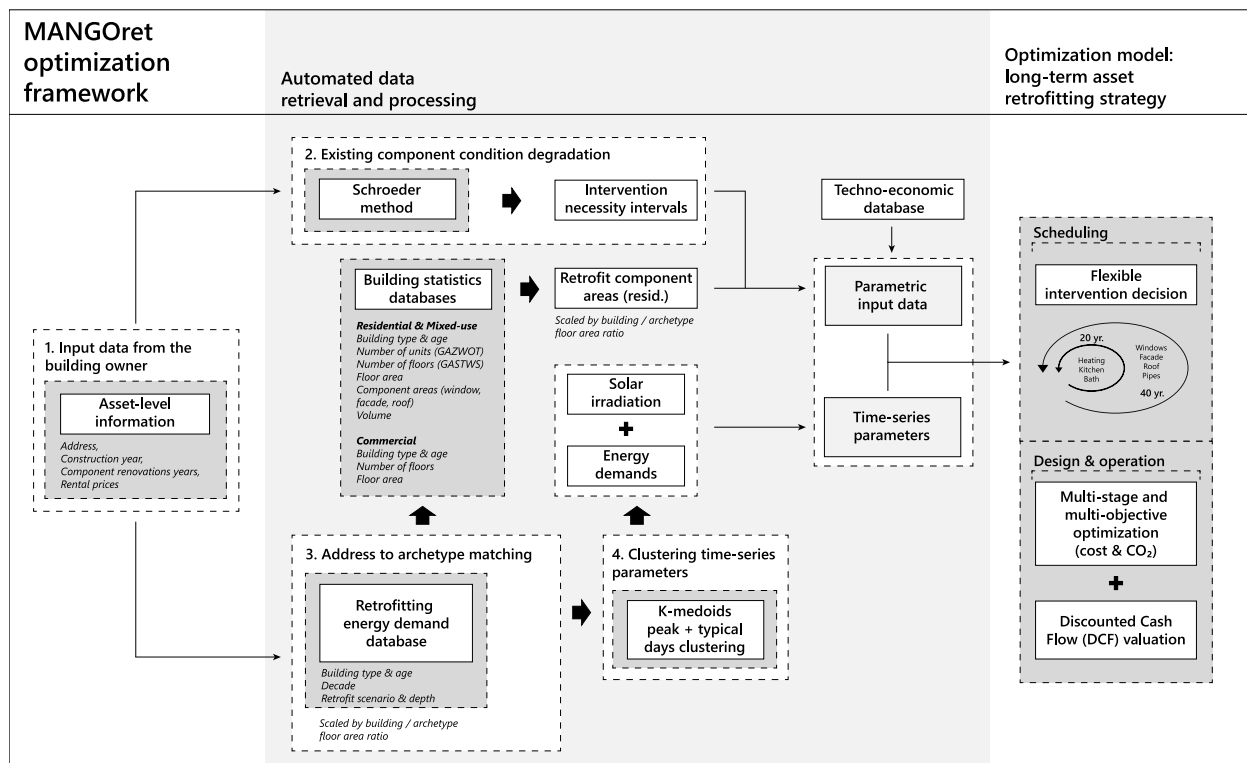
Fig. 1. MANGOret optimization framework considering three sections — Input data from the building owner (step 1), Automated data retrieval and processing (steps 2–4), which supply the necessary time-series and parametric input data to the MANGOret optimization model.

- From the real estate management perspective, the MANGOret model includes critical elements such as the possible rental income after the retrofit (according to legal mandates) in order to calculate the building value. The optimization is able to be scaled up for many contextual assets at once to automate investment planning.

This paper is structured as follows: Section 2 describes the main features of the MANGOret optimization framework. Section 3 introduces the illustrative case study that is used to demonstrate the value of the model. Section 4 presents the results of the paper along with model discussion. Finally, concluding remarks are given in Section 5.

2. MANGOret: A model framework for the optimal, long-term investment planning of building retrofits

Here we describe the key characteristics of the MANGOret optimization *framework*, along with the mathematical formulation of the MANGOret optimization *model*. Due to the significant amount of diverse input data required for the MANGOret model, it was necessary to create a framework which could adequately generate such data for any building in a scalable manner. In this paper, we demonstrate the MANGOret framework for the case of several buildings from an LSI portfolio in Switzerland, but nonetheless the approach can be replicated in other countries.

The MANGOret framework is depicted in the Fig. 1 workflow. The preliminary steps 1–4 relate to retrieving and processing the necessary building input data. In **Step 1 (Input data from the building owner)**, we gather a small set of relevant data which is necessary to conduct both steps 2 and 3. In **Step 2 (Existing component condition degradation)**, we determine a range of years for when various components must first be retrofitted ('necessity intervals') via the Schroeder component condition degradation method (further described in Section 2.2). In **Step 3 (Address to archetype matching)**, we develop an archetypal energy demand database (further described in Section 2.3)

to retrieve the relevant retrofitting packages' energy demands and statistical building data from government databases for any building address. In this database, all buildings contained within the building registry are assigned an archetype with simulated energy demand profiles for different retrofitting packages and climate scenarios. Since we take a multi-year perspective for the holistic building D-MES and envelope retrofit investment strategy, we utilize typical days to reduce computational complexity. In **Step 4 (Clustering time-series parameters)**, we conduct a peak and typical days k-medoids clustering of the time-series parameters (solar irradiation and energy demands). Combined with the techno-economic database shown in Appendix B, these automated data retrieval and processing steps form the necessary input data for the MANGOret optimization model.

Represented in the right side of Fig. 1, the MANGOret model conducts a multi-stage and multi-objective optimization (cost vs. CO_2), and further DCF valuation based on rental income, to output a long-term asset retrofitting strategy. In the following, we first outline the MANGOret optimization model formulation and subsequently discuss the automated data retrieval and processing steps.

2.1. Optimization model formulation

The MANGOret model considers a portfolio of energy technologies and retrofitting packages shown in the Fig. 2 superstructure representation. The presented technologies and retrofitting packages are chosen as part of the illustrative case of the MANGOret optimization framework, with other technologies and retrofitting possibilities able to be added.

MANGOret builds upon the MANGO model [50], utilizing the latter's capabilities for the long-term, multi-stage design and operation of D-MES. The MANGOret model adds a complete consideration of the retrofitting investment decision, with the main additions categorized as:

- Consideration of which thermal envelope retrofitting package, and thus relevant demand profile, to choose among several components options (Roof, Facade, Window) and their combinations,
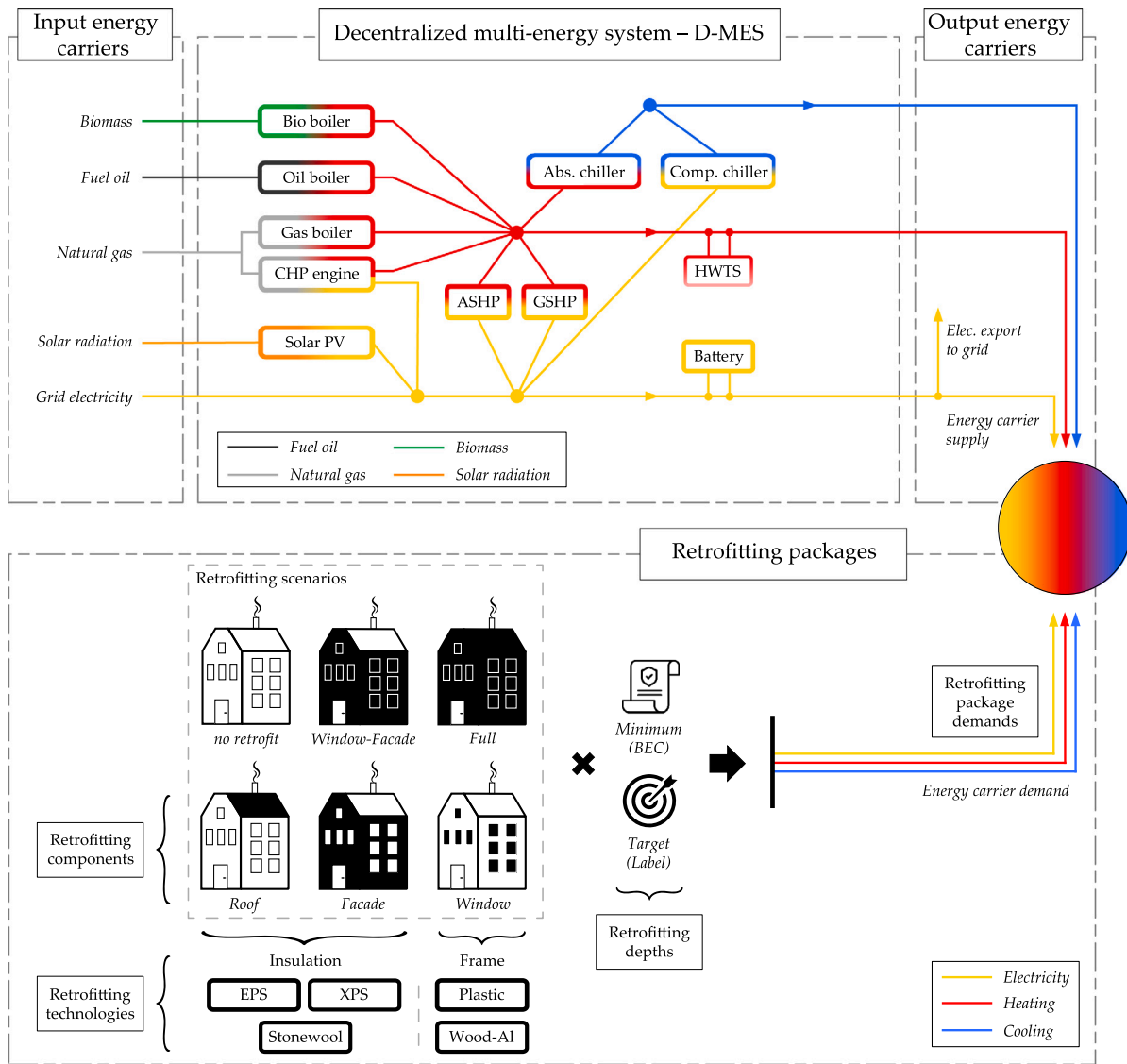
Fig. 2. Superstructure representation of both the building-level D-MES (top) and retrofitting (bottom) aspects of the MANGOret model. The top of the figure presents the candidate energy conversion and storage technologies which supply energy demands for the building. The bottom of the figure presents the various considered retrofitting aspects – components, depths, technologies – which combine to form a chosen retrofitting package with their simulated demands. The model simultaneously considers the energy systems and retrofitting sections, with the colorful circle representing the balance of demand and supply (see Eq. (3)).

taken from an archetypal energy demand database (see Section 2.3). Further, we consider various retrofitting depths (Minimum vs. Target) along with technology options for each component such as insulation and Window types.

- Mathematical formulation of real estate considerations regarding a value-added rental price formula to output potential revenues and building value. The legally-mandated rental price constraints are the main drivers of real estate retrofitting budgets [15].
- Investments in non-energy miscellaneous technologies (kitchens, bathrooms, pipes) which constitute a significant part of retrofit budgets. These are not shown in Fig. 2 as they are not energy considerations.
- Consideration of embodied emissions for all technologies and components (energy and non-energy).
- Incorporation of a range of years for when it is first necessary to initiate a retrofit for all components according to the Schroeder probabilistic scheduling method (based on component condition).
- Incorporation of existing conversion and storage technology installations.

- Incorporation of model periods to represent a number of years in order to reduce computational complexity for the operational aspects of the computation.

Given the candidate technologies, energy carriers, retrofitting packages, and objective functions to be optimized, MANGOret simultaneously takes design decisions regarding *what, where, and when* actions for the building D-MES and envelope retrofits. The complete model formulation and detailed explanation of all parameters, variables, constraints and objective functions provided in Appendix A.

The model is formulated as a MILP in Python using the Pyomo open-source optimization modeling language [69,70], solved in this paper with the state-of-the-art solver Gurobi [71] on high performance computing clusters at ETH Zurich. We describe the model formulation in the following.

2.1.1. Sets

Table 1 presents a summary and description of all model sets used in MANGOret. From the MANGO formulation, we have added relevant sets related to retrofitting along with (i) the addition of model

Table 1

MANGOret model sets and indices. While energy system locations are maintained from the original formulation in MANGO, they are not used as always one building site is considered at a time in developing building-specific retrofitting strategies.

Set	Index	Description
$\mathcal{P}$	p	Periods considered in the model horizon
$\mathcal{D}$	d	Set of representative days considered for each period
$\mathcal{T}$	t	Time steps considered for each day
$\mathcal{W}_{cs} \subseteq \mathcal{P}$	w_{cs}	Investment stages for conversion and storage technologies
$\mathcal{W}_f \subseteq \mathcal{P}$	w_f	Investment stages for retrofitting components
$\mathcal{L}$	l	Energy system locations.
$\mathcal{E}C$	ec	All energy carriers in the energy system
$\mathcal{E}C_i \subseteq \mathcal{E}C$	ec_i	Energy carriers that can be imported by the energy system
$\mathcal{E}C_e \subseteq \mathcal{E}C$	ec_e	Energy carriers that can be exported from the energy system
$\mathcal{E}C_d \subseteq \mathcal{E}C$	ec_d	Energy carriers for which demands are established
$\mathcal{F}$	f	Retrofitting components
$\mathcal{J}$	j	Retrofitting depths
$\mathcal{G}$	g	Retrofitting technologies
$\mathcal{H}$	h	Retrofitting technology demand package
$\mathcal{N}$	n	Miscellaneous technologies
C	c	Energy conversion technologies
$C_{ext} \subseteq C$	c_{ext}	Existing energy conversion technologies
$C_{sol} \subseteq C$	c_{sol}	Solar energy conversion technologies
$C_d \subseteq C$	c_d	Dispatchable energy conversion technologies
$C_{d_h} \subseteq C_d$	c_{d_h}	Dispatchable energy conversion technologies which mainly supply heating
$C_{d_c} \subseteq C_d$	c_{d_c}	Dispatchable energy conversion technologies which mainly supply cooling
S	s	Energy storage technologies
$S_{ext} \subseteq S$	s_{ext}	Existing energy storage technologies

periods as a further delineation of the temporal resolution, and (ii) the separation of investment stages into the energy system (conversion and storage) and retrofitting technologies.

We separate multiple sets for individual thermal envelope components ($\mathcal{F}$) – Roof, Facade, Window – and subsequently a set to incorporate a depth element ($\mathcal{J}$) — e.g. $Roof_{Min}$, $Roof_{Tar}$, $Facade_{Min}$, $Facade_{Tar}$, $Window_{Min}$, and $Window_{Tar}$ for the case presented here. These two depths are modeled as the minimum intervention based on the Building Energy Code (BEC) and the target intervention based on a green building label, originally described in Murray et al. [48]. The retrofitting technologies ($\mathcal{G}$) are represented as different options, for the example of Facade and Roof insulation materials: oil-based extruded and expanded polystyrene (XPS and EPS, respectively) along with mineral stone wool, and for Windows: plastic and wood-aluminum frames.

The retrofitting depths are linked with their combinations in ($\mathcal{H}$) – termed retrofitting package demands – to reference the demand profiles from the archetypal energy demand database. For example, additionally with individual technology profiles (e.g. $Window_{Min}$, $Facade_{Min}$, and $Roof_{Min}$), we add the combinations $Window - Facade$ and the $Full$ retrofit considering all three, with $_{Min}$ and $_{Tar}$ depths. To reduce complexity, we have only simulated the aforementioned relevant combinations in the archetypal demand database, although MANGOret could utilize any number of retrofitting components, depths, technologies, and package demands. The various retrofitting technology options' parameters (costs and embodied emissions) are linked to the required technology-specific insulation thicknesses (Roof and Facade) or Window panes necessary to meet the simulated demands at the respective depths.

Further, we include a sets of existing technologies to account for components already installed in the building, with their respective remaining lifetime. The years in which existing conversion technologies retire ($cl_c + 1$) are added to the set of investment stages for conversion and storage technologies ($\mathcal{W}_{cs}$) in order to allow for further technology installations in those stages. This is supplemented by miscellaneous technologies such as kitchens, bathrooms, and pipes, $\mathcal{N}$, which do not impact the energy or envelope retrofitting aspects of the building.

Multi-year model periods ($\mathcal{P}$) are added in order reduce the model's temporal resolution. While in this paper, the horizon of the model is always 30 calendar years ($\mathcal{Y}$) representing 2021–2050, the addition

of periods allows for the bundling of years to reduce computational complexity. For example, if optimizing for 10 periods over 30 years, the real years (y_p) 1–3 would be represented by period 1, while real years 4–6 would be represented by period 2, and so on. These relationships between periods p, years y, days d, and hourly time steps t are shown in Fig. 3.

For parameter values which correspond to operational aspects over an entire period, such as import/export prices and energy carrier carbon factors, the average of all values corresponding to the period is taken. For parameter values which correspond to an investment stage, such as technology costs, efficiencies, etc., values from the first year in each period are taken (e.g. in the above example, costs for period 2 would be taken from real year 4).

2.1.2. Parameters

The MANGOret model requires various parameters to perform a simultaneous optimization of building D-MES and envelope retrofits. All model parameters, their mathematical notation and definition are discussed in more detail in Appendix A.2 and are supplemented by the techno-economic database in Appendix B. All parameters from the MANGO model which are not listed pertaining to conversion and storage technologies still apply. Taken from steps 1–4 of the MANGOret framework, the main parameter categories include:

- Real estate-relevant parameters connected to the building-specific limitations or characteristics, such as floor area, window area, facade area, roof area along with availability of roof area for solar technology installations. These parameters come from two sources — from building owners and government building statistical databases.
- Energy demand profiles per retrofitting package (h) that accurately reflect short-term variability (hourly basis) and long-term patterns for the entire 30-year model horizon. Profiles are taken from the developed archetypal energy demand database (see Section 2.3).
- Renewable energy availability profiles (e.g. solar irradiation) that accurately reflect short-term variability and long-term patterns. Solar irradiance data for each building location are taken from the Renewables.ninja API which connects to the MERRA-2 database [72–74].
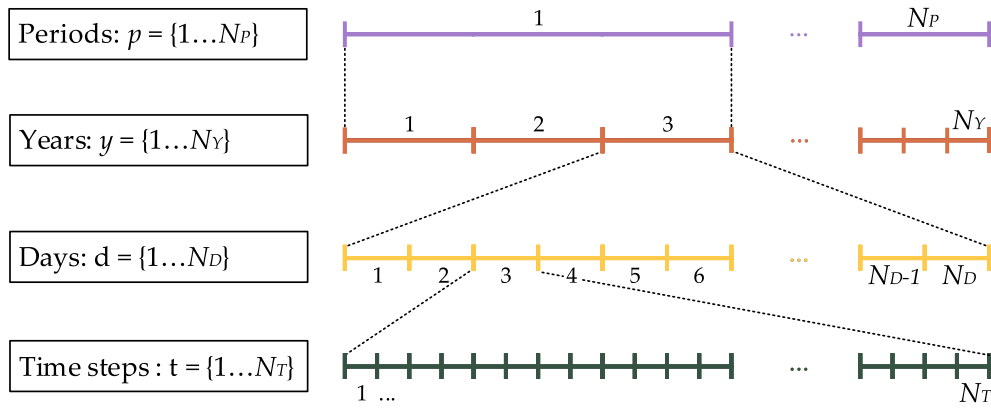
Fig. 3. Temporal horizon representation in the MANGOret model using a sequence of periods, years, days, and time steps. Example shown with each period represented by 3 years.

- Economic parameters, such as the evolution of energy carrier prices, technology costs, maintenance costs, along with base-rents, etc.
- Technical parameters pertaining to the operation and the performance of technologies, such as conversion efficiencies and lifetimes, etc. depending on the technology.
- Emission factors for energy carriers and linearly scaled parameters for embodied emissions of all considered technologies.
- Ranges of years for which retrofitting components along with existing technologies must first be retrofitted. These are taken from the output of the Schroeder method (see Section 2.2).

2.1.3. Decision variables

The main MANGOret decision variables pertain to the design and operation of building D-MES and envelope retrofits over the modeled time horizon. Here, we discuss the decision variables most important for MANGOret with further detail provided in Appendix A.3 and Table A.6. All decision variables from the MANGO model which are not listed pertaining to energy system operation and design still apply.

The model considers *all at once* all relevant existing building investment decisions related to energy retrofits along with 'renovations' of miscellaneous non-energy components. The retrofitting functionality is primarily achieved through a series of binary decision variables (explained further in Appendix A.5). The utilization of these binary variables – namely Y^{retnew}, $Y^{retactive}$, Y^{retdem}, and $Y^{retoccur}$ – presents a novel approach for envelope retrofit optimization. The main retrofitting-relevant decision variables are:

- Y^{retnew}_{g,l,w_f} : Binary variable denoting the installation of retrofitting technology g, at location l, in investment stage w_f
- $Y^{retactive}_{g,l,p}$: Binary variable denoting that retrofitting technology g, at location l, is active in period p
- $Y^{retdem}_{h,l,p}$: Binary variable representing the active retrofitting package demand h which the model takes as demand input, at location l, in period p
- $Y^{retoccur}_{l,w_f}$: Binary variable representing the occurrence of the retrofitting package at location l, in investment stage w_f
- $Y^{retoccur_{scaff}}_{l,w_f}$: Binary variable representing the occurrence of the retrofitting package at location l, in investment stage w_f relevant for project costs such as scaffolding
- Y^{misc}_{n,l,w_f} : Binary variable denoting the installation of new capacity of miscellaneous technology n, at location l, in investment stage w_f

The main real estate-relevant decision variables are:

- $rent_{l,p}$: Rent per period for location l, in period p

- $VAI_{l,p}$: Value-added investment portion per period supplemented to the rent for location l, in period p
- T^{value} : Total lifetime value of building (location l), defined as the sum of discounted rental revenue over the horizon, minus discounted total cost of energy systems and retrofits (T^{cost} objective, see Section 2.1.4)

The main energy system-relevant decision variables are:

- $NCAP^{conv}_{c,l,w_{cs}}$: New capacity of conversion technology c, installed at location l, in investment stage w_{cs}
- $NCAP^{stor}_{s,l,w_{cs}}$: New capacity of storage technology s, installed at location l, in investment stage w_{cs}
- $Y^{conv}_{c,l,w_{cs}}$: Binary variable denoting the installation of new capacity of conversion technology c, at location l, in investment stage w_{cs}
- $Y^{stor}_{s,l,w_{cs}}$: Binary variable denoting the installation of new capacity of storage technology s, at location l, in investment stage w_{cs}

The variables in the model pertaining to D-MES operating aspects are indexed per period p, day d, and hour t in addition to their specific indices:

- $P^{imp}_{ec_i,l,p,d,t}$: Import of energy carrier ec_i, at energy system location l
- $P^{conv}_{c,l,w_{cs},p,d,t}$: Input energy to conversion technology c, installed at energy system location l, in investment stage w_{cs}[2]
- $P^{exp}_{ec_e,l,p,d,t}$: Exported energy of carrier ec_e, at energy system location l

2.1.4. Objective functions

We utilize the two most commonly considered objectives in optimization — minimization of the discounted total investment costs (T^{cost}) and/or CO_2 emissions (T^{CO_2}) over the multi-year horizon. In the following, we describe the updated retrofitting-relevant T^{cost} and T^{CO_2} objective functions from their original formulations in MANGO [50].

Total cost T^{cost} is defined in Eq. (1), composed of terms that represent the total investment expenditure, the total operating expenditure and the salvage value of the building D-MES and envelope retrofit at the end of the model horizon. Each of these terms encompasses

---

[2] The definition domain for the variables $P^{conv}_{c,l,w_{cs},p,d,t}$ includes the conditions: $y_p \geq w_{cs}$ and $y_p \leq w_{cs}+cl_c-1$, which defines the operating period of conversion technology c, with cl_c being the lifetime of the technology in real years y_p. This ensures that a technology cannot operate in the years before the investment stage when the generation technology is installed and also that it cannot operate beyond its lifetime cl_c. For instance, if a technology is installed in stage $w_{cs} = 1$ and has a lifetime of 15 years, it will be operational between $y_p \geq 1$ and $y_p \leq 15$.

conversion, storage, retrofitting, and miscellaneous technologies. The exact mathematical definitions of the individual terms in Eq. (1) are given in Appendix A.4.

$$
\min T^{cost} = \underbrace{\sum_{l,w_{cs}} \left(C_{l,w_{cs}}^{INV,TECH} \right)}_{\text{Energy system investment expenditure}}
$$

$$
+ \underbrace{\sum_{l,w_f} \left(C_{l,w_f}^{INV,RET} + C_{l,w_f}^{INV,MISC} \right)}_{\text{Retrofitting investment expenditure}} \tag{1}
$$

$$
+ \underbrace{\sum_{l,p} \left(C_{l,p}^{IMP} + C_{l,p}^{MAINT} - R_{l,p}^{EXP} \right)}_{\text{Operating expenditure}} - \underbrace{\sum_{l} R_{l}^{SLVG}}_{\text{Salvage value}}
$$

Investment expenditure is composed of the over all energy system locations l and investment stages w_{cs} (for energy systems) & and w_f (for retrofits) of the individual expenditures for energy conversion and storage technologies, $C_{l,w_{cs}}^{INV,TECH}$, retrofitting technologies, $C_{l,w_f}^{INV,RET}$, and miscellaneous technologies, $C_{l,w_f}^{INV,MISC}$. The operating expenditure is defined as the sum over all energy system locations l and periods p of the individual expenditure due to energy carrier imports, $C_{l,p}^{IMP}$, technology maintenance, $C_{l,p}^{MAINT}$, and, the revenue due to energy carrier exports, $R_{l,p}^{EXP}$.

The salvage value is defined as the sum of the individual salvage value terms (R_{l}^{SLVG}), representing the remaining value that is retained by technologies at location l that have not reached the end of their lifetime at the end of the model horizon. The salvage value is credited back to the total system cost to offset part of the investment costs in technologies that have been utilized only for a fraction of their lifetime in the model. Hence, the use of these salvage values can mitigate the distorting end-of-horizon effects [50]. The amount of salvage value depends on the investment stage a technology was installed, its operational lifetime, and its initial investment cost (see exact definition in Eq. (A.14)). Technologies reaching the end of their lifetime during the modeled horizon are assumed to have no salvage value.

All terms of Eq. (1) are discounted to present values with the building-specific discount rate r_l as this can vary between real estate markets. All investment expenditures are assumed to occur at the beginning of the year corresponding to each investment stage w_{cs} or w_f, operating expenditures discounted according to the calendar year in which they occur, while the salvage value is paid back after the end of the model horizon.

The second objective function considered in the model relate to the total CO_2 emissions of the building's energy system and technology embodied emissions, is expressed as the sum over all energy system locations l and periods p of individual emission terms, $E_{l,p}^{CO_2}$, as shown in Eq. (2):

$$
\min T^{CO_2} = \underbrace{\sum_{l,p} E_{l,p}^{operCO_2}}_{\text{Operational and indirect emissions}}
$$

$$
+ \underbrace{\sum_{l,w_{cs}} E_{l,w_{cs}}^{embCO_2,TECH} + \sum_{l,w_f} \left(E_{l,w_f}^{embCO_2,RET} + E_{l,w_f}^{embCO_2,MISC} \right)}_{\text{Technology embodied emissions}}
$$

$$
\tag{2}
$$

The $E_{l,p}^{operCO_2}$ term includes only operational CO_2 emissions and, more specifically, direct emissions due to local energy carrier utilization (e.g. fossil fuel combustion) and indirect emissions due to energy imports (e.g. grid electricity imports). The $E_{l,p}^{embCO_2}$ term includes the linear, capacity- or size-scaled embodied CO_2eq emissions of conversion, storage, retrofitting, and miscellaneous technologies. The exact mathematical definitions for all components of $E_{l,p}^{operCO_2}$ and $E_{l,p}^{embCO_2}$ terms are given in Appendix A.4.

MANGOret can be utilized in both individual building along with multi-building site configurations. In the above objective function formulas, we present the cost and emissions aspects as the summation over all building locations l. This demonstrates a strategy to consider an optimal retrofitting investment strategy for a portfolio of buildings without any linking constraints between buildings, such as budgets, manpower, etc. However, in this paper we consider one building at a time to provide building-specific retrofitting strategies. Considering several buildings at once would increase computational effort largely due to the large number of variables from all technology choices which make it difficult to solve multiple buildings in one optimization problem.

As in the original MANGO formulation, MANGOret can be used in both single- and multi-objective optimization modes considering all cost and CO_2 objectives. We solve the multi-objective problem using the augmented ϵ-constraint method from Ref. [75], as it has been shown to avoid the production of weakly Pareto optimal solutions.

2.1.5. Constraints

In order to create feasible asset retrofitting strategies in an optimization model, it is imperative to formulate constraints that define balances, limitations, bounds, or minimum requirements involving the model's decision variables. The addition of retrofitting and real-estate aspects present a novelty for optimization models, constraining in a way that would achieve a long-term investment strategy considering the simultaneous design of building D-MES and envelope retrofits. All energy-relevant constraints from the original MANGO formulation are still utilized. The main constraints in the MANGOret model relate to:

- Energy balances for conversion and storage technologies considering the chosen retrofit package's energy demands.
- Retrofitting-relevant technology installation and sizing constraints assuring the consideration of their investment decisions over the time horizon.
- Legally mandated rental constraints including the main rent formula calculation considering component pass-on rates along with linear parameters such as rent escalation and structural vacancy.

Retrofitting energy balance

The overall energy balance constraint is shown in Eq. (3). In broad terms, it states that the end-user energy demands, $dem_{ec_d,h,l,p,d,t}$, at location l, for energy carrier ec_d, must be balanced by energy imports, conversion, storage, and exports for every period p, day d and time step t in the model horizon. Similar to Refs. [31,43], a binary variable $Y_{h,l,p}^{retdem}$ is used to select the active retrofitting package which the model takes as demand input.

$$
\underbrace{\sum_{h} dem_{ec_d,h,l,p,d,t} \cdot Y_{h,l,p}^{retdem}}_{\text{Retrofitting package demand}} = \underbrace{P_{ec_i,l,p,d,t}^{imp}}_{\text{Import}}
$$

$$
+ \underbrace{\sum_{\substack{c,w_{cs} \\ p \geq w_{cs} \\ p \leq w_{cs}+cl_c-1}} \left(P_{c,l,w_{cs},p,d,t}^{conv} \cdot \eta_{c,ec,w_{cs}}^{conv} \cdot cdeg_{c,ec,w_{cs},p} \right)}_{\text{Conversion technologies}}
$$

$$
+ \underbrace{\sum_{\substack{s,w_{cs} \\ p \geq w_{cs} \\ p \leq w_{cs}+sl_s-1}} \left[stc_{s,ec} \cdot (Q_{s,l,w_{cs},p,d,t}^{dis} - Q_{s,l,w_{cs},p,d,t}^{ch}) \right]}_{\text{Storage technologies}} \tag{3}
$$

$$
- \underbrace{P_{ec_e,l,p,d,t}^{exp}}_{\text{Export}}
$$

$$
\forall\ ec \in \mathcal{EC},\ l \in \mathcal{L},\ p \in \mathcal{P},\ d \in \mathcal{D},\ t \in \mathcal{T}
$$

Retrofitting-relevant constraints

There are a series of constraints related to the retrofitting-functionality of the MANGOret model. These constraints rely on a number of binary variables. In the following, we present the most important

constraints to explain each binary definition with one example for continuity.

The purpose of Eqs. (4) to (11) is to constrain the model to properly consider retrofitting through a series of binary variables — namely Y^{retnew}, $Y^{retactive}$, Y^{retdem}, and $Y^{retoccur}$. The model's optimal retrofitting decision begins with Y^{retnew}, which denotes the installation of a new capacity of a retrofitting technology (g) with an associated depth (j) related to the retrofitting component (f). For example, the model could decide to retrofit (thus, $Y^{retnew} = 1$ in that period) the Facade and Window components in period 1 with retrofitting depths and technologies $Facade_{Min}$ and $Facade_{MinXPS}$, $Window_{Min}$ and $Window_{MinWoodAl}$, respectively. This is followed by the Roof component in period 3 with depth $Roof_{Min}$ and technology $Roof_{MinXPS}$.

Eq. (4) tracks the new installed retrofitting technology Y^{retnew} to keep the correct retrofitting technology active with $Y^{retactive}$. In the previous example, both $Facade_{MinXPS}$, and $Window_{MinWoodAl}$ would have $Y^{retactive} = 1$ in all model periods while $Roof_{MinXPS}$ would have $Y^{retactive} = 1$ from period 3 onwards.

$$Y^{retactive}_{g,l,p} = \sum_{\substack{w_f \\ w_f \leq p \\ w_f \geq p - gl_g + 1}} Y^{retnew}_{g,l,w_f}, \tag{4}$$
$$\forall g \in \mathcal{G}, l \in \mathcal{L}, \ p \in \mathcal{P}$$

Eq. (5) mandates that a retrofitting technology must be active ($= 1$) in any given year within the 'necessity interval' parameter range output from the Schroeder method (see Section 2.2). We utilize binary matrices to match retrofitting components (f) to retrofitting depths (j) with the binary matrix $mapcomp_{j,f}$, and further to retrofitting technologies (g) with the binary matrix $mapdepth_{g,j}$. A similar formulation is taken for miscellaneous technologies.

$$\sum_{\substack{j,g,p \\ p \geq intmin_{f,p} \\ p \leq intmax_{f,p} \\ mapcomp_{j,f}=1 \\ mapdepth_{g,j}=1}} Y^{retactive}_{g,l,p} \geq 1, \tag{5}$$
$$\forall \ f \in \mathcal{F}, \ l \in \mathcal{L}$$

Eq. (6) assures that the active retrofitting technology $Y^{retactive}$ is matched to the relevant retrofitting packages' demands Y^{retdem} using the binary matrix $mapdem_{g,h}$. In practical terms, this is relevant for combining multiple individual retrofits to use the relevant *combined* retrofitting package demand. In the above example, this would mean the model utilizes the $Window - Facade_{Min}$ package from periods 1 through 3, and then upon the installation of a technology with depth $Roof_{Min}$ (in this case, $Roof_{MinXPS}$) in period 3, switching to the $Full_{Min}$ package with the associated technologies. More information on retrofitting package demands is provided in Section 2.3.

$$\sum_{\substack{g \\ mapdepth_{g,j}=1}} Y^{retactive}_{g,l,p} = \sum_{\substack{g,h \\ mapdepth_{g,j}=1 \\ mapdem_{g,h}=1}} Y^{retdem}_{h,l,p}, \tag{6}$$
$$\forall \ j \in \mathcal{J}, \ l \in \mathcal{L}, p \in \mathcal{P}$$

Eq. (7) forces the model's consideration of one retrofitting packages' demand profile Y^{retdem} per period. Further, Eq. (8) forces the model's consideration of a maximum of one $Y^{retactive}$ per retrofitting depth (j) per period.

$$\sum_{h} Y^{retdem}_{h,l,p} = 1, \tag{7}$$
$$\forall \ l \in \mathcal{L}, p \in \mathcal{P}$$
$$\sum_{\substack{g, \\ mapdepth_{g,j}=1}} Y^{retactive}_{g,l,p} \leq 1, \tag{8}$$
$$\forall \ j \in \mathcal{J}, \ l \in \mathcal{L}, p \in \mathcal{P}$$

The following two retrofits occurrence constraints Eqs. (9) and (10) track generally when a new retrofit occurs. Simply put, whenever

there is any new retrofit activity ($Y^{retnew} = 1$), then $Y^{retoccur} = 1$ in order to trigger a switch in the retrofit package demand. Eq. (11) expresses $Y^{retoccur_{scaff}}$ as a binary variable used to track when a certain retrofit activity is triggered to apply a fixed retrofitting project cost for scaffolding which is signified for Facade and Roof components. From the above example, both $Y^{retoccur}$ and $Y^{retoccur_{scaff}}$ would equal 1 in periods 1 and 3.

$$Y^{retoccur}_{l,w_f} \leq \sum_{g} Y^{retnew}_{g,l,w_f}, \tag{9}$$
$$\forall \ l \in \mathcal{L}, w_f \in \mathcal{W}$$

$$Y^{retoccur}_{l,w_f} \geq (1/|\mathcal{G}|) \cdot \sum_{g} Y^{retnew}_{g,l,w_f}, \tag{10}$$
$$\forall \ l \in \mathcal{L}, w_f \in \mathcal{W}$$

$$Y^{retoccur_{scaff}}_{l,w_f} \geq (1/|\mathcal{G}_{scaff}|) \cdot \sum_{g} Y^{retnew}_{g,l,w_f}, \tag{11}$$
$$\forall \ l \in \mathcal{L}, w_f \in \mathcal{W}$$

We further constrain both the number and/or capacity sizing of conversion, storage, and miscellaneous technologies to prevent the model from over-installing technologies. Appendix A.5 details the remaining constraints.

Rent constraints

We capture the legally-mandated aspects of rent calculation in Eqs. (12) and (13), allowing the model to determine the rent based on the chosen optimal investment strategy including all technologies' respective pass-on rates. The rent formula in Eq. (12) is based on previous research on real estate decision-making in Europe, signifying the justified rent increases from value-added technology investments [15]. The formula is split based on consideration of period 1 and all periods thereafter. For period 1, Eq. (12) states that the rent is equal to the base rent of the building at location l plus any value-added investments made in that period, outputting the period 1 rent ($rent_{l,p=1}$). In further periods ($rent_{l,p>1}$), the model is constrained that any rent increase must be justified by further investments or otherwise through the linear parameters. The Value-Added Investment ($VAI_{l,p}$) portion is part of the rental formulas formulated in Eq. (13).

We consider linear real estate market effects by introducing prospective rental escalation ($rentescal_{l,p}$) and structural vacancy ($structvaca_{l,p}$) parameters depending on the market attractiveness of each individual building at location l. Other than for these two parameters, we do not capture rental increases from any other source such as from macroeconomic factors. The total building value, presented in Eq. (15), is calculated using a DCF methodology [9] commonly used in real estate. The value is calculated simply as the discounted sum of the total rental revenue minus the discounted sum total investment costs, over all periods.

We constrain the rent to 90% of the market quantile in each ZIP code with the following constraint in Eq. (14).

$$\underbrace{rent_{l,p}}_{\text{Rent in period } p} = VAI_{l,p} \cdot \underbrace{(1 + rentescal_{l,p})^{|Y_p|}}_{\text{Rent escalation}}$$
$$\cdot \underbrace{(1 - structvaca_{l,p})^{|Y_p|}}_{\text{Structural vacancy}} \cdot \underbrace{\sum_{i=y_p}^{y_p+|Y_p|-1} \frac{1}{(1+r_l)^i}}_{\text{Real year discounting}}$$
$$+ \begin{cases} \underbrace{(baserent_l \cdot fa_{l,p} \cdot |Y_p|)}_{\text{Base rent in period 1}} & \text{if } p = 1 \\ \underbrace{rent_{l,p-1}}_{\text{Rent in previous period}} & \text{if } p \geq 1, \end{cases} \quad \forall \ l \in \mathcal{L}, \ p \in \mathcal{P} \tag{12}$$

$$VAI_{l,p} = \sum_{\substack{c,s,w_{cs} \\ w_{cs}=p}} \left(C_{l,w_{cs}}^{INV,TECH} \cdot passon_{c,s}/cl_c \text{ OR } sl_s \right)$$

$\underbrace{\qquad}_{\text{Value-added investment}}$ $\underbrace{\qquad\qquad\qquad\qquad\qquad\qquad\qquad}_{\text{Energy system technology investment}}$

$$+ \underbrace{\sum_{\substack{g,w_f \\ w_f=p}} \left(C_{l,w_f}^{INV,RET} \cdot passon_g/gl_g \right)}_{\text{Retrofitting technology investment}} + \underbrace{\sum_{\substack{n,w_f \\ w_f=p}} \left(C_{l,w_f}^{INV,MISC} \cdot passon_n/nl_n \right)}_{\text{Miscellaneous technology investment}}$$

$$\forall\, l \in \mathcal{L},\ p \in \mathcal{P}$$

(13)

$$rent_{l,p} \leq maxrent_{l,p} \tag{14}$$

$$T^{value} = \left(\sum_p rent_{l,p} \right) - T^{cost} \tag{15}$$

2.2. Retrofit scheduling

When developing long-term building investment strategies, it is necessary to determine *what* retrofit is necessary, along with *when* it is necessary to intervene. Here, we discuss the approach to retrofit scheduling in the MANGOret optimization framework considering component condition. Further detail and description is provided in Appendix A.6.

Methodologies to determine the most favorable retrofit schedule for a specific existing component or a combination are generally categorized in literature into two classes — deterministic and probabilistic. Both methods generally approach the question of '*when*' by estimating the remaining expected service life of components to determine intervention timing. Further, a large set of these retrofit analysis methods manifest the *when* and *what* decision as two separate, decoupled steps [76]. Models which do consider the interdependencies of retrofitting technologies (*what*) and the importance of a long-term horizon (*when*) at once, typically do not consider component conditions and thus take the expected remaining service life approach [31].

As a parametric input into the MANGOret optimization framework, we utilize a hybrid approach of *both* deterministic and probabilistic classes to determine the Life-Cycle Cost (LCC) of the individual component retrofit considering their condition, with the possibility of coupling interventions. As shown in step 2 of Fig. 1, based on the last component renovation yeras from the building owner, we utilize the Schroeder method [77,78] to output the range of years ('necessity intervals') for which a component must be retrofitted based on its condition, termed as $intmin_{n,f,p}$ (minimum intervention period) and $intmax_{n,f,p}$ (maximum intervention period) parameters in MANGOret. After the first intervention for each retrofitted component, the deterministic end-of-life approach is taken, formulated in Eq. (A.17).

An example of the two-phase Schroeder degradation method is shown in Fig. 4, based on assumed component condition preferences from Ref. [77]. We specifically focus on Roof, Facade, and Window components due to their large impact on energy demands as shown in Ref. [48], along with existing heating systems and miscellaneous technologies due to their impact on retrofit budgets.

MANGOret chooses the optimal retrofitting schedule for each component based on the 'necessity interval' ranges, considering the techno-economic decision space to align various component retrofits. For example, this would be done to reduce disturbance (by coupling retrofits) or from an economic perspective by saving on projects costs such as scaffolding [76]. In MANGOret, we capture both examples with the preferred alignment of external retrofits. We do so by adding retrofit project cost constraints with scaffolding costs (see Appendix A.5) for when an external Roof and/or Facade retrofit is initiated. The outputs of the Schroeder method for the case study are reported in Table A.7.

2.3. Archetypal energy demand database

Obtaining the required energy demand input data is often a challenging step in optimization models, particularly if high-resolution data (hourly or sub-hourly) is desired [80]. Considering the limited data availability relating to retrofitting packages' energy demands at an hourly resolution, we adopt a similar approach previously conducted for European residential buildings [81] to develop a database with various retrofitting packages for archetypal buildings. The resulting database would allow architects, energy engineers, and asset managers to assess a long-term time series of energy demands for a considered retrofitting package, for any particular building over many building types, along with rich spatial and temporal resolution. As our illustrative case study is based in Switzerland (see Section 3), we utilize the available resources to generate energy demand profiles for a large set of Swiss archetypal buildings, which could be matched to any Swiss address with coordinates, adding to the scalability of the MANGOret framework.

First, we developed building archetypes by utilizing a clustering methodology applied across Swiss government building stock and open source data extracted from multiple databases — the Federal Register of Buildings and Dwellings (GWR) [82], Company Structure Statistics (STATENT) [83], and OpenStreetMap [84]. Since important building-specific parameters such as component areas are typically not available from building owners, we take them from the GWR database [82]. Other information such as building constructions, ages, material properties, etc. are taken from various other sources.

In all, we developed 2124 Swiss building archetypes based on 16 building types, 7 Swiss geographic zones, and 9 age categories shown cartographically in Fig. 5. Our clustering resulted in 1–5 archetypes per category which is a combination of building type, age, and location. The archetypal buildings were then modeled and simulated in a building energy simulation software from the methodology presented in Ref. [48], utilizing the CESAR (Combined Energy Simulation And Retrofitting) tool [85] built on the standard building energy software EnergyPlus [86]. CESAR creates individual EnergyPlus models for each specific building and assigns construction types based on the initially defined age categories. Next, weather files were modified for specific climate change scenarios and years of analysis utilizing a similar set of data generated from Ref. [87]. The resulting buildings were then simulated with weather files for their specific location.

Overall, each archetype was simulated from 2020–2060 in 10-year time-steps with the 11 retrofitting packages (considering two retrofitting depths) for heating, cooling, and electricity demands. We further simulated each archetype over 3 climate change scenarios based on Representative Concentration Pathways (RCPs 2.6°C, 4.5°C, and 8.5°C). For this paper, we utilize a time horizon to 2050 and RCP 2.6°C. The 10-year time-step simulations correspond to a range of years in the model, for example the 2030 profiles accounting for the range of real years 2025–2034. The final output is a temporal, spatial, and retrofit-specific Swiss building energy demand database with an hourly resolution, with the ability to match any Swiss building address to an archetype through the clustering parameters. As an estimation of the particular buildings' aggregate energy demands (keeping the integrity of the profiles), the archetypal energy demands are scaled by the ratio of floor areas between the building of interest and the archetype.

Finally, the energy demand and solar irradiance time-series parameters are clustered using a k-medoids peak + typical day clustering from the approach used in Ref. [88]. For this paper, peak days were used for heating and cooling demands along with 5 typical 'normal' days, resulting in 7 total typical days. An example of the richness of the archetypal demand database is shown in Fig. 6, with the left-side demonstrating the average daily profiles of the retrofitting packages for heating and cooling for example years 2020 and 2040. On the right-side, the average annual heating demands per floor area are presented.
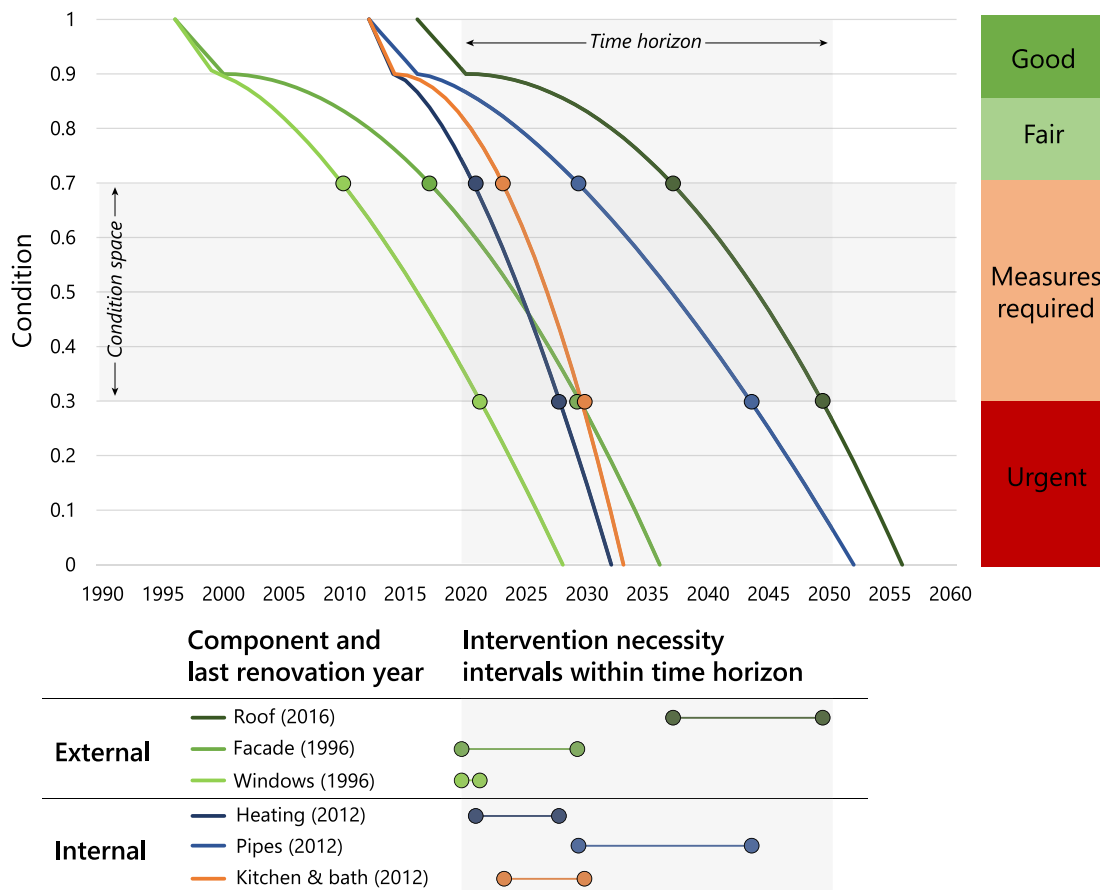
Fig. 4. Example of Schroeder method component degradation curves for the considered set of components. The condition space considered for retrofit 'necessity intervals' is set to 30%–70%. Each component's degradation is based on its last renovation year, expected lifetime, and degradation parameters according to the Schroeder method [79]. When the minimum necessity interval lies before the beginning of the considered time horizon (2021), the interval is set to 2021, as shown for Facade and Windows. Heating technology intervals only apply for existing technologies.

For example, between the extreme scenarios of 'no retrofit' and the $Full_{Tar}$ retrofit (e.g. a deep retrofit with a green building label), heating demands are reduced by over 4 times and cooling demands increase by almost 3 times. The general trend for this building shows that deeper retrofits reduce heating demands while increasing cooling demands. Further information on the database is presented in Appendix A.7.

3. Illustrative case study

3.1. Retrofitting considerations

The portfolio of energy technologies and retrofitting packages considered in MANGOret are shown in the superstructure representation in Fig. 2. The technologies discussed as follows are chosen as part of the illustrative example of the MANGOret optimization framework, with others able to be added.

In terms of conversion technologies, the candidate heating technologies include electrically-driven Air-Source Heat Pumps (ASHP), Ground-Source Heat Pumps (GSHP), fuel oil, natural gas, and biomass boilers, and gas-fired Combined Heat and Power (CHP) engines. The candidate cooling technologies are absorption and compression chillers. In terms of RE technologies, only solar Photovoltaic (PV) panels are considered due to urban constraints. Additionally, Hot Water Thermal Storage Tanks (HWTS) and lithium-ion batteries are considered to store thermal and electrical energy, respectively. D-MES can import all energy carriers but can only export electricity as they are grid connected.

The retrofitting technologies include insulation materials for the Facade and Roof: oil-based XPS and EPS along with mineral stone

wool, and for Windows: plastic and wood-aluminum frames. These retrofitting technologies also have a depth element — the minimum BEC or target green building label. Further, the technologies comprise the various considered retrofitting packages which can be combined towards deeper retrofits (see Section 2.1).

Existing technologies for each building are also included in the model, where applicable. Generally buildings owners lack data on technical system sizes of heating systems, for example fuel oil or gas boilers [15]. Thus, these existing components are modeled as technologies without a pre-determined size. Therefore, for the available set of existing technologies, MANGOret sizes and installs them based on the respective retrofit package demand profile in the beginning of the horizon, without investment cost but with maintenance cost.

In this paper, we utilize 6 model periods with each period representing 5 years for the 30-year horizon. Retrofitting investment stages (w_f) are set at each period, while energy system investment stages (w_{cs}) are set at periods 1, 3, and 5, with additional stages able to be added in the case of existing technology retirement (e.g. natural gas boiler).

3.2. Building case study composition

We apply MANGOret to four case study buildings taken from an LSI portfolio to demonstrate the value of optimal multi-stage D-MES and envelope investment planning with a long-term horizon of 30 years (2021–2050). These four buildings, described in Table 2, were chosen to demonstrate the variety of strategies relevant across building types, sizes, ages, locations, and real estate markets.
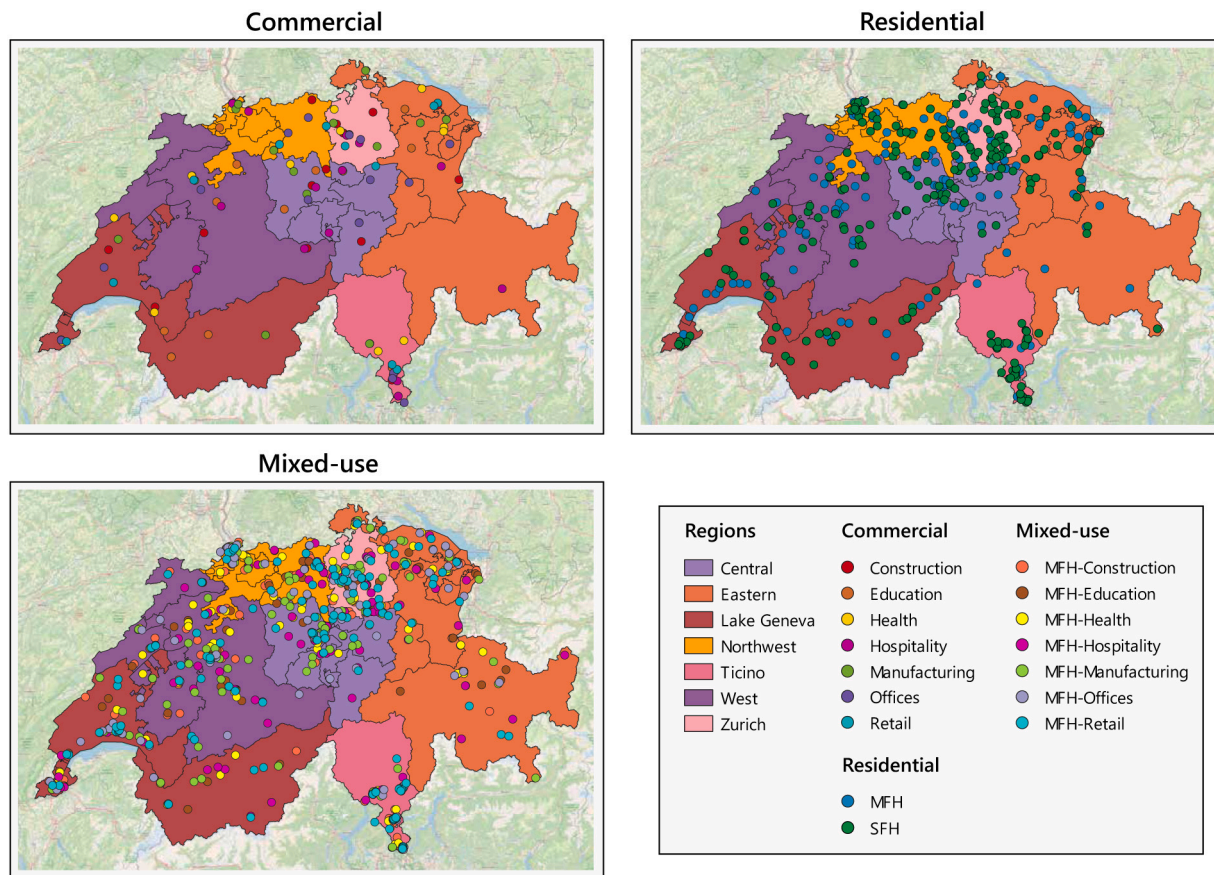
Fig. 5. Location of the Swiss archetype buildings which were simulated in the archetypal energy demand database considering residential (Single Family House (SFH) = 221, Multi-Family House (MFH) = 179), mixed-use (824), and commercial (100 with 9 age categories = 900) building types. The total number of archetypes developed and simulated for the database is 2,124.

Table 2
Building-specific parameters are assumed to be constant over the 30-year time horizon. Floor area corresponds to both gross internal rentable floor area and energy reference area. Solar roof area is assumed to be 80% of roof area. Pipes correspond to number of traditional standing radiators serving an average floor area of 30 m^2. Dynamic real estate markets (e.g. Zurich) are exemplified with higher values for rental escalation than structural vacancy.

Characteristic	Building 1	Building 2	Building 3	Building 4
Building type	Mixed-use	Residential	Residential	Commercial
Location	Zurich	Montreux	Zurich	St. Gallen
Construction year	1859	1964	1938	1967
Floor area (m^2)	1,285	2,727	3,347	8,605
Number of floors (#)	8	6	8	9
Base rent (CHF/m^2)	618	113	185	377
Rent escalation	2%	1%	2%	1%
Structural vacancy	1%	1%	1%	1%
Roof area (m^2)	321	341	669	1448
Solar roof area (m^2)	257	273	536	1,158
Facade area (m^2)	1,178	1,282	3,169	5,443
Window area (m^2)	190	329	465	1,397
Kitchen and bathrooms (#)	12	20	25	96
Pipes (#)	21	45	56	143
Existing heating (remaining life)	Gas (9)	Gas & Oil (12, 4)	Gas (9)	Oil (9)

Building 1 is a mixed-use building in the center of Zurich old-city with retail stores on the lower floor, with private residences and small offices above. Building 2 is a Multi-Family House (MFH) residence in a residential neighborhood in Montreux. Building 3 is a MFH block-style residential property in Zurich city. Building 4 is a large commercial property with retail and office units in St. Gallen. At the beginning of the horizon, all buildings have existing fossil-fueled heating systems (natural gas and/or oil) and do not have any installed RE. All buildings are assumed to have HWTS with a remaining lifetime of 5 years.

Following the steps of the Fig. 1 workflow, in step 1 we gathered relevant contextual aspects about the buildings from the building owner such as the address, construction year, last component renovation years, and base-year rental prices. In step 2, the component renovation years are utilized in the Schroeder retrofit scheduling method to output the intervention necessity intervals for each retrofitting component (see Section 2.2). Next, in step 3, we matched the specific buildings to an archetypal building for which we have energy demand data (see Section 2.3). For each archetypal building in the database, we simulated energy demand profiles for several retrofitting packages and
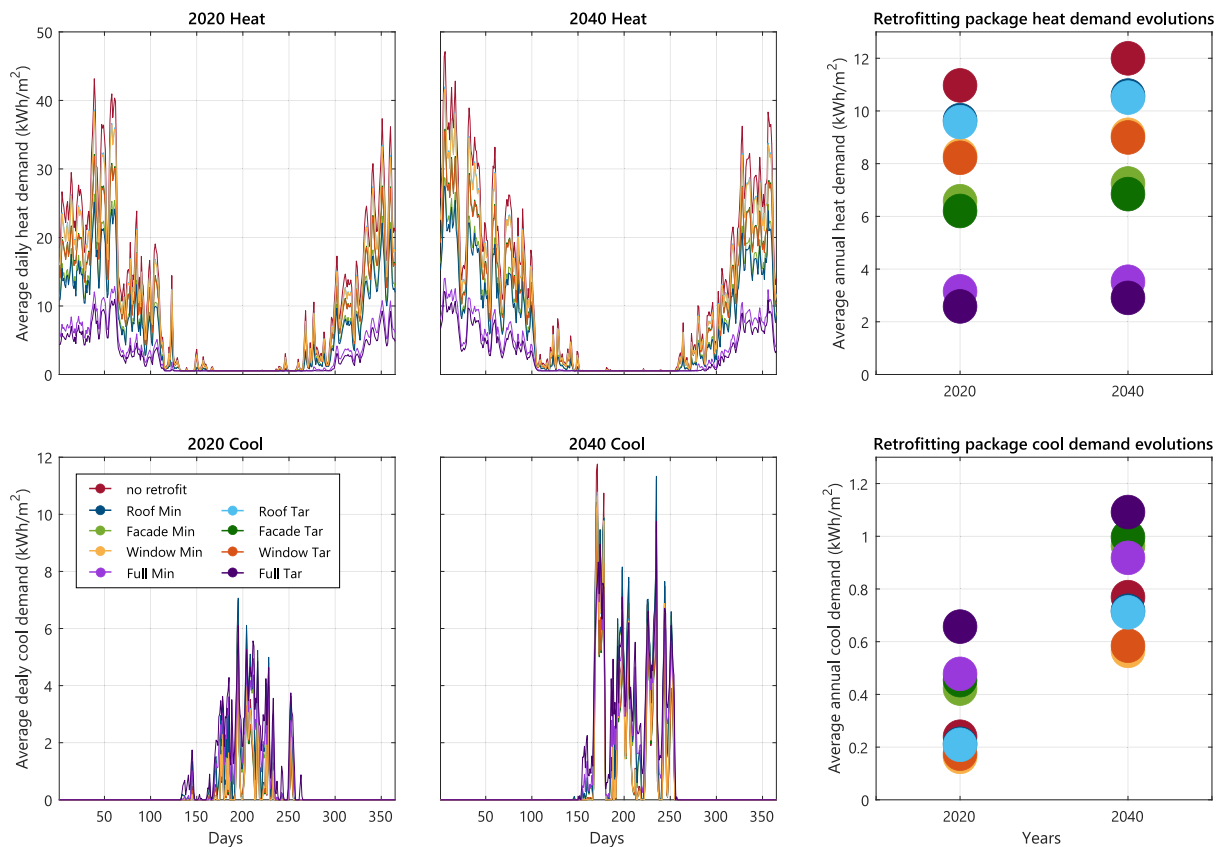
Fig. 6. Example of the simulated retrofitting packages' heating and cooling energy demands per floor area (presented as daily averages for clarity) for a multi-family house archetype in Zurich, Switzerland in the RCP 2.6°C scenario shown for the example years 2020 and 2040. Residential building electricity demands are not shown here as demands from appliances and lighting do not present much variation over the year [85].

retrieved relevant data such as retrofit component areas taken and scaled from Swiss government building statistics databases.

Building-specific parameters were used where possible. Due to limited data availability, for certain parameters constant values were used for the case study such as the discount rate (5%) and inflation rate (1%). Building-specific existing heating system types and their remaining expected service life were acquired from owners, along with market-specific rent escalation and structural vacancy parameters. Further, the Swiss CO$_2$ tax of 96 CHF/tonCO$_2$ is used for fossil fuels (oil and natural gas) as the cost would be passed on to the building owner [89]. All relevant techno-economic and building-specific parameters are reported in Appendix B.

4. Results

In this section, we present the main results of applying the MANGOret optimization framework to the four Swiss building case studies. We highlight the main insights that long-term investment planning of building D-MES and envelope retrofits can offer building sector stakeholders. First, the economic and environmental performance of optimal retrofitting investment strategies are presented in Section 4.1. Second, the cost and emissions trade-offs of technology choices and their investment schedules are discussed in Section 4.2. Third, we present the impact of model periods on optimal results in Section 4.3. Finally, a model discussion is provided in Section 4.4.

4.1. Economic and environmental performance of optimal building retrofitting investments

Fig. 7 presents the four buildings' Pareto fronts on an aggregate (left) and average annual per floor area (right) basis from the cost

vs. CO$_2$ emissions multi-objective optimization. Each aggregate point represents the total emissions and discounted costs of the 30-year optimal strategies. As the selected buildings are assorted by floor area from smallest (Building 1) to largest (Building 4), the aggregate values of cost and emissions follow suit. Overall, as is typical for optimization studies, costs and emissions are such that decreasing the former implies increasing the latter. Further, generally steep increases in cost are observed for the minimum emissions points. However, the same pattern of buildings' size to their aggregate cost and emissions values is not necessarily observed with the average annual per floor area metrics, with all buildings' Pareto fronts lying in similar ranges. Comparing between the two metrics reveals that there could be more attractive cost-effective emissions-reduction opportunities between different buildings.

As a target for existing buildings in 2050, the Swiss Society of Engineers and Architects (SIA) suggests 10 kgCO$_2$/m^2 split halfway between both embodied and operational emissions [90]. In this case study, only some buildings' Pareto points are able to reach this threshold. In fact, all optimal solutions for Building 4 would miss this target. Nevertheless, Building 4 shows the largest potential aggregate reduction in emissions of 510 tCO$_2$ between minimum emissions and minimum cost Pareto points for an overall 10% increase in cost, demonstrated by the 'flat' slope. While the average annual costs per floor area are considerably high for Building 4, nevertheless in the context of the building's retrofitting investments which 'have to be done anyway', such a large aggregate reduction in CO$_2$ could potentially justify the proportional increase in cost.

We provide further granularity on the optimal retrofitting investment strategies for two buildings in Fig. 8 — residential Building 3 (left) and commercial Building 4 (right). These buildings were chosen as they present the most interesting comparison between building types,
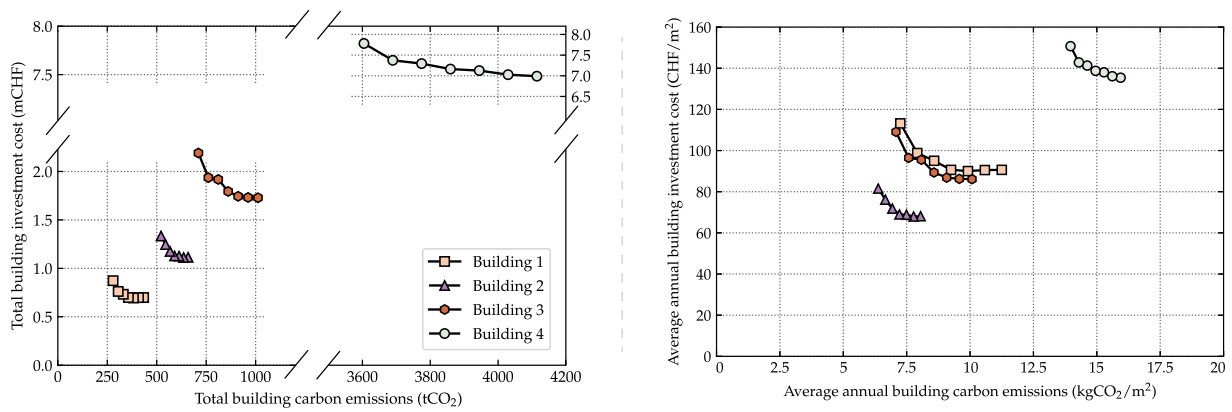
Fig. 7. Pareto fronts illustrating the total building cost and CO_2 emissions in aggregate (left) and average annual per floor area (right) values for the optimal retrofitting investment strategies for the four building case studies. Note the aggregate (left) plot has broken axes on both the x and y due to the large values from the commercial Building 4 in comparison to the other buildings.
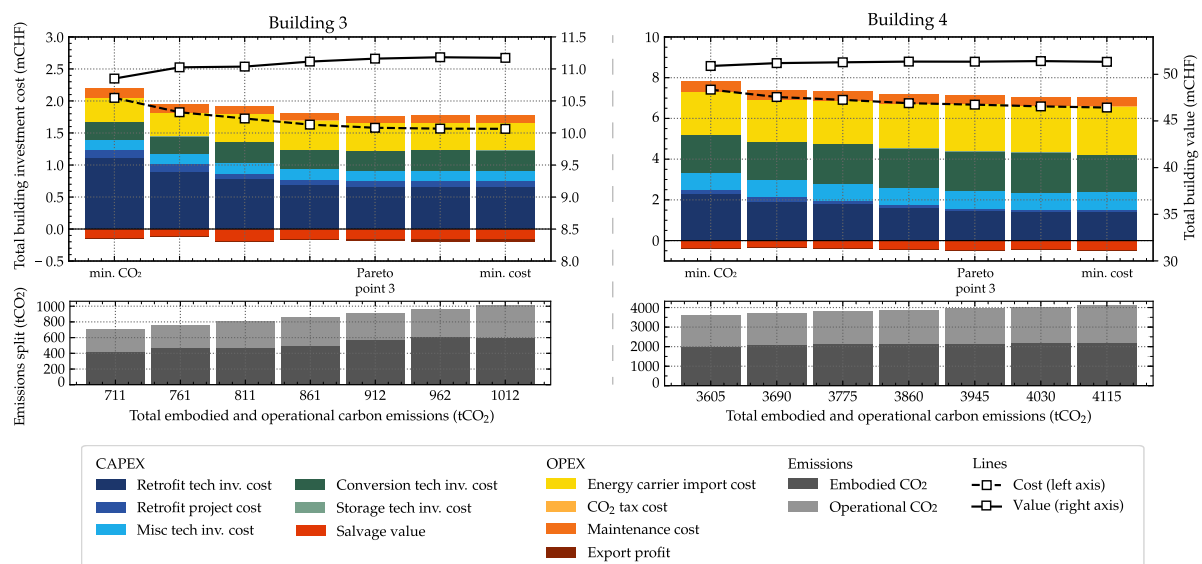

Fig. 8. Pareto front with compositions of investment costs (CAPEX and OPEX) illustrating the total cost and CO_2 emissions for the optimal retrofits for — the residential Building 3 and the commercial Building 4. The solid line signifies the value of the building (right axis) and the dotted line signifies the total cost Pareto front (left axis). The bottom of the figure presents the split between embodied and operational CO_2 emissions.

sizes, along with differentiation between aggregate and average annual per floor area results. Here, the optimal cost Pareto front is shown in the dotted line (left axis) for each Pareto points' CO_2 emission value. We detail the categorical compositions of both capital investment expenditures (CAPEX) and operating expenditures (OPEX) in various colors along with the building values with the solid line (right axis).

The representation in Fig. 8 allows building sector decision-makers to make the following observations for cost, CO_2, and value: (i) the optimal trade-offs for multiple long-term investment strategies demonstrate that achieving low-CO_2 necessitates increased investment costs which subsequently decrease building value, (ii) decreasing CO_2 emissions is primarily driven by increased CAPEX investments into retrofits and miscellaneous technologies even with the subsequently smaller investments in conversion technologies, (iii) decreasing building value in low-CO_2 points is due to the rate of increase of CAPEX investments outweighing the potential value-added revenue increases from rents, and (iv) both embodied and operational emissions decrease in relatively equal proportions over the 30-year horizon for all optimal strategies, with embodied emissions representing the majority.

The novelty presented here for the trade-offs between cost, CO_2, and value are due to the legally-mandated rental formulas (see Eqs. (12)

and (13)). These formulas present legal constraints on rental price increases through value-added investments or otherwise with changing tenant contracts. Building value is calculated by the subtraction of discounted rental income and investments (colors). Between the 'extreme' minimum cost and emissions Pareto points for the example of Building 3, total costs increase by CHF 462k (27% increase in cost between the points) while the discounted rental income increases CHF 138k (1.1% increase in rental income), resulting in a reduced building value of CHF 324k (2.9% decrease in value). The total CO_2 reduction considering both operational and embodied emissions is 301 tCO_2 (30% decrease in emissions) between the extreme Pareto points on both ends of the Pareto front. Notwithstanding value-added investments, we utilize market-based rent escalation and structural vacancy to allow for linear effects relating to tenant turnover, for the example of Building 3 being 2% and 1% respectively.

Achieving low-CO_2 buildings necessitates increased CAPEX investments. While the CAPEX proportion of total investments generally increases in minimum emissions points, nevertheless the proportions vary only slightly. For Building 3's Pareto points, CAPEX costs remain around 70% (OPEX costs are 30%) with a range of $\pm$ 7%. Building 4 shows a similar pattern with CAPEX remaining around 64%

with a range of ± 3%. With further granularity into CAPEX budgets, retrofitting and miscellaneous technologies present a significant portion, ranging from 53% for minimum cost points to 64% in the minimum emissions point. While low-CO_2 points demonstrate smaller investments in conversion technologies due to deeper retrofits, they do not necessarily attain lower OPEX costs. The trade-offs between higher CAPEX costs and emissions to achieve low-CO_2 retrofits could potentially lead to split-incentive issues unless owners can recoup their increased CAPEX investment from the decreased OPEX credited to tenants.

The overall decrease in building value in low-CO_2 points is due to the rate of increase of CAPEX investments outweighing the potential value-added rental revenue increases. Nevertheless, for all buildings the total investment costs over the 30-year horizon present only a portion of the discounted rental income from the first period. In buildings with a higher base rent, the proportion of rents to investments will be much higher thus varying the value of the buildings. This aligns with research stating that retrofitting is profitable in more attractive real estate markets or otherwise with higher pass-on rates [15].

The bottom of Fig. 8 shows the split of embodied and operational CO_2 emissions for each buildings' Pareto points. Interestingly, the optimization decreases both embodied and operational CO_2 emissions in relatively equal proportions for each Pareto point. For Building 3, embodied emissions are around 60% and operational emissions are at 40% with a range of ± 3%, while for Building 4 these values vary marginally. This points to the similar cost trade-offs of both embodied and operational emissions reductions in the optimization problem.

Often in multi-objective optimizations studies, the 'extreme' points in the Pareto are compared to accentuate trade-offs between costs and emissions. Nevertheless, there are solutions in the Pareto front which provide for a more beneficial balance of objectives presenting 'minimal regret' solutions near the minimum cost point. As an example, we run a simple Euclidean distance calculation for the normalized values of the two objectives towards the 'utopia' point at the origin [91]. Such an approach is one way to assure equal weights in the multi-objective function.

We find that for the example of Building 3, Pareto point 3 provides the shortest distance. In comparison, between the minimum cost point and Pareto point 3, we observe an increase in total cost of CHF 15k (0.9% increase in cost between the points), an increased rental income of just CHF 2.4k (0.02% increase in rental income) resulting in a reduced building value of CHF 12k (0.1% decrease in value), and a total CO_2 reduction of 100 tCO_2 (10% decrease in emissions). Using Pareto point 3 versus the minimum cost point thus gives a decision-maker a more 'balanced' multi-objective choice — they must invest a negligible extra amount to achieve a large decrease in emissions. Therefore, we henceforth use Pareto point 3 as a comparison with the minimum emissions point. Relating to the issue of split-incentive issue between building owners' (CAPEX) and tenants' (OPEX) costs in retrofits, the slightly increased costs in Pareto point 3 are largely due increased OPEX which would put more burden on tenants.

4.2. Technology choices and schedules of optimal building retrofitting investments

Fig. 9 presents the building investment cost composition and nominal rental income per floor area for each period for the minimum emissions (top-left) and Pareto point 3 (top-right) strategies for Building 3. This figure simultaneously depicts the answers for the *when* and *what* questions of optimal retrofitting investment strategies relating to various investment categories, along with the revenue side, over the long-term horizon.

In the context of low-CO_2 buildings, we show that to achieve minimum emissions, deep retrofits of all components are conducted as early as possible (in period 1) to reduce energy demands and in turn emissions. In Pareto point 3, along with the minimal cost solution, the optimal solution is to wait 'as long as possible' until the components must be retrofitted due to the condition-based necessity constraints. This is equivalent of the 'real-world' minimum cost approach of retrofitting at component end-of-life which is demonstrated in both minimum cost and Pareto point 3. For the example of Building 3, the component condition degradation methodology (see Section 2.2) dictates that Windows must be retrofitted in period 1 while Facade and Roof must be retrofitted latest in period 3.

On the bottom of the figure we present the difference between the per period cost components of the minimum emissions and Pareto point 3 (bottom-left) along with the total difference over the 30-year horizon (bottom-right). Here, we present clearly that the deeper, earlier retrofits required to achieve minimum emissions subsequently benefit from reduced costs for conversion technologies and energy carrier imports, albeit with the former outweighing the latter greatly. This demonstrates the importance of considering the interdependencies of the demand- and supply-sides of the energy balance in buildings' retrofitting schedules over the long-term horizon. It must be noted that all values presented here are discounted — while the discounted difference between the compared Pareto points' budgets is large due to differing retrofit schedules, the nominal difference is much less.

Regarding rental revenues, Building 3 demonstrates a linear increase of rents due to the market parameters in a dynamic real estate market. The influence of value-added investments (see Eq. (13)) can be seen in the difference graph with positive differences denoting the higher value-added investments of the minimum emissions point, particularly when the deep retrofit is conducted period 1. The total nominal rent is slightly higher in the minimum emissions point but nevertheless the increased investment costs outweigh the discounted rents, and thus the building value decreases.

Similarly to Fig. 9 for the minimum emissions and Pareto point 3 of Building 3, Fig. 10 depicts the answers for the *when* and *what* questions of optimal retrofitting investment strategies relating to specific technologies. The figure is broken into the sections: (top) investment cost evolution for all technologies per period, (middle) contributions of technology embodied emissions per period, and (bottom) operational emissions per period.

Importantly, the optimal technology choices differ between the minimum emission and Pareto point 3 strategies. The higher retrofitting investment costs in the minimum emissions point are due to choosing higher cost, lower embodied emission technologies such as Stonewool and EPS insulation for the Facade and Roof, respectively, along with Wood-Aluminum frame Windows. On the other hand, cost optimal solutions including Pareto point 3 choose the cheapest available options in XPS insulation for Facade and Roof along with plastic frame Windows. Embodied emissions from conversion and storage technologies is dominated by solar PV and less so with the ASHP and compression chiller. Nevertheless, the largest portion of embodied emissions is due to retrofitting and miscellaneous technologies, with all conversion and storage technologies, except for solar PV, contributing minimally to the total. Due to later retrofits, the cost optimal points generally have higher salvage values.

Here we show the importance of capturing embodied emissions for retrofits as they account for a slightly larger proportion than operational emissions across all Pareto points, aligning with the findings of Shadram et al. [92]. It is worth noting that in this paper, we only account for the embodied emissions of non-structural retrofitting components such as Facade and Roof insulation, Windows, kitchens & bathrooms, pipes, conversion, and storage technologies. Nevertheless, the vast majority of embodied emissions are due to the structural components such as concrete, brick, and steel [93] but are not considered in this retrofitting-focused study as the building structure is 'irreversible'.

To achieve minimum emissions, the model minimizes PV installations and associated conversion technologies to smaller capacities
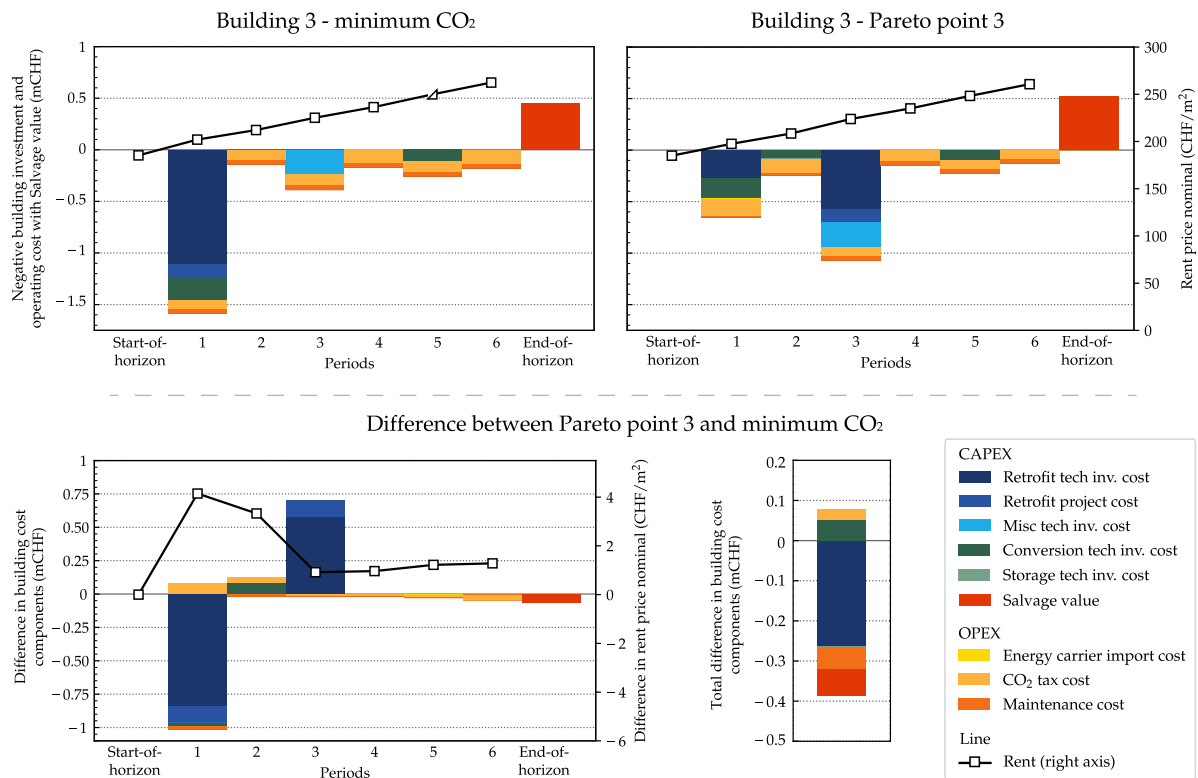
Fig. 9. Compositions of investment cost categories per period represented as negative values, with revenues from salvage as positive, for the minimum emissions (top-left) and Pareto point 3 (top-right) for Building 3. On the right axis, we present the nominal rent per floor area in each period as the positive revenue stream. The bottom of the figure presents the period-by-period difference in investment cost compositions (bottom-left) between Pareto point 3 and the minimum emissions point, along with the total difference over the 30-year horizon (bottom-right).

relative to the cost optimal points due to their high embodied emissions. In the low-CO_2 strategy, the building is primarily heated with an ASHP and solar PV system along with a small biomass boiler for peak demands. All of these technologies are installed in period 1 when the deep retrofit is conducted, with the heating system reinstalled in period 5. Similarly, Pareto point 3 relies on a larger solar PV and ASHP system, further choosing to install and operate the (free) existing gas boiler. In contrast to the minimum emissions point, Pareto point 3 installs solar PV in period 2 and relies on a small fuel oil boiler in period 5 to meet peak demands, albeit it is rarely used. Both strategies show a reliance on compression chillers to meet cooling demands. Batteries are utilized in the CO_2 optimal points, with HWTS being present in both albeit of smaller size in the minimum emissions point.

This presents an interesting new narrative for decarbonizing the building stock, as the optimization model conducts a deep & 'green' retrofit right away to reduce demands and energy system capacities, even of RE technologies (solar PV). The building still relies on the grid due to the constrained roof area for solar PV, with cost optimal points importing a larger amount of electricity. While the hydro and nuclear-dominated Swiss grid has a relatively low life-cycle CO_2 emission factor (see Table B.8) for Europe, potentially with a 'dirtier' grid the optimal operation strategy would decide to reduce reliance on the grid even further. Overall, due to increased sector-coupling and thermal electrification, the decarbonization of the electricity grid is critical for the building sector. While the relative contributions of the above points are specific to Building 3, nevertheless we observe the similar patterns for all buildings.

The technology choices on both the demand- and supply-sides of the energy balance dictate the energy and emissions distributions for the Pareto points. Fig. 11 presents the Pareto points' average annual energy and emissions types per floor area. Similarly to Wu et al. [43], operational emissions are more 'flexible' in their reduction compared

to embodied emissions which innately have discrete choices. This is demonstrated in the 'steps' of the total emissions points due to the contribution of embodied emissions, versus the smoother increase in the operational emissions points. Logically, this is explained by the direct correlation between operational emissions and energy consumption, versus that of embodied emissions which have several choices of retrofitting technologies available per depth.

Our results show that to reduce emissions from existing buildings, both operational and embodied, *necessitates* reductions in energy consumption by investing in deeper & 'greener' envelope retrofits. This is due to the correlation of emissions reductions with energy consumption, demonstrating the importance of considering both the demand- and supply-sides of the building retrofitting investment decision. For the example of comparing Building 3's extreme Pareto points, emissions are reduced 30% (from 10 to 7 kgCO_2/m^2) while energy consumption is reduced 32% (from 69 to 47 kWh/m^2). Further, the increased energy consumption of all buildings relative to their energy demands (from the archetypal energy demand database) are largely due to thermal electrification from heat pumps which dominate heating technology solutions. In the following, we discuss the impact on results of considering various approximations of the long-term temporal resolution through model periods granularity.

4.3. Considerations of periods in the long-term horizon

In this paper, we implement model periods which represent a number of years in order to make the model smaller and faster through drastically reducing variables and binaries. Nonetheless, clustering the temporal resolution into periods presents an approximation of the optimal result versus a 'full' 30 period and year horizon due the inability to track year-to-year variations. Here, we compare technology investments and schedules, along with computational effort, for Building 3's
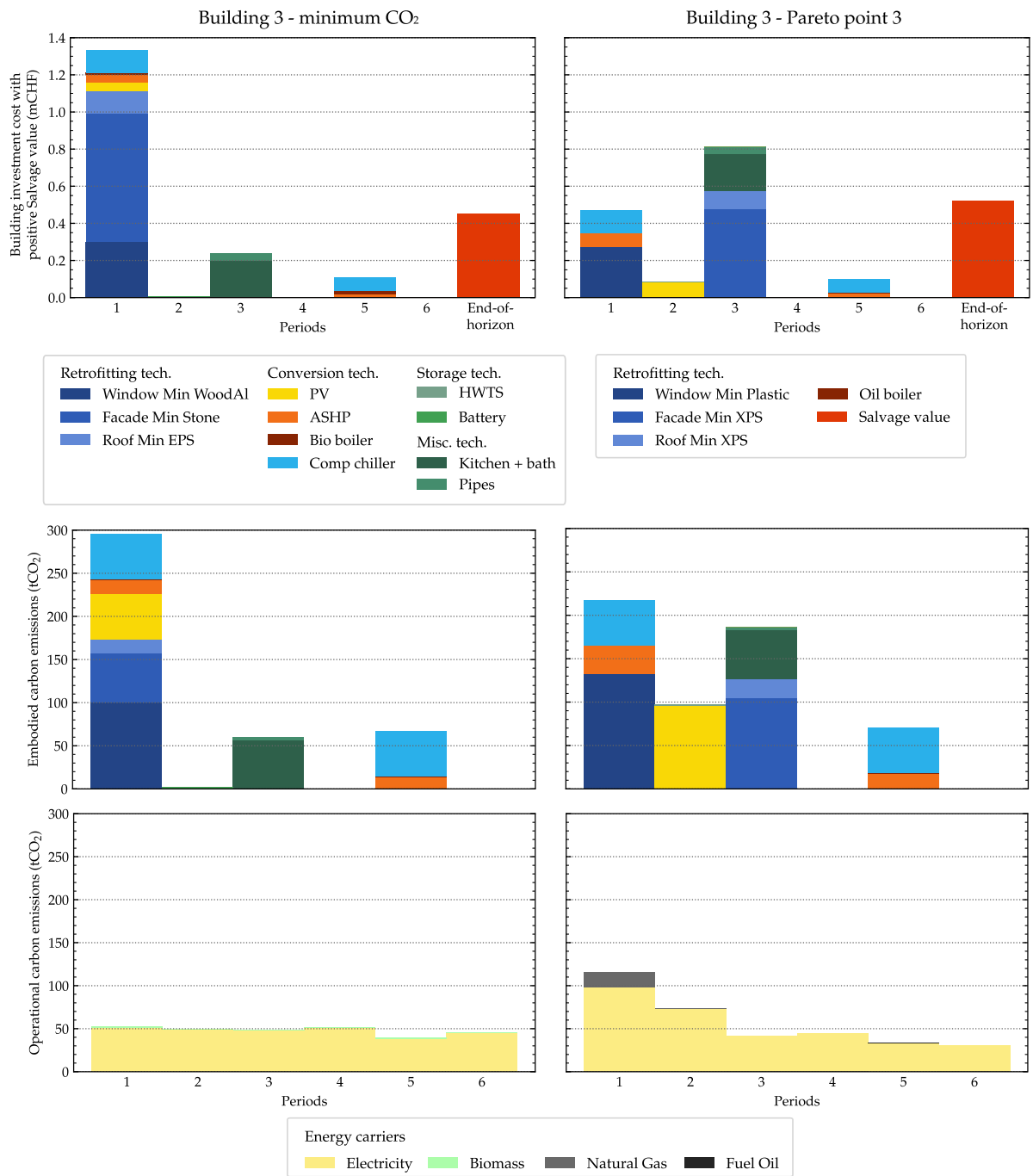
Fig. 10. Compositions of investment costs by technology (top) for the minimum emissions (left) and Pareto point 3 (right) for Building 3. Compositions of embodied missions by technology (middle) are presented in a similar color scheme to the top of the figure. While both strategies share the set of technology choices, there are differences. As such, the legend for Pareto point 3 (right) is updated with the different technology choices which are different from the minimum emissions legend (left). Operational emissions presented in the bottom of the figure.

minimum cost optimization considering 30, 15, and 10 periods along with the base-case of 6 periods presented earlier in the results.

Due to the variations in parameters over the long-term horizon, results in Table 3 show that the chosen number periods significantly influence the design, operation, and scheduling of retrofits and thus the overall objective results. In comparison to the 30 period case, with lower numbers of periods the model results consistently over-estimate costs and building value, and under-estimate CO_2 emissions, likely due to improved accuracy in optimizing for operation-relevant variables (p, d, t) on a year-to-year basis in the minimum cost objective. This is exemplified by the fact that when moving towards higher temporal

granularity (from 6 to 30 periods), the aggregate values and share of operational emissions increases above that of embodied emissions. Importantly, model run time increases exponentially with the 6 period minimum cost optimization taking just over 6 minutes while the 30 periods takes over 60 hours.

Fig. 12 presents the technology design (*what*) and scheduling (*when*) across the four period cases. The cost optimization presents little differences with regards to technology choices between the cases. The only differences are in the 30 period case, in which a small oil boiler is installed in real year 15 and a small battery in real year 26.
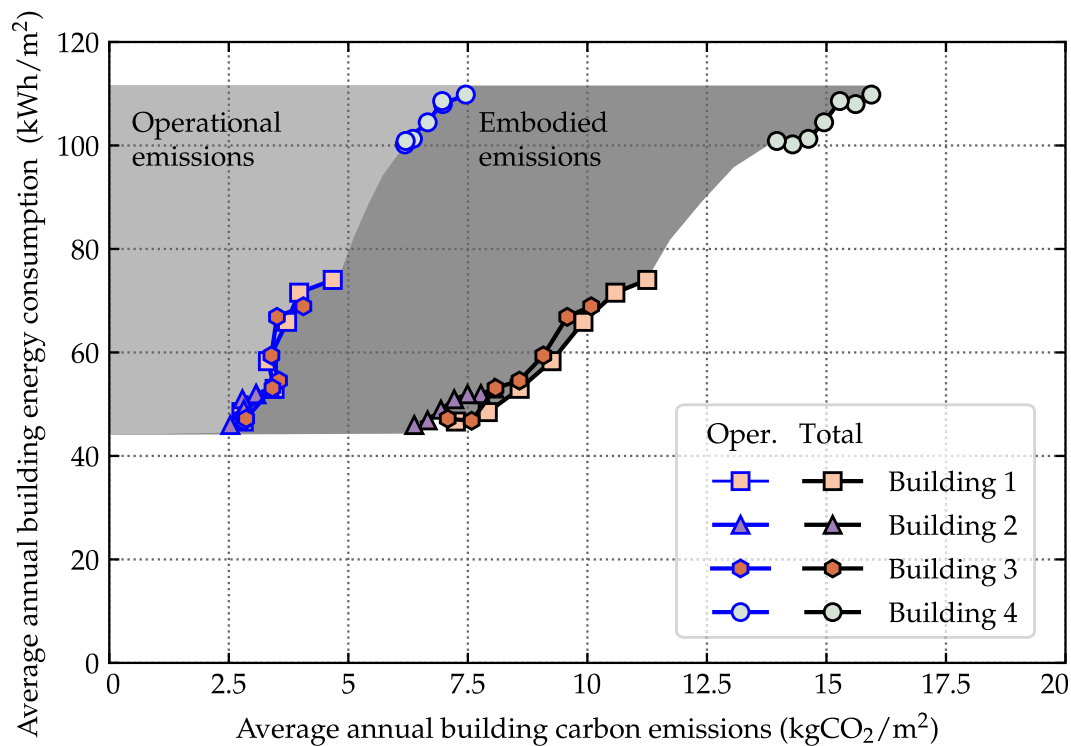
Fig. 11. Average annual energy consumption compared to carbon emissions per floor area for all buildings' Pareto fronts. Total emissions shown in black while operational emissions shown in blue. The composition of operational and embodied emissions are highlighted in gray tones.

Table 3
Comparison of the objective results for the minimum cost optimization for Building 3 over the four period cases. Here, we compare the period scenarios by using 3 system investment stages (w_{cs}) for 6 periods, 6 w_{cs} for 10 and 30 periods, and, 7 w_{cs} for 30 periods. Results show that higher temporal granularity (more periods) improves accuracy on objective function results but exponentially increases solving time.

	6 periods	10 periods	15 periods	30 periods	Diff. 30 vs. 6	Diff. 30 vs. 10
Cost (kCHF)	1,565	1,532	1,473	1,469	−6.14%	−4.11%
Value (kCHF)	11,173	11,033	10,983	10,890	−2.54%	−1.30%
CO_2 (tonCO_2)	1,012	1,008	1,060	1,217	+20.3%	+20.8%
Emb. CO_2 share (%)	59.7%	57.2%	57.3%	50.4%	+1.46%	+5.96%
Oper. CO_2 share (%)	40.3%	42.8%	42.7%	49.6%	+32.5%	+28.7%
Run time (h)	0.11	1.20	4.31	62.5		

The most pronounced difference between the period cases relates to the increased accuracy in scheduling technology installations on a real year basis (y_p). This is likely due to a better accuracy for technological developments along with ability to plan for technology retirements at end of life with higher granularity. For example, the 30 period case installs solar PV in real year 8 (2028) while in the 10 period case, it is installed between real years 1 to 3, in the 15 periods case between real years 7 to 8, and for the 6 period case between real years 6 to 10. Variations are also seen in the installation of the first and second ASHP, along with the Facade, Roof, and kitchen & bathroom internal renovation which is subject to the necessity interval constraints. Here, accuracy continually decreases with the 30 periods case conducting this project in real year 16 while for the 6 periods case it is conducted between real years 11 and 15.

4.4. Model discussion

In this section, we provide our perspective on the added value which the MANGOret optimization framework can bring to energy engineers and building owners. Finally, we discuss limitations of the framework.

As discussed in the Introduction, optimal retrofit investment planning must take into account a long-term horizon considering all technological, economic, and contextual developments relevant to the building. MANGOret incorporates the entire retrofitting decision-space to

give building owners the value of investment flexibility for the energy and non-energy aspects relevant for budgeting. Owners are able to investigate the trade-offs between multiple objectives (*how* to prioritize) for several buildings at once (*where*). Here, MANGOret can develop multiple strategies for any contextual building in a scalable matter by utilizing automated data retrieval and processing steps, a key interest for LSIs who must develop significant numbers of asset-level retrofitting strategies in MYP processes. Both energy engineers and owners are able to answer questions regarding *when* and *what* to do for optimal retrofits considering the interdependencies of scheduling technology investments between the demand- and supply-sides of the building.

The overall goal of presenting the MANGOret framework and model is to provide a methodological contribution to the domains of energy optimization and real estate management. We bridge the gap between predominant methodologies utilized in both domains with a novel methodology for optimal MYP relevant for existing buildings. A key novelty relates to demonstrating the cost, value, and CO_2 emissions trade-offs of optimal investment decisions. This provides important information for owners on both the cost and revenue sides, allowing them to choose an investment strategy based on desired CAPEX budgets, rental revenues, values, and/or CO_2 constraints. Energy-focused retrofitting investment methodologies which do not consider the rental revenue-side of investments could potentially miss strategic trade-offs. Further, we argue that the MANGOret framework and model presents
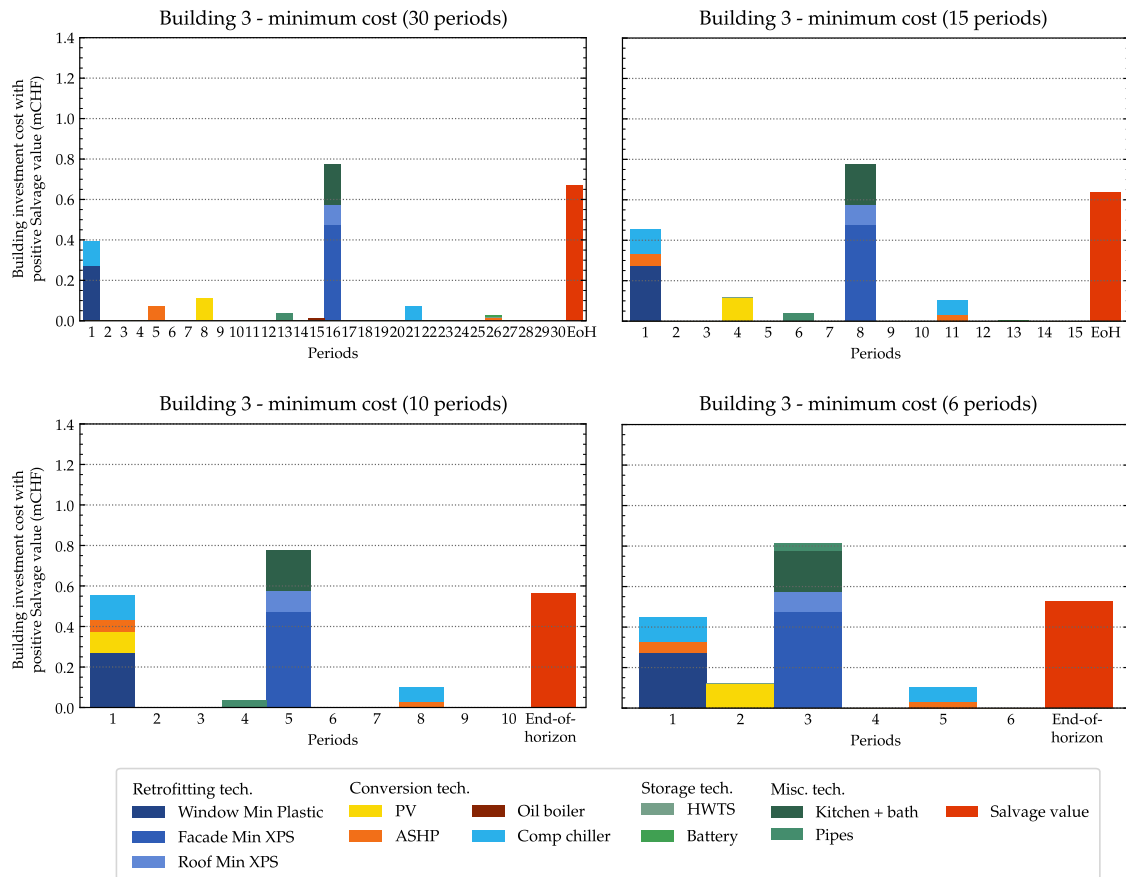
Fig. 12. Compositions of investment costs by technology for the minimum cost optimization for Building 3 over the four period cases. We present the cases of 30 periods (top-left) with each period representing one year, 15 periods (top-right) with each period representing 2 years, 10 periods (bottom-left) with each period representing 3 years, and 6 periods (bottom-right) with each period representing 5 years.

an added-value to meet the needs of reducing existing building energy demands along with both embodied and operational emissions.

While we present the quality of results the model can generate, nevertheless we leave important analyses regarding model sensitivities to parameters for further work. One aspect relevant for rental revenues relates to the legally mandated component pass-on rates which define the extent to which value-added investments can be passed on to the tenant [94].[3] Building owners' preferred choice of the optimal asset retrofitting strategy (output from MANGOret) will likely depend on whether they can achieve a certain expected building value post-retrofit. Therefore, such a legal constraint considerably affects the retrofit decision-making of an economic-driven building owner. Generally for all retrofitting components, Swiss legislation allows for pass-on rates of 50%–70% for value-added retrofits, while rates of heating systems range from 100% for RE-based systems to 0% for fossil-based systems (see Appendix B) [96]. Different values for these legal parameters could therefore significantly change the model results with respect to rental revenues and building values. Here, the issue of rental affordability comes into the frame [15].

While MANGOret presents a novel consideration of the long-term perspective required to adequately plan investments into existing buildings, nonetheless the model outputs a wealth of information relevant

for D-MES such as storage considerations, sector coupling, and RE-integration. As the value of most of these aspects was discussed in MANGO [50], we chose to present the real estate budgeting and planning perspective relevant for building owners and MYP processes. Nevertheless, the MANGOret framework is also relevant for energy engineers in developing early-stage optimal retrofitting design and operation strategies.

Limitations

In this paper, we formulate the long-term retrofitting investment problem in an aggregate manner by combining the cost considerations of owners and tenants into one (the 'building'). Taking such a perspective can be likened to an 'all-in' rental contract where the owner internalizes the OPEX of tenants' energy and water usage (utilities) into the gross rent. However, the utility costs are generally paid separately by tenants and thus not considered in owners' MYP, as they can only pass on investments to the net rent, leading to issues such as the split-incentive [97]. Changing the objective functions to only consider owner-relevant CAPEX costs could potentially change optimal solutions. Nevertheless the question of accounting for costs and emissions between owners and tenants is not considered.

While the MANGOret optimization framework is currently formulated as a deterministic problem with assumed perfect foresight, we imagine it would nevertheless be valuable for real-world retrofit investment planning. In a recent work by Bohlayer et al. the impact of various multi-period optimization under uncertainty approaches were compared [91]. Given the uncertainty present in the model's long-term horizon, MANGOret could be run every few years for each building, aligning with owners' current 5–10 year horizons in their MYP processes [15].

---

[3] In Switzerland, value-enhancing investments and pass-on rates are regulated in Switzerland in Art. 14 VMWG (Additional Services of the Landlord) [94]. According to this article, the building owner has to prove the value increasing share of investments in order to increase net rents. There exist legal uncertainties for whether the owner can increase rents after a tenant leaves, with certain market increases being justifiable [95].

Further, since existing buildings are extremely contextual depending on construction style, the potential of various retrofitting packages' on energy demands and envelope retrofits could vary. We demonstrate MANGOret for the case study of four buildings in Switzerland, generally typified by a solid concrete construction. Nevertheless, the MANGOret framework can be applied to other countries with a different set of input data primarily relating to: the archetypal energy demand database, the government building statistics databases, and the techno-economic database.

5. Conclusions

Situated between the domains of energy optimization and real estate management, this paper presented MANGOret — a novel optimization framework and model for the long-term investment planning of existing building D-MES and envelope retrofits. The three main contributions relate to MANGOret's: (i) scalable, data-driven framework to optimize investments – both energy and non-energy – for any existing building, (ii) long-term retrofitting design solutions, operating strategies, and investment schedules which simultaneously consider the demand- and supply-sides of the retrofit along with both embodied and operational emissions, and (iii) inclusion of important budgeting elements relevant for building owners' multi-year retrofit investment planning such as rental revenues and building value.

First, the contextual nature of existing buildings make retrofit investment planning arduous and time-consuming. To aid in the planning process especially for large numbers of buildings, the model relies on a framework encompassing a series of automated data retrieval and processing steps. Importantly, the framework consists of an archetypal energy demand database connected to various building statistics databases to reference the retrofitting packages' energy demands and buildings' contextual information.

Second, from the energy perspective, the model generates long-term investment strategies considering energy and non-energy technology design, operation, and scheduling. The model is able to consider the interdependent investment and scheduling trade-offs between demand- and supply-side measures for a number of technologies. Further, embodied emissions of all technologies relevant for building sector decarbonization are considered. By considering a 30-year horizon 0 to 2050 for all aspects within the framework, MANGOret is able to harness the strategic value of investment flexibility to optimally phase investments across the multi-objective cost and CO_2 decision space. Third, from the real estate management perspective, the model includes a key novelty relevant for building owners' MYP processes relating to the possible building rental income post-retrofit, formulated from value-added investment regulations. This provides important insights to the additional trade-offs of building value with the traditional cost vs. CO_2 multi-objective optimization. Overall, we show the value of optimal MYP by considering all relevant technologies' cost and emissions contributions over a long-term horizon for a case study of four buildings in Switzerland.

Aligning with previous studies, our results show that higher investment costs are necessary to achieve low-CO_2 retrofits relative to minimum cost strategies. Nevertheless, we show that these trade-offs do not necessarily have to be weighed at the extremes of the Pareto, instead presenting 'minimal regret' solutions in the Pareto front which reduce CO_2 at negligible cost increases. We provide relevant insights for real estate owners by demonstrating the trade-off of decreasing building value with low-CO_2 retrofits largely due to high investment costs outweighing rental revenue increases. While all presented cost and value results in this paper are discounted, the nominal difference between earlier (minimum CO_2) and later retrofits (minimum cost) is smaller than that of the discounted difference. As suggested in previous research, this puts the prominence of the risk-adjusted discount rate into the frame [98].

The increased investment costs in low-CO_2 retrofitting strategies is primarily due to larger CAPEX investments towards deeper & 'greener' envelope retrofits, driven by lower embodied emission technology choices. Non-energy miscellaneous technologies also present an important part of retrofitting budgets. Relating to scheduling, achieving low-CO_2 retrofits is largely due to conducting deeper retrofits at earlier investment stages, subsequently reducing the required investments in conversion technologies due to lower energy demands. Our results demonstrate that optimal emission reductions in buildings necessitate subsequent reductions in energy consumption due to their direct correlation. These results directly contradict studies which argue that decarbonizing supply-side solutions should be prioritized to the expense of EE solutions due to their high costs [99].

This presents a strategic change for owners to retrofit building envelopes before their end-of-life. Here, we highlight the importance of incorporating embodied emissions in D-MES and envelope optimization studies as they encompass the majority of total emissions. This is particularly important for RE technologies such as solar PV which present a large fraction of embodied emissions in our results. Nevertheless, our results reaffirm the present-day attractiveness of grid-connected buildings powered by solar PV and heat pumps, corresponding to a significant portion of solutions.

Future studies should seek to relate multiple asset-level optimal retrofitting strategies together at a portfolio-level relevant for MYP, or otherwise at the district-level if many adjacent buildings relevant for energy planning. Considering portfolios, owners would potentially choose different optimal strategies (Pareto points) between the decision-space of various assets (Pareto front) subject to desired CAPEX budgets, value targets, and/or CO_2 constraints. Further, the influence of various techno-economic and contextual uncertainties, along with policy scenarios, over the long-term horizon could strongly influence results. Efforts to include policy aspects within an optimization modeling framework could give further insights to practitioners and policymakers, with major hurdles being the consideration of building contextuality versus model scalability [100–102]. While this would potentially be computationally expensive to run in such a complex model, it would nevertheless present interesting results for building sector decarbonization. Related to advancing embodied emissions considerations, future studies could integrate material- and technology-level life-cycle analysis data into the considered set of technologies.

CRediT authorship contribution statement

Ivalin Petkov: Conceptualization, Methodology, Software, Formal analysis, Investigation, Data curation, Writing – original draft, Visualization, Funding acquisition. **Georgios Mavromatidis:** Conceptualization, Methodology, Software, Writing – review & editing, Supervision. **Christof Knoeri:** Conceptualization, Methodology, Writing – review & editing, Supervision, Funding acquisition. **James Allan:** Data curation, Software, Writing – review & editing. **Volker H. Hoffmann:** Writing – review & editing, Supervision, Funding acquisition.

Declaration of competing interest

The authors declare that they have no known competing financial interests or personal relationships that could have appeared to influence the work reported in this paper.

Acknowledgments
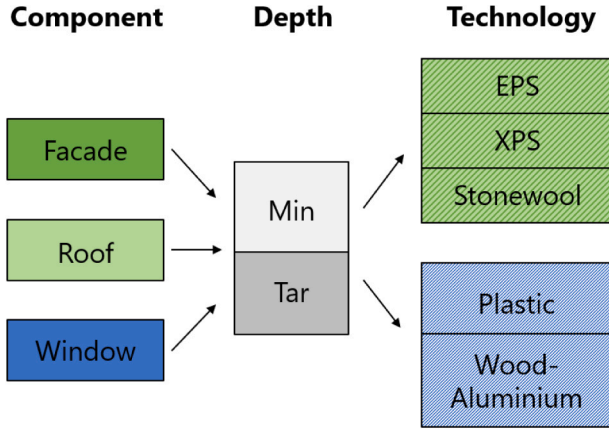
Component   Depth   Technology

Fig. A.13. Relationship between retrofitting components, depths, and technologies.

thank Portia Murray for her assistance on the archetypal energy demand database. All the optimization model runs were performed on the Euler cluster managed by the HPC team at ETH Zurich.

Appendix A. Complete MANGOret model formulation

In this Appendix, the complete formulation of the MANGOret (Multi-scAle eNerGy Optimization — retrofitting) model is presented. As we build on the MANGO model formulation which considers solely D-MES design and operation [50], we have chosen to present only the additional retrofitting aspects unless otherwise necessary.

A.1. Sets

The sets consider the spatial and temporal dimensions of the model as well as the considered energy technologies, retrofitting aspects, and energy carriers. The parameters, variables, and constraints are indexed over the sets described in Table 1. The relationship between the sets of retrofitting components (f), depths (j), and technologies (g) are visually depicted in Fig. A.13.

A.2. Parameters

The model considers a series of technical, economic, environmental and other parameters, which are presented in Tables A.4 and A.5, respectively. The values for the key model parameters used for this paper's case study are given in Appendix B.

The three 'mapping' binary matrices shown in Fig. A.14 allow to create relationships between sets of retrofitting components (f), depths (j), technologies (g), and demand packages (h). The matrices are: (1) $mapcomp_{j,f}$ — the 'raw' retrofitting components (f) which need to retrofitted with a certain retrofitting depth (j) in the first necessity interval, (2) $mapdepth_{g,j}$ — with the retrofitting depth (j) to the selected retrofitting technology (g), and (3) $mapdem_{g,h}$ — with the retrofitting technology (g) and the relevant demand profile (h) taking into account possible combinations leading up to 'full' retrofits.

A.2.1. Parameter definitions

Eqs. (A.1) to (A.4) show the definition of model parameters related to the salvage value of conversion, storage, retrofitting, and miscellaneous technologies salvage value at the end of their lifetime. These are taken from the methodology applied in the TIMES model [103].

$$cslvg_{c,w_{cs}} = \frac{1 - (1 + r_l)^{\max_{p\in P}(p)\cdot|Y_p|+1-w_{cs}-cl_c}}{1 - (1 + r_l)^{-cl_c}},$$

$$\forall\, c \in C,\; w_{cs} \in \mathcal{W} \mid \{w_{cs} \geq \max_{p\in P}(p) + 1 - cl_c\} \tag{A.1}$$

$$sslvg_{s,w_{cs}} = \frac{1 - (1 + r_l)^{\max_{p\in P}(p)\cdot|Y_p|+1-w_{cs}-sl_s}}{1 - (1 + r_l)^{-sl_s}},$$

$$\forall\, s \in S,\; w_{cs} \in \mathcal{W} \mid \{w_{cs} \geq \max_{p\in P}(p) + 1 - sl_s\} \tag{A.2}$$

$$rslvg_{g,w_f} = \frac{1 - (1 + r_l)^{\max_{p\in P}(p)\cdot|Y_p|+1-w_f-gl_g}}{1 - (1 + r_l)^{-gl_g}},$$

$$\forall\, g \in \mathcal{G},\; w_f \in \mathcal{W} \mid \{w_f \geq \max_{p\in P}(p) + 1 - gl_g\} \tag{A.3}$$

$$mslvg_{n,w_f} = \frac{1 - (1 + r_l)^{\max_{p\in P}(p)\cdot|Y_p|+1-w_f-nl_n}}{1 - (1 + r_l)^{-nl_n}},$$

$$\forall\, n \in \mathcal{N},\; w_f \in \mathcal{W} \mid \{w_f \geq \max_{p\in P}(p) + 1 - nl_n\} \tag{A.4}$$

A.3. Decision variables

The model's decision variables are presented in Table A.6. Any time a decision variable ins multiplied by a binary, for the example of $P^{imp}_{ec_i,l,p,d,t}$ and $P^{exp}_{ec_e,l,p,d,t}$ with $Y^{retdem}_{h,l,p}$, we linearize them according to the strategy described on page 84 of Ref. [104].

A.4. Objective functions

In this paper, we utilize two objective functions — the minimization of the lifetime, discounted energy system costs (T^{cost}) and/or CO_2 emissions (T^{CO_2}), presented in the following. Retrofit and miscellaneous technologies are added to the initial (T^{cost}) function presented in MANGO which considers conversion and storage technologies. Further, we add embodied emissions aspects of all conversion, storage, retrofitting, and miscellaneous technologies to the (T^{CO_2}) function. The mathematical definitions of the two objective functions are given in Eqs. (A.5) and (A.6) respectively.

While developing the model, we experimented with a third real estate-relevant objective of maximizing the total lifetime building value (T^{value} — inversely, minimizing the negative of value). The total building value is calculated using a DCF of the total rent income summed over all periods minus the discounted costs of energy system and retrofitting technologies in the respective years. We have chosen not to utilize it in the MANGOret case study due to the difficulties in adequately constraining the model towards real-world parameters. For the example of the value maximization objective, the model chooses to install the largest possible energy system in the balance of decreasing costs and increasing rental revenues with all of the constraints already set forth in the model. Nonetheless, this results in 'unrealistic' energy systems designs which are often too-large for real-world buildings.

$$\min T^{cost} = \sum_{l,w_{cs}} C^{INV,TECH}_{l,w_{cs}} + \sum_{l,w_f} \left(C^{INV,RET}_{l,w_f} + C^{INV,MISC}_{l,w_f} \right)$$
$$+ \sum_{l,p} \left(C^{IMP}_{l,p} + C^{MAINT}_{l,p} - \sum_{l,p} R^{EXP}_{l,p} \right) - \sum_l R^{SLVG}_l \tag{A.5}$$

$$\min T^{CO_2} = \sum_{ec_i,h,p,d,t} \left(P^{imp}_{ec_i,l,p,d,t} \cdot c_{ec_i,p} \cdot nd_{p,d} \right)$$
$$+ \Bigg[\sum_{\substack{c,w_{cs}\\ w_{cs}=p}} \left(NCAP^{conv}_{c,l,w_{cs}} \cdot c_{c,w_{cs}} \right) + \sum_{\substack{s,w_{cs}\\ w_{cs}=p}} \left(NCAP^{stor}_{s,l,w_{cs}} \cdot c_{s,w_{cs}} \right)$$
$$+ \sum_{\substack{n,w_f\\ w_f=p}} \left(Y^{misc}_{n,l,w_f} \cdot misca_{n,l,p} \cdot c_{n,w_f} \right)$$
$$+ \sum_{\substack{j,g,f,w_f\\ w_f=p\\ mapcomp_{j,f}=1\\ mapdepth_{g,j}=1}} \left(Y^{retnew}_{g,l,w_f} \cdot compa_{f,l,p} \cdot c_{g,w_f} \right) \Bigg] \tag{A.6}$$

$$\max T^{value} = \sum_l \left(\sum_p rent_{l,p} \right) - T^{cost} \tag{A.7}$$

Table A.4

Technical, environmental, and other MANGOret model parameters.

Parameter	Unit	Description
Technical parameters		
$dem_{ec_d,h,l,p,d,t}$	[kWh]	Energy demand for energy carrier ec_d, for retrofitting package h, at location l, in period p, day d and time step t
$fa_{l,p}$	[m^2]	Total floor area of building location l in period p
$compa_{f,l}$	[m^2]	Total area available of retrofitting component f (e.g. Facade, Window, Roof) at location l
$rsa_{l,p}$	[m^2]	Total roof area available for solar technologies at location l, in period p
fsa	[–]	Factor for the total floor area available for storage technologies
saf_s	[kWh/m^2]	Factor for storage capacity per unit floor area for storage technology s
$misca_{n,l}$	[–]	Total number of miscellaneous technologies (e.g. number of kitchens, number of radiators) at location l
$max_{c_{dh}}$	[–]	Parameter for the maximum possible number of dispatchable conversion technologies which mainly supply heating
$max_{c_{dc}}$	[–]	Parameter for the maximum possible number of dispatchable conversion technologies which mainly supply cooling
Technology lifetime parameters		
cl_c	[periods]	Lifetime of conversion technology c
sl_s	[periods]	Lifetime of storage technology s
gl_g	[periods]	Lifetime of retrofitting technology g
nl_n	[periods]	Lifetime of miscellaneous technology n
Environmental parameters		
$c_{ec_i,p}$	[kgCO$_2$/kWh]	Carbon emission factor for imported energy carrier ec_i in period p
$c_{c,w_{cs}}$	[kgCO$_2$/kW]	Linear, capacity-dependent embodied carbon emission factor for conversion technology c, in investment stage w_{cs}
$c_{s,w_{cs}}$	[kgCO$_2$/kWh]	Linear, capacity-dependent embodied carbon emission factor for storage technology s, in investment stage w_{cs}
c_{g,w_f}	[kgCO$_2$/m^2]	Linear, size-dependent embodied carbon emission factor for retrofitting technology g, in investment stage w_f
c_{n,w_f}	[kgCO$_2$/unit]	Linear, unit-dependent embodied carbon emission factor for miscellaneous technology n, in investment stage w_f
Other parameters		
y_p	[years]	Real representative years of each period
Y_p	[years]	Number of years representing each period
$nd_{p,d}$	[days]	Number of calendar days represented by each representative day d, in period p
$big\,M$	[–]	"Big M" — Sufficiently large value

Table A.5

Economic MANGOret model parameters. Fixed, linear, and maintenance costs of conversion and storage technologies are kept the same as in the original MANGO model formulation.

Parameter	Unit	Description
$i_{ec_i,p}$	[CHF/kWh]	Price for importing energy carrier ec_i, in period p
$e_{ec_e,p}$	[CHF/kWh]	Compensation for exporting energy carrier ec_e, in period p
$fc^{conv}_{c,w}$	[CHF]	Fixed cost for the installation of conversion technology c, in investment stage w_{cs}
$lc^{conv}_{c,w}$	[CHF/kW]	Linear, capacity-dependent cost for the installation of conversion technology c, in investment stage w_{cs}
$fc^{stor}_{s,w}$	[CHF]	Fixed cost for the installation of storage technology s, in investment stage w_{cs}
$lc^{stor}_{s,w}$	[CHF/kWh]	Linear, capacity-dependent cost for the installation of storage technology s, in investment stage w_{cs}
fc^{ret}_{g,w_f}	[CHF]	Fixed cost for the installation of retrofitting technology g, in investment stage w_f
lc^{ret}_{g,w_f}	[CHF/m^2]	Linear, size-dependent cost for the installation of retrofitting technology g, in investment stage w_f
$proj^{ret}_{g,w_f}$	[CHF]	Retrofitting project fixed cost (e.g. scaffolding) for the installation of retrofitting technology g which are relevant for scaffolding (e.g. facade and Roof), in investment stage w_f
fc^{misc}_{n,w_f}	[CHF]	Fixed cost for the installation of miscellaneous technology n, in investment stage w_f
lc^{misc}_{n,w_f}	[CHF/m^2]	Linear, size-dependent cost for the installation of miscellaneous technology n, in investment stage w_f
om^{conv}_c	[–]	Parameter used to calculate the annual maintenance cost for conversion technology c as a fraction of its total investment cost
om^{stor}_s	[–]	Parameter used to calculate the annual maintenance cost for storage technology s as a fraction of its total investment cost
om^{ret}_g	[–]	Parameter used to calculate the annual maintenance cost for retrofitting technology g as a fraction of its total investment cost
om^{misc}_n	[–]	Parameter used to calculate the annual maintenance cost for miscellaneous technology n as a fraction of its total investment cost
$cslvg_{c,w_{cs}}$	[–]	Salvage percentage of initial investment cost for conversion technology c that was installed in stage w_{cs} and has not reached the end of its lifetime at the end of the model horizon (Defined for: $\{w_{cs} \geq \max_{p \in P}(p) + 1 - cl_c\}$)
$sslvg_{s,w_{cs}}$	[–]	Salvage percentage of initial investment cost for storage technology s — same formula applies as for $cslvg_{c,w_{cs}}$
$rslvg_{g,w_f}$	[–]	Salvage percentage of initial investment cost for retrofitting technology g that was installed in stage w_f and has not reached the end of its lifetime at the end of the model horizon (Defined for: $\{w_f \geq \max_{p \in P}(p) + 1 - gl_g\}$)
$mslvg_{n,w_f}$	[–]	Salvage percentage of initial investment cost for miscellaneous technology n — same formula applies as for $rslvg_{g,w_f}$
$baserent_l$	[CHF/m^2]	Base rent for location l at the beginning of the horizon
$maxrent_{l,p}$	[CHF/m^2]	Maximum market rent feasible to be charged (taken as the 90% quantile at the beginning of the horizon in the relevant ZIP code) for location l, in period p
$rentescal_{l,p}$	[–]	Rent escalation parameter depending on market attractiveness for location l, in period p
$structvaca_{l,p}$	[–]	Structural vacancy parameter depending on market attractiveness for location l, in period p
$passon_{c,s,g,n}$	[–]	Pass-on cost for conversion (c), storage (s), retrofitting (g), and miscellaneous (n) technologies as a fraction of their total investment cost
$intmin_{n,f,p}$	[–]	Minimum necessity interval period (lower bound) for miscellaneous technologies (n) and retrofitting components (f) for location l
$intmax_{n,f,p}$	[–]	Maximum necessity interval period (upper bound) for miscellaneous technologies (n) and retrofitting components (f) for location l
$mapcomp_{j,f}$	[–]	Binary matrix of retrofitting depths (j) to retrofitting components (f)
$mapdepth_{g,j}$	[–]	Binary matrix of retrofitting technologies (g) to retrofitting depths (j)
$mapdem_{g,h}$	[–]	Binary matrix of retrofitting technologies (g) to retrofitting technology demands (h)
r_l	[–]	Building-specific discount rate

		Retrofitting component (f)	Retrofitting technology (g)																
			Façade						Window				Roof						noretrofit
			Façade Min			Façade Tar			Window Min		Window Tar		Roof Min			Roof Tar			
			EPS	XPS	Stonewool	EPS	XPS	Stonewool	Plastic	Wood-Al	Plastic	Wood-Al	EPS	XPS	Stonewool	EPS	XPS	Stonewool	
Retrofitting package (h)	Retrofitting depth (j)	Façade Min																	
		Façade Tar																	
		Window Min																	
		Window Tar																	
		Roof Min																	
		Roof Tar																	
		noretrofit																	
		Window-Façade Min																	
		Full Min																	
		Window-Façade Tar																	

Fig. A.14. The three binary mapping matrices $mapcomp_{j,f}$, $mapdepth_{g,j}$, $mapdem_{g,h}$ conceptually depicted in one matrix with black boxes representing 1's and white boxes representing 0's.

Table A.6
MANGOret model decision variables.

Parameter	Unit	Description
Energy system operation		
$P^{conv}_{c,l,w,p,d,t}$	[kWh]	Input energy to conversion technology c, installed at energy system location l, in investment stage w, and operating in period p, day d, and time step t (Defined for: $\{y \geq w$ and $p \leq w + cl_c - 1\}$)
$P^{imp}_{ec_i,l,p,d,t}$	[kWh]	Import of energy carrier ec_i, at energy system location l, in period p, day d, and time step t
$P^{exp}_{ec_e,l,p,d,t}$	[kWh]	Exported energy of energy carrier ec_e, at energy system location l, in period p, day d, and time step t
Energy system design		
$NCAP^{conv}_{c,l,w_{cs}}$	[kW, m²]	New capacity of conversion technology c, installed at location l, in investment stage w_{cs}
$NCAP^{stor}_{s,l,w_{cs}}$	[kWh]	New capacity of storage technology s, installed at location l, in investment stage w_{cs}
$Y^{conv}_{c,l,w_{cs}}$	[–]	Binary variable denoting the installation of new capacity of conversion technology c, at location l, in investment stage w_{cs}
$Y^{stor}_{s,l,w_{cs}}$	[–]	Binary variable denoting the installation of new capacity of storage technology s, at location l, in investment stage w_{cs}
Retrofitting aspects		
Y^{retnew}_{g,l,w_f}	[–]	Binary variable denoting the installation of new capacity of a retrofitting technology g, at location l, in investment stage w_f
$Y^{retactive}_{g,l,p}$	[–]	Binary variable denoting the active retrofitting technology g, at location l, in period p
$Y^{retoccur}_{l,w_f}$	[–]	Binary variable representing the change of the retrofitting package at location l, in investment stage w_f
$Y^{retoccur_{scaff}}_{l,w_f}$	[–]	Binary variable representing the change of the retrofitting package at location l, in investment stage w_f relevant for project costs such as scaffolding
$Y^{retdem}_{h,l,p}$	[–]	Binary variable representing the change of the retrofitting package h, at location l, in period p
Y^{misc}_{n,l,w_f}	[–]	Binary variable denoting the installation of new capacity of miscellaneous technology n, at location l, in investment stage w_f
Cost and emission performance		
T^{cost}	[CHF]	Total lifetime cost for energy systems and retrofits
T^{CO_2}	[kgCO₂]	Total lifetime energy system CO_2 emissions
T^{value}	[CHF]	Total lifetime value of building (location l), defined as the sum of discounted rental income over the horizon, minus discounted total cost of energy systems and retrofits
$rent_{l,p}$	[CHF]	Rent per period for location l, in period p
$VAI_{l,p}$	[CHF]	Value-added investment portion per period supplemented to the rent for location l, in period p
$C^{IMP}_{l,p}$	[CHF]	Total cost due to energy carrier imports at location l, in period p
$C^{MAINT}_{l,p}$	[CHF]	Total maintenance cost for all conversion, storage, retrofitting, and miscellaneous technologies installed at location l, in period p
$C^{INV}_{l,w}$	[CHF]	Total investment cost for conversion and storage technologies (TECH) along with retrofitting technologies (RET) and miscellaneous technologies (MISC) installed at location l, in investment stages w_{cs} and w_f, respectively
$R^{EXP}_{l,p}$	[CHF]	Total income due to energy carrier exports at location l, in period p
R^{SLVG}_{l}	[CHF]	Salvage value of all conversion, storage, retrofitting, and miscellaneous technologies at location l not reaching the end of their lifetime at the end of the model horizon

The T^{cost} objective is composed of summation terms including the investment costs for energy technologies ($C^{INV,TECH}_{l,w_{cs}}$), retrofitting technologies ($C^{INV,RET}_{l,w_f}$), and miscellaneous technologies ($C^{INV,MISC}_{l,w_f}$) at each location l and investment stages w_{cs} and w_f, the energy carrier import costs ($C^{IMP}_{l,p}$), maintenance costs ($C^{MAINT}_{l,p}$) and revenues due to energy carrier exports ($R^{EXP}_{l,p}$) at each location l and period p, and, finally, the salvage value at each building location l at the end of the model horizon due to technologies not reaching the end of their lifetime (R^{SLVG}_{l}). Definitions for these terms are given in Eqs. (A.8) to (A.14).

Note that all cost terms are discounted to present value using the building-specific discount rate r_l. Cost terms pertaining to investment expenditure are assumed to occur at the beginning of the investment stage, hence, the exponent $w_{cs} - 1$ or $w_f - 1$, for energy system, retrofitting, and miscellaneous technologies respectively, in the discounting term of Eqs. (A.8) to (A.10). The same applies to the salvage revenue term (R^{SLVG}_{l}) with the discounting term using the term $|Y_p|$

which denotes the cardinality of the set, in this case refers to the number of years representing each period.

Due to the addition of model periods representing multiple years at once, discounting is altered from the original MANGO formulation for model decision variables C^{IMP}, C^{MAINT}, and R^{EXP}. Here, we discount based on the real year of consideration in each period by discounting for all elements of exponent i from all real years y_p to $y_p + |Y_p| - 1$.

$$
\begin{aligned}
C^{INV,TECH}_{l,w_{cs}} = & \sum_c \left[lc^{conv}_{c,w_{cs}} \cdot NCAP^{conv}_{c,l,w_{cs}} + fc^{conv}_{c,w_{cs}} \cdot Y^{conv}_{c,l,w_{cs}} \right] \cdot \frac{1}{(1+r_l)^{w_{cs}-1}} \\
& + \sum_s \left[lc^{stor}_{s,w_{cs}} \cdot NCAP^{stor}_{s,l,w_{cs}} + fc^{stor}_{s,w_{cs}} \cdot Y^{stor}_{s,l,w_{cs}} \right] \\
& \cdot \frac{1}{(1+r_l)^{w_{cs}-1}}, \ \forall \ l \in \mathcal{L}, \ w_{cs} \in \mathcal{W}
\end{aligned}
$$

(A.8)

$$
\begin{aligned}
C_{l,w_f}^{INV,RET} = & \sum_g \left[fc_{g,w_f}^{ret} \cdot Y_{g,l,w_f}^{retnew} \right] \cdot \frac{1}{(1+r_l)^{w_f-1}} \\
& + \sum_{\substack{j,g \\ mapcomp_{j,f}=1 \\ mapdepth_{g,j}=1}} \left[lc_{g,w_f}^{ret} \cdot Y_{g,l,w_f}^{retnew} \cdot compa_{f,l,p} \right] \cdot \frac{1}{(1+r_l)^{w_f-1}} \\
& + \sum_f \left[proj_{g,w_f}^{ret} \cdot Y_{l,w_f}^{retoccur_{scaff}} \cdot compa_{f,l,p} \right] \cdot \frac{1}{(1+r_l)^{w_f-1}}, \\
& \forall \, l \in \mathcal{L}, \, w_f \in \mathcal{W}
\end{aligned}
\tag{A.9}
$$

$$
\begin{aligned}
C_{l,w_f}^{INV,MISC} = & \sum_g \left[fc_{n,w_f}^{misc} \cdot Y_{n,l,w_f}^{misc} \right] \cdot \frac{1}{(1+r_l)^{w_f-1}} \\
& + \sum_g \left[lc_{n,w_f}^{misc} \cdot Y_{n,l,w_f}^{misc} \cdot misca_{n,l,p} \right] \cdot \frac{1}{(1+r)^{w_f-1}}, \\
& \forall \, l \in \mathcal{L}, \, w_f \in \mathcal{W}
\end{aligned}
\tag{A.10}
$$

$$
C_{l,p}^{IMP} = \sum_{ec_i,d,t} \left[P_{ec_i,l,p,d,t}^{imp} \cdot i_{ec_i,p} \cdot nd_{p,d} \right] \cdot |Y_p| \cdot \sum_{i=y_p}^{y_p+|Y_p|-1} \frac{1}{(1+r_l)^i}, \, \forall \, l \in \mathcal{L}, \, p \in \mathcal{P}
\tag{A.11}
$$

$$
\begin{aligned}
C_{l,p}^{MAINT} = & \sum_{\substack{c,w_{cs} \\ p \geq w_{cs} \\ p \leq w_{cs}+cl_c-1}} \left[lc_{c,w_{cs}}^{conv} \cdot NCAP_{c,l,w_{cs}}^{conv} + fc_{c,w_{cs}}^{conv} \cdot Y_{c,l,w_{cs}}^{conv} \right] \\
& \cdot om_c^{conv} \cdot |Y_p| \cdot \sum_{i=y_p}^{y_p+|Y_p|-1} \frac{1}{(1+r_l)^i} \\
& + \sum_{\substack{s,w_{cs} \\ p \geq w_{cs} \\ p \leq w_{cs}+sl_s-1}} \left[lc_{s,w_{cs}}^{stor} \cdot NCAP_{s,l,w_{cs}}^{stor} + fc_{s,w_{cs}}^{stor} \cdot Y_{s,l,w_{cs}}^{stor} \right] \\
& \cdot om_s^{stor} \cdot |Y_p| \cdot \sum_{i=y_p}^{y_p+|Y_p|-1} \frac{1}{(1+r_l)^i} \\
& + \sum_{\substack{j,g,f,w_f \\ p \geq w_f \\ p \leq w_f+gl_g-1 \\ mapcomp_{j,f}=1 \\ mapdepth_{g,j}=1}} \left[lc_{g,w_f}^{ret} \cdot Y_{g,l,w_f}^{retnew} \cdot compa_{f,l,p} + fc_{g,w_f}^{ret} \cdot Y_{g,l,w_f}^{retnew} \right] \\
& \cdot om_g^{ret} \cdot |Y_p| \cdot \sum_{i=y_p}^{y_p+|Y_p|-1} \frac{1}{(1+r_l)^i} \\
& + \sum_{\substack{n,w_f \\ p \geq w_f \\ p \leq w_f+nl_n-1}} \left[lc_{n,w_f}^{misc} \cdot Y_{n,l,w_f}^{misc} \cdot misca_{n,l,p} + fc_{n,w_f}^{misc} \cdot Y_{n,l,w_f}^{misc} \right] \\
& \cdot om_n^{misc} \cdot |Y_p| \cdot \sum_{i=y_p}^{y_p+|Y_p|-1} \frac{1}{(1+r_l)^i}, \, \forall \, l \in \mathcal{L}, \, p \in \mathcal{P}
\end{aligned}
\tag{A.12}
$$

$$
R_{l,p}^{EXP} = \sum_{ec_e,d,t} \left[P_{ec_e,l,p,d,t}^{exp} \cdot e_{ec_e,p} \cdot nd_{p,d} \right] \cdot |Y_p| \cdot \sum_{i=y_p}^{y_p+|Y_p|-1} \frac{1}{(1+r_l)^i}, \, \forall \, l \in \mathcal{L}, \, p \in \mathcal{P}
\tag{A.13}
$$

$$
\begin{aligned}
R_l^{SLVG} = & \sum_{\substack{c,w_{cs} \\ w_{cs} \geq |\mathcal{Y}|-cl_c+1}} \left[lc_{c,w_{cs}}^{conv} \cdot NCAP_{c,l,w_{cs}}^{conv} + fc_{c,w_{cs}}^{conv} \cdot Y_{c,l,w_{cs}}^{conv} \right] \\
& \cdot cslvg_{c,w_{cs}} \cdot \frac{1}{(1+r_l)^{|Y_p|}} \\
& + \sum_{\substack{s,w_{cs} \\ w_{cs} \geq |\mathcal{Y}|-sl_s+1}} \left[lc_{s,w_{cs}}^{stor} \cdot NCAP_{s,l,w_{cs}}^{stor} + fc_{s,w_{cs}}^{stor} \cdot Y_{s,l,w_{cs}}^{stor} \right] \\
& \cdot sslvg_{c,w_{cs}} \cdot \frac{1}{(1+r_l)^{|Y_p|}} \\
& + \sum_{\substack{j,g,f,w_f \\ p \geq w_f \\ p \leq w_f+gl_g-1 \\ mapcomp_{j,f}=1 \\ mapdepth_{g,j}=1}} \left[lc_{g,w_f}^{ret} \cdot Y_{g,l,w_f}^{retnew} \cdot compa_{f,l,p} + fc_{g,w_f}^{ret} \cdot Y_{g,l,w_f}^{retnew} \right] \\
& \cdot rslvg_{g,w_f} \cdot \frac{1}{(1+r_l)^{|Y_p|}} \\
& + \sum_{\substack{n,w_f \\ p \geq w_f \\ p \leq w_f+nl_n-1}} \left[lc_{n,w_f}^{misc} \cdot Y_{n,l,w_f}^{misc} \cdot misca_{n,l,p} + fc_{n,w_f}^{misc} \cdot Y_{n,l,w_f}^{misc} \right] \\
& \cdot mslvg_{n,w_f} \cdot \frac{1}{(1+r_l)^{|Y_p|}}, \\
& \forall \, l \in \mathcal{L}, \, p \in \mathcal{P}
\end{aligned}
\tag{A.14}
$$

A.5. Constraints

A.5.1. Retrofitting energy balance

Eq. (A.15) describes how the energy demands of the end-users at the different locations are met at each time step of the model via energy imports, conversion, storage charging and discharging, while also allowing for exports. Note that the main retrofitting-relevant change from MANGO includes the addition of the binary variable $Y_{h,l,p}^{retdem}$ which denotes which retrofitting packages' energy demand should be used.

$$
\begin{aligned}
\sum_h dem_{ec_d,h,l,p,d,t} \cdot Y_{h,l,p}^{retdem} = & P_{ec_i,l,p,d,t}^{imp} \\
& + \sum_{\substack{c,w_{cs} \\ p \geq w_{cs} \\ p \leq w_{cs}+cl_c-1}} \left(P_{c,l,w_{cs},p,d,t}^{conv} \cdot \eta_{c,ec,w_{cs}}^{conv} \cdot cdeg_{c,ec,w_{cs},p} \right) \\
& + \sum_{\substack{s,w_{cs} \\ p \geq w_{cs} \\ p \leq w_{cs}+sl_s-1}} \left[stc_{s,ec} \cdot (Q_{s,l,w_{cs},p,d,t}^{dis} - Q_{s,l,w_{cs},p,d,t}^{ch}) \right] \\
& - P_{ec_e,l,p,d,t}^{exp} \\
& \forall \, ec \in \mathcal{EC}, \, l \in \mathcal{L}, \, p \in \mathcal{P}, \, d \in \mathcal{D}, \, t \in \mathcal{T}
\end{aligned}
\tag{A.15}
$$

A.5.2. Retrofitting-relevant constraints

This section outlines the remaining retrofitting-relevant constraints used in the MANGOret model not described in the manuscript. Eqs. (A.16) and (A.17) outline the remaining constraints relating to the model's retrofitting functionality. Next, Eqs. (A.18) to (A.27) outline all constraints relevant to the number and/or sizing of conversion, storage, or miscellaneous technologies.

Eq. (A.16) mandates that a miscellaneous technology must be active (= 1) in any given year through the summation of Y^{misc}.

$$
\sum_{\substack{w_f \\ w_f \geq intmin_{n,p} \\ w_f \leq intmax_{n,p}}} Y_{n,l,w_f}^{misc} = 1,
\tag{A.16}
$$

$$
\forall \, n \in \mathcal{N}, \, l \in \mathcal{L}
$$

The 'retrofit continuity constraint' in Eq. (A.17) assures that another retrofit (based on component lifetime) is conducted in all further intervals after the first necessity interval, representing the deterministic approach for scheduling.

$$Y_{g,l,w_f}^{retnew} \geq \left(Y_{g,l,w_f}^{retnew} - gl_g \right)$$
$$\forall g \in \mathcal{G}, \, l \in \mathcal{L}, w_f \in \mathcal{W} \mid \{w_f - gl_g \geq 1\} \tag{A.17}$$

Next, we constrain the model for both the number and/or capacity sizing of conversion, storage, and miscellaneous technologies. This is necessary in order to prevent the model from over-installing technologies. First, we define two constraints in Eq. (A.18) that both existing conversion and storage technologies can only be installed in year 1.

$$Y_{c_{ext},l,w_{cs}}^{conv} = 0 \quad \text{AND} \quad Y_{s_{ext},l,w_{cs}}^{stor} = 0 \mid \{w_{cs} \neq 1\}$$
$$Y_{c_{ext},l,w_{cs}}^{conv} \leq 1 \quad \text{AND} \quad Y_{s_{ext},l,w_{cs}}^{stor} \leq 1 \mid \{w_{cs} = 1\},$$
$$\forall c_{ext} \in C, s_{ext} \in S, l \in \mathcal{L}, w_{cs} \in \mathcal{W} \tag{A.18}$$

In Eqs. (A.19) and (A.20), we define the maximum number of heating and cooling dispatchable technologies allowed to be alive in a given period, respectively, based on real-world real estate management constraints.

$$\sum_{\substack{c_{dh},w_{cs} \\ p \geq w_{cs} \\ p \leq w_{cs}+cl_c-1}} Y_{c_{dh},l,w_{cs}}^{conv} \leq max_{c_{dh}},$$
$$\forall \, ec_d \in \mathcal{EC}, \, l \in \mathcal{L}, \, p \in \mathcal{P} \mid$$
$$\{ec_d = Heat\} \tag{A.19}$$

$$\sum_{\substack{c_{dc},w_{cs} \\ p \geq w_{cs} \\ p \leq w_{cs}+cl_c-1}} Y_{c_{dc},l,w_{cs}}^{conv} \leq max_{c_{dc}},$$
$$\forall \, ec_d \in \mathcal{EC}, \, l \in \mathcal{L}, \, p \in \mathcal{P} \mid$$
$$\{ec_d = Cool\} \tag{A.20}$$

Next, we set limits for the capacity sizes of conversion and storage technologies. First, Eq. (A.21) sets a constraint for the maximum capacity of dispatchable technologies according to the relevant maximum energy demand per energy carrier of any retrofitting package which that technology could serve, in order to avoid over-investment and retain a safety factor. Second, Eq. (A.22) utilizes two parameters to convert the maximum kWh of storage based on a space utilization factor per technology (saf_s) and the maximum floor area available (fsa) for the example of a utility room.

$$NCAP_{c_d,l,w_{cs}}^{conv} \leq max(dem_{ec_d,h,l,p,d,t})$$
$$\forall \, c_d \in C, \, l \in \mathcal{L}, w_{cs} \in \mathcal{W} \mid$$
$$\{ \, ec_d \in \mathcal{EC} \text{ AND } p \geq w_{cs} \text{ AND } p \leq w_{cs} + cl_c - 1 \text{ AND } \eta_{c_d,ec,w}^{conv} > 0\} \tag{A.21}$$

$$\sum_{\substack{s,w_{cs} \\ p \geq w_{cs} \\ p \leq w_{cs}+sl_s-1}} NCAP_{s,l,w_{cs},p}^{stor} / saf_s \leq fa_{l,p} \cdot fsa,$$
$$\forall \, l \in \mathcal{L}, w_{cs} \in \mathcal{W}, p \in \mathcal{P} \mid$$
$$\{w_{cs} = p\} \tag{A.22}$$

Eqs. (A.23) to (A.25) state that there can only be one conversion, storage, and miscellaneous technology type (e.g. one ASHP, one battery, one kitchen & bathroom) installed in any given stage, to avoid multiple of the same technology installed in the same investment stage

Table A.7
Intervention necessity intervals for each of the four case study buildings reported in real years (y_p) as outputs from the Schroeder method (see Section 2.2).

Component	Building	intmin	intmax
Roof	Building 1	2	15
	Building 2	1	3
	Building 3	3	16
	Building 4	5	18
Facade	Building 1	13	26
	Building 2	3	16
	Building 3	3	16
	Building 4	5	18
Windows	Building 1	1	6
	Building 2	9	21
	Building 3	1	7
	Building 4	1	9
Kitchen + bath	Building 1	2	8
	Building 2	10	16
	Building 3	10	16
	Building 4	1	3
Pipes	Building 1	9	23
	Building 2	1	10
	Building 3	1	13
	Building 4	1	13

while they are alive.

$$\sum_{\substack{w_{cs}' \\ w_{cs}' \geq w_{cs} \\ w_{cs}' \leq w_{cs}+cl_c-1}} Y_{c,l,w_{cs}'}^{conv} \leq 1,$$
$$\forall \, c \in C, \, l \in \mathcal{L}, w_{cs} \in \mathcal{W} \tag{A.23}$$

$$\sum_{\substack{w_{cs}' \\ w_{cs}' \geq w_{cs} \\ w_{cs}' \leq w_{cs}+sl_s-1}} Y_{s,l,w_{cs}'}^{stor} \leq 1,$$
$$\forall \, s \in S, \, l \in \mathcal{L}, \, w_{cs} \in \mathcal{W} \tag{A.24}$$

$$\sum_{\substack{w_f' \\ w_f' \geq w_f \\ w_f' \leq w_f+nl_n-1}} Y_{n,l,w_f'}^{misc} \leq 1,$$
$$\forall \, n \in \mathcal{N}, \, l \in \mathcal{L}, \, w_f \in \mathcal{W} \tag{A.25}$$

To add an additional real world constraint on specific heating system types to simplify real estate owners' decisions, we state in Eqs. (A.26) and (A.27) that there can only one of either a ASHP or GSHP alive, or only one of either an oil or gas boiler alive in any given stage.

$$\sum_{\substack{w_{cs}' \\ w_{cs}' \geq w_{cs} \\ w_{cs}' \leq w_{cs}+cl_c-1}} Y_{ASHP,l,w_{cs}'}^{conv} + Y_{GSHP,l,w_{cs}'}^{conv} \leq 1,$$
$$\forall \, l \in \mathcal{L}, w_{cs} \in \mathcal{W} \tag{A.26}$$

$$\sum_{\substack{w_{cs}' \\ w_{cs}' \geq w_{cs} \\ w_{cs}' \leq w_{cs}+cl_c-1}} Y_{Oil,l,w_{cs}'}^{conv} + Y_{Gas,l,w_{cs}'}^{conv} \leq 1,$$
$$\forall \, l \in \mathcal{L}, w_{cs} \in \mathcal{W} \tag{A.27}$$

A.6. Further information on the Schroeder method

While many methodologies for considering retrofit scheduling exist for both deterministic and probabilistic classes, most real estate owners use deterministic methods for their simplicity and robustness [105]. Deterministic approaches deem the necessity to replace a component based on their remaining End-of-Life (EOL) or otherwise expected service life, treated simplistically as a single value, further mandating
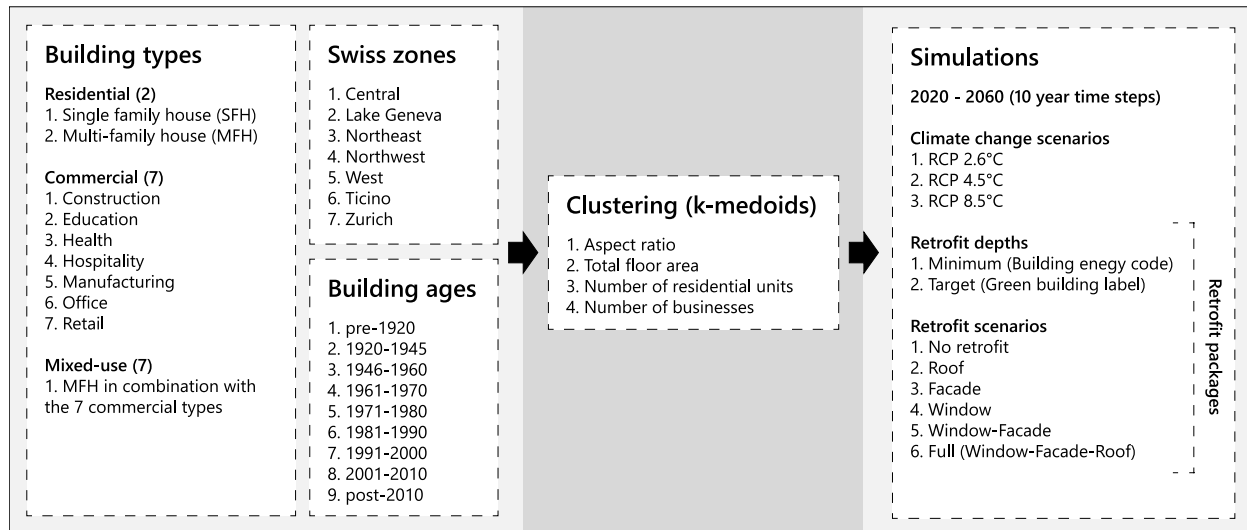
Fig. A.15. Detail on the classes of building types, Swiss geographic zones, and building ages which were clustered to develop the archetypes. These archetypes were then simulated for each ten year time step from 2020–2060, over 3 climate scenarios, and over the 11 retrofitting packages.

an installation directly after the components' retirement. Here, managers evaluate the techno-economic attractiveness of retrofitting the component, along with the possibility to align various component's EOL in order to reduce management or project costs. This is important as the allowable retrofitting budget considers all components to be retrofitted: energy systems, retrofits, and non-energy [15].

However, deterministic elements are limited in considering a more expanded techno-economic decision space of various intervention years and technology options [76]. This is because building components degrade at various rates, inherently allowing for flexibility in investment decisions on a year-to-year basis to align with budgeting or managerial constraints. Building owners often utilize such flexibility in retrofit scheduling to determine step-by-step renovation measures [76,106, 107], implying that probabilistic methods would be better suited to capture real-world aspects.

A number of probabilistic methodologies are available for retrofit scheduling, typically taking a Life-Cycle Costing (LCC) approach [76, 107,108]. One intuitive methodology widely used in the real estate industry for supporting strategic maintenance and renovation decisions for mixed-use portfolios is named after the original author, Jules Schroeder [78,79]. The methodology is based on a two-phase non-linear method to degrade components' value over their remaining expected service life, covering all of the main components considered in renovations.[4] The main benefit of the probabilistic Schroeder method is its simplicity. Relying on a few standardized parameters such as component lifetimes, degradation factors, among others, the method creates degradation curves for each component to output a range of years in which a renovation would be suitable [79], as shown in the manuscript in Fig. 4. Table A.7 reports the necessity intervals for each case study building, as the output of the Schroeder method.

A.7. Further information on the archetypal energy demand database

Each existing building presents a certain uniqueness depending on the building type, construction quality, and age, which vary the

retrofitting packages' energy demands [109]. Since a complete understanding of the retrofitting project is not available until technical planning several years before project start, typically engineers rely on deterministic norms (e.g. kWh/m^2) to estimate retrofitting packages' energy demands for various building types, constructions, and ages in a certain climate zone [51]. Advancing beyond norms to estimate retrofitting packages' energy demands, a wide range of studies have employed urban building energy modeling and simulation for archetypal buildings in a certain city, state, or country [110,111]. We build on these studies by utilizing a combination of government and open-source databases to develop the archetypal energy demand database for Switzerland.

The GWR database of residential buildings is used to identify residential single and multi-family homes [82]. Further, we utilize the STATENT database to identify commercial building use [83]. This is combined with the building geometry that is provided from OpenStreetMap data [84]. A significant part of the methodologies used in the creation of this database are reported in Murray et al. [48,112], where a similar set of retrofitting packages (h) – combinations of retrofitting depths (j) – were utilized although without the use of retrofitting technologies (g). In all, there are 11 retrofitting packages simulated for heating, cooling, and electricity demands to 2050.

Depicted in Fig. A.15, buildings are clustered based on their location (Switzerland's 7 major geographic zones), major building types, and ages. These building types also include the most common categories of mixed-use buildings if the building types include both residential and businesses. Within each of these sub-categories, the buildings are clustered according to their total floor area, the number of occupants for residential buildings, and number of employees for commercial buildings.

The clusters are identified using the k-medoids technique, which identifies a maximally representative building for each cluster, and assigns this as the archetype. K-medoids is a variation of the unsupervised k-means algorithm that assigns the centroid of the cluster to one of the buildings within the set of the buildings, commonly used for building energy systems [139]. K-means would normally assign the centroid to the theoretical feature center of the group, but using this dataset, this would result in an artificial building. To simulate real buildings, the k-medoids method is used. The number of centroids for each sub-category is chosen for the number that results in the highest silhouette value, and thus the most representative clustering. This resulted typically

---

[4] Examples of considered components are: Windows, insulation and renovation of the Facade, Roof, and Basement; thermal distribution and production; electrical systems; along with other non-energy related elements such as lifts, sanitary facilities, interior walls, etc.

Table B.8

Energy carrier import prices and export compensation, along with the CO_2 emission factor for grid electricity during the 30-year planning horizon. All price and compensation units are in CHF/kWh and the CO_2 emission factor in $kgCO_2$/kWh. Constant values were used for life cycle emissions parameters for the following energy carriers: natural gas (c_{gas} = 0.228 $kgCO_2$/kWh), fuel oil (c_{oil} = 0.301 $kgCO_2$/kWh), and biomass (c_{bio} = 0.027 $kgCO_2$/kWh) [113].

	Import prices				Export compensation	CO_2 emission factors
Ref.		[114,115]	[114,115]	[114,115]	[114,115]	[115,116]
Year	Fuel oil, i_{oil,y_p}	Natural gas, i_{gas,y_p}	Biomass, i_{bio,y_p}	Grid electricity, i_{elec,y_p}	Grid electricity, e_{elec,y_p}	Grid electricity, c_{elec,y_p}
2021	0.093	0.069	0.072	0.161	0.054	0.102
2022	0.095	0.070	0.074	0.163	0.054	0.101
2023	0.096	0.071	0.076	0.165	0.055	0.099
2024	0.097	0.072	0.079	0.167	0.056	0.098
2025	0.099	0.073	0.081	0.169	0.056	0.096
2026	0.100	0.075	0.085	0.171	0.057	0.095
2027	0.102	0.076	0.089	0.173	0.058	0.094
2028	0.105	0.078	0.093	0.175	0.058	0.092
2029	0.107	0.080	0.096	0.177	0.059	0.091
2030	0.109	0.081	0.100	0.180	0.060	0.089
2031	0.112	0.083	0.103	0.181	0.060	0.088
2032	0.113	0.084	0.106	0.183	0.061	0.087
2033	0.115	0.085	0.108	0.185	0.062	0.085
2034	0.117	0.086	0.111	0.187	0.062	0.084
2035	0.118	0.088	0.114	0.188	0.063	0.082
2036	0.120	0.088	0.116	0.189	0.063	0.081
2037	0.121	0.089	0.118	0.189	0.063	0.079
2038	0.122	0.090	0.120	0.189	0.063	0.078
2039	0.124	0.091	0.122	0.189	0.063	0.077
2040	0.125	0.092	0.124	0.190	0.063	0.075
2041	0.126	0.093	0.125	0.191	0.064	0.074
2042	0.127	0.093	0.126	0.192	0.064	0.072
2043	0.128	0.094	0.128	0.193	0.064	0.071
2044	0.128	0.094	0.129	0.194	0.065	0.070
2045	0.129	0.095	0.130	0.195	0.065	0.068
2046	0.130	0.095	0.131	0.195	0.065	0.067
2047	0.131	0.096	0.133	0.196	0.065	0.065
2048	0.131	0.096	0.134	0.196	0.065	0.064
2049	0.132	0.097	0.135	0.197	0.066	0.063
2050	0.133	0.098	0.136	0.197	0.066	0.075

Table B.9

Dynamic linear cost and efficiency coefficients of GSHP, ASHP & comp. chiller, CHP, PV, and battery technologies during the 30-year planning horizon based on the learning curve coefficient (μ) for each technology, $C_y = C_o \cdot e^{-\mu y}$. All linear cost ($lc$) units are in CHF/kW. In the Table, references labeled with * are used to obtain current (2021) cost values and efficiencies for the technologies, while references labeled with $^+$ are used to create projections for the future.

	GSHP		ASHP & Comp. chiller		CHP	PV		Battery
μ	0.035		0.027		0.005	0.021		0.019
Ref.	[117]*, [118]$^+$	[119]*, [120]$^{*,+}$, [121]$^{*,+}$	[122]*, [123]*, [118]$^+$	[119]*, [120]$^{*,+}$, [121]$^{*,+}$	[124]$^{*,+}$	[125]$^+$, [124]*	[125]*, [126]$^+$	[127]*, [128]$^+$, [129]$^+$
Year	$lc^{conv}_{GSHP,w_{cs}}$	$\eta^{conv}_{GSHP,w_{cs}}$	$lc^{conv}_{ASHP,w_{cs}}$, $lc^{conv}_{CC,w_{cs}}$	$\eta^{conv}_{ASHP,w_{cs}}$, $\eta^{conv}_{CC,w_{cs}}$	$\eta^{conv}_{CHP,w_{cs}}$	$lc^{conv}_{PV,w_{cs}}$	$\eta^{conv}_{PV,w_{cs}}$	$lc^{stor}_{BAT,w_{cs}}$
2021	1827	3.75	858	3.05	900	267	16.6%	367
2022	1765	3.79	835	3.08	896	261	16.8%	360
2023	1704	3.83	813	3.11	891	256	17.0%	354
2024	1645	3.87	791	3.14	887	251	17.2%	347
2025	1589	3.91	770	3.17	882	246	17.4%	341
2026	1534	3.95	750	3.20	878	241	17.6%	334
2027	1481	3.99	730	3.24	873	236	17.7%	328
2028	1430	4.02	710	3.27	869	231	17.9%	322
2029	1381	4.06	691	3.30	865	226	18.1%	316
2030	1334	4.10	673	3.33	860	221	18.3%	310
2031	1288	4.14	655	3.36	856	217	18.5%	304
2032	1243	4.18	638	3.39	852	213	18.7%	298
2033	1201	4.22	621	3.43	848	208	18.9%	293
2034	1159	4.26	604	3.46	843	204	19.0%	287
2035	1120	4.30	588	3.49	839	200	19.2%	282
2036	1081	4.33	572	3.52	835	196	19.4%	277
2037	1044	4.37	557	3.55	831	192	19.6%	271
2038	1008	4.41	542	3.58	827	188	19.8%	266
2039	973	4.45	528	3.61	823	184	20.0%	261
2040	940	4.49	514	3.65	818	180	20.1%	257
2041	907	4.53	500	3.68	814	176	20.3%	252
2042	876	4.57	487	3.71	810	173	20.5%	247
2043	846	4.61	474	3.74	806	169	20.7%	242
2044	817	4.65	461	3.77	802	166	20.9%	238
2045	789	4.68	449	3.80	798	162	21.1%	233

Table B.9 (*continued*).

	GSHP		ASHP & Comp. chiller		CHP	PV		Battery
μ	0.035		0.027		0.005	0.021		0.019
Ref.	[117]*, [118]+	[119]*, [120]*,+, [121]*,+	[122]*, [123]*, [118]+	[119]*, [120]*,+, [121]*,+	[124]*,+	[125]+, [124]*	[125]*, [126]+	[127]*, [128]+, [129]+
Year	$lc^{conv}_{GSHP,w_{cs}}$	$\eta^{conv}_{GSHP,w_{cs}}$	$lc^{conv}_{ASHP,w_{cs}}$, $lc^{conv}_{CC,w_{cs}}$	$\eta^{conv}_{ASHP,w_{cs}}$, $\eta^{conv}_{CC,w_{cs}}$	$\eta^{conv}_{CHP,w_{cs}}$	$lc^{conv}_{PV,w_{cs}}$	$\eta^{conv}_{PV,w_{cs}}$	$lc^{stor}_{BAT,w_{cs}}$
2046	762	4.72	437	3.84	794	159	21.3%	229
2047	736	4.76	425	3.87	790	156	21.3%	225
2048	710	4.80	414	3.90	786	153	21.6%	221
2049	686	4.84	403	3.93	782	150	21.8%	216
2050	662	4.88	392	3.96	779	146	22.0%	212

Table B.10

Constant linear costs, conversion efficiency, lifetime, O&M cost, pass-on rates, and embodied emissions characteristics of all conversion technologies. Where there are missing values (–), parameters change over the 30-year planning horizon (see Table B.9). Comp. chillers are modeled with the same efficiency as ASHPs, with ASHPs not being able to be used reversibly. Other miscellaneous parameters such as the maximum number of heating $max_{c_{dh}}$ and cooling $max_{c_{dc}}$ technologies, are set at 2 and 1 respectively based on consultations from the building owner.

Technical characteristic	GSHP	ASHP	Oil boiler	Natural gas boiler	Biomass boiler	CHP	Abs. chiller	Comp. chiller	PV
Linear conversion technology cost, $lc^{conv}_{c,w_{cs}}$ (CHF/kW)	–	–	441 [130]	649 [119]	825 [63]	–	549 [131]	–	–
Conversion factor, $\eta_{c,ec,w_{cs}}$	–	–	92% [130]	91% [117]	89% [130]	55% (thermal) 35% (electrical) [117]	76% [131]	–	–
Conversion technology lifetime, cl_c (y_p)	23 [117]	21 [122]	22 [127]	20 [117]	20 [117]	20 [117]	20 [131]	20 [131]	27 [132]
Maintenance cost factor, om^{conv}_c	0.8% [133]	0.8% [133]	2.3% [122]	2.4% [122]	2.1% [134]	5.0% [134]	2.0% [131]	0.8% [118]	1.7% [127]
Pass-on rate, $passon_c$ [96]	100%	100%	0%	0%	100%	50%	50%	100%	100%
Embodied emissions, $c_{c,w_{cs}}$ (kgCO$_2$/kW) [113]	273	364	51	51	51	364	364	364	254

Table B.11

Constant techno-economic characteristics of thermal and the battery electrical storage technologies. The floor area available for storage technologies fsa in utility rooms is set to 5%. Storage technology floor area factors saf_s in kWh/m^2 were set at HWTS - 9, and Battery - 5 based on industry-standards.

Technical characteristic	Thermal	Battery
Charge/discharge efficiency, η^{ch}_s/η^{dis}_s	91% [34]	96% [117]
Maximum charge/discharge rate, $q^{ch,max}_s/q^{dis,max}_s$	25% [34]	25% [125]
Self-discharge rate, η^{self}_s	0.750% [134]	0.054% [135]
Linear storage technology cost, $lc^{stor}_{s,w_{cs}}$ (CHF/kWh)	13 [117]	–
Storage technology lifetime, sl_s (y_p)	23 [136]	13 [125]
Yearly storage degradation coefficient, $sydeg_s$	0%	2.0% [137,138]
Maintenance cost factor, om^{stor}_s [134]	1.5%	2.5%
Pass-on rate, $passon_s$ [96]	50%	50%
Embodied emissions, $c_{s,w_{cs}}$ (kgCO$_2$/kWh) [113]	5	157

between 1–5 centroids for each sub-category of building defined by location, age and building type. Lastly, a k-Nearest Neighbors (kNN) classification algorithm is trained to assign each building of a certain location, type and age sub-category to the nearest centroid (archetype). Since the original dataset was not comprehensive for every building in Switzerland, additional buildings can also be assigned to a centroid using this kNN model.

Some assumptions were made in the clustering process based on data retrieved from the databases. For example, buildings which were classified as SFH mixed-use were simulated assuming SFH only. This is because mixed-use SFHs often do not exist in reality and this was seen to be an anomaly of the clustering procedure. There were several other buildings types assigned in the clustering: Water, Arts, Power, Transportation, Mining, Agriculture, Trade. Inspection of the clustering assignment led us to believe that these were headquarter buildings of different companies and therefore, these buildings were all simulated as the Office archetype.

We used a nearest-neighbor spatial join to match the case study addresses to the assigned buildings in the database. This process had a mean join distance of 12.6 m and a maximum join distance of 208 m.

For the cases with a large join distance, we assume that the correct archetype was assigned to the building due to the likelihood of similar buildings being located near each other. As more data becomes available, the quality and completeness of input data will improve leading to an improvement in archetype classification and higher accuracy in the spatial join.

Archetypal energy demand approaches employ a wide range of input data assumptions, building energy simulation models, and calibration methodologies, making validation and verification of building energy models difficult [140,141]. Particularly important, while difficult to capture in parametric analysis, is the consideration of the energy performance gap [142]. While the developed database is deterministic, we are able to capture uncertainty of climate change RCP scenarios which has been shown to be important [143,144] due to the potential effects of climate change to reduce heating and increase cooling demand, for the example of Europe [145]. In future work, such an rich archetypal database could be up-scaled to provide high-level insights on energy demands, along with other risk factors for demands such as economic shocks [146]. This could lend further insight into studies focusing on the Swiss heating [147–150] and cooling [151] demands over time considering climate change, or all of them together [152].

Appendix B. Techno-economic database parameter values

Tables B.8 to B.14 comprise all dynamic and static parameters of the techno-economic database.

Embodied emissions parameters of all technologies are presented as static values. While circular economy initiatives in the building industry are making strides in reducing these figures from today, due to data unavailability they are kept constant for all technologies. Further, life cycle grid electricity emission factors (kg CO$_2$-eq) for the beginning of the time horizon are taken from a Swiss government project according to the ecoinvent methodology.

Table B.12
Constant techno-economic characteristics of Window component retrofitting technologies.

Technical characteristic — $Window$	$Min_{Plastic}$	$Tar_{Plastic}$	Min_{WoodAl}	Tar_{WoodAl}
Linear retrofit tech. cost, lc_{g,w_f}^{ret} (CHF/m²) [153]	586	644	645	709
Retrofit component lifetime, gl_g (y$_p$) [154]	32	32	32	32
Maintenance cost factor, om_g^{ret} [153]	0.5	0.5%	0.5%	0.5%
Pass-on rate, $passon_g$ [96]	20%	20%	25%	25%
Embodied emissions, c_{g,w_f} (kgCO₂/m²) [113]	285	342	217	260

Table B.13
Constant techno-economic characteristics of Facade and Roof component retrofitting technologies. The pass-on rate for all Facade technologies is 65% while the pass-on rate for all Roof technologies is 20% [96]. The fixed retrofit project cost for scaffolding is set to 15 CHF/m² per facade area.

Technical characteristic — $Roof\&Facade$	Min_{XPS}	Tar_{XPS}	Min_{EPS}	Tar_{EPS}	Min_{Stone}	Tar_{Stone}
Linear retrofit tech. cost, lc_{g,w_f}^{ret} (CHF/m²) [153]	150	165	180	198	218	240
Retrofit component lifetime, gl_g (y$_p$) [154]	40	40	40	40	40	40
Maintenance cost factor, om_g^{ret} [153]	0.5%	0.5	0.5%	0.5%	0.5%	0.5%
Embodied emissions, c_{g,w_f} (kgCO₂/m²) [48,113,155]	33	40	24	29	18	22

Table B.14
Constant techno-economic characteristics of miscellaneous technologies. Due to data unavailability, costs and lifetimes for kitchens and bathrooms are based on interviews with the building owner.

Technical characteristic	Kitchen + bathrooms	Pipes
Linear misc. technology cost, lc_{n,w_f}^{ret} (CHF/unit)	8000	348 [153]
Misc. component lifetime, nl_n (y$_p$)	20	40 [154]
Maintenance cost factor, om_n^{misc} [153]	0.5%	0.5%
Pass-on rate, $passon_n$ [96]	75%	10%
Embodied emissions, c_{n,w_f} (kgCO₂/unit) [113]	2250	27.3

References

[1] Levesque A, Pietzcker RC, Baumstark L, Luderer G. Deep decarbonisation of buildings energy services through demand and supply transformations in a 1.5° c scenario. Environ Res Lett 2021;16(5):054071. http://dx.doi.org/10.1088/1748-9326/ABDF07.

[2] Grubler A, Wilson C, Bento N, Boza-Kiss B, Krey V, McCollum DL, Rao ND, Riahi K, Rogelj J, De Stercke S, Cullen J, Frank S, Fricko O, Guo F, Gidden M, Havlík P, Huppmann D, Kiesewetter G, Rafaj P, Schoepp W, Valin H. A low energy demand scenario for meeting the 1.5° c target and sustainable development goals without negative emission technologies. Nat. Energy 2018;3(6):515–27. http://dx.doi.org/10.1038/s41560-018-0172-6.

[3] IEA, UNEP. 2019 global status report for buildings and construction. Tech. rep., International Energy Agency (IEA), United Nations Environment Programme (UNEP); 2019, URL https://webstore.iea.org/download/direct/2930?fileName=2019_Global_Status_Report_for_Buildings_and_Construction.pdf.

[4] Sandberg NH, Heidrich O, Dawson R, Dimitriou S, Vimm-r T, Filippidou F, Stegnar G, Šijanec Zavrl M, Brattebø H. Dynamic building stock modelling: Application to 11 European countries to support the energy efficiency and retrofit ambitions of the EU. Energy Build 2016;132:26–38. http://dx.doi.org/10.1016/J.ENBUILD.2016.05.100.

[5] SFOE. Energy strategy 2050: Once the new energy act is in force. Tech. rep., Swiss Federal Office of Energy (SFOE); 2018, p. 1–25, URL http://www.bfe.admin.ch/energiestrategie2050/index.html?lang=en{&}dossier_id=07008.

[6] European Commission - Joint Research Centre. Achieving the cost-effective energy transformation of Europe's buildings. Tech. rep., 2019, p. 1–56, URL https://publications.jrc.ec.europa.eu/repository/bitstream/JRC117739/cost_optimal_energy_renovations_online.pdf.

[7] European Commission. A Renovation Wave for Europe - greening our buildings, creating jobs, improving lives. Tech. rep., 2020, URL https://eur-lex.europa.eu/resource.html?uri=cellar:0638aa1d-0f02-11eb-bc07-01aa75ed71a1.0003.02/DOC_1{&}format=PDF.

[8] Kontokosta CE. Modeling the energy retrofit decision in commercial office buildings. Energy Build 2016;131:1–20. http://dx.doi.org/10.1016/j.enbuild.2016.08.062.

[9] Geltner DM, Miller NG, Clayton J, Eichholtz P. Commercial real estate: Analysis and investments. 3rd ed.. Mason, OH, USA: Oncourse Learning; 2014, p. 1–826, 3rd edition.

[10] Hecher M, Hatzl S, Knoeri C, Posch A. The trigger matters: The decision-making process for heating systems in the residential building sector. Energy Policy 2017;102:288–306. http://dx.doi.org/10.1016/j.enpol.2016.12.004.

[11] Federal Statistical Office of Switzerland (Bundesamt für Statistik). Bau- und wohnbaustatistik (construction and housing statistics). 2018.

[12] 2° Investing Initiative and Wüest Partner. Bridging the gap: Measuring progress on the climate goal alignment and climate actions of Swiss Financial Institutions. Tech. rep., Swiss Federal Office for the Environment (SFOE); 2020, p. 1–104, URL https://www.bafu.admin.ch/bafu/en/home/topics/climate/info-specialists/climate-and-financial-markets.html{#}-194175513.

[13] SSF. EU action plan on sustainable finance: Effects on Swiss financial institutions. Tech. rep., Swiss Sustainable Finance (SSF); 2019, p. 12, URL https://eur-lex.europa.eu/legal-content/EN/TXT/?uri=CELEX:52018DC0097.

[14] EBA. EBA action plan on sustainable finance. Tech. rep., European Banking Authority (EBA); 2019, p. 1–22, URL https://eba.europa.eu/sites/default/documents/files/document_library//EBAActionplanonsustainablefinance.pdf.

[15] Petkov I, Knoeri C, Hoffmann VH. The interplay of policy and energy retrofit decision-making for real estate decarbonization. Environ Res: Infrastruct Sustain 2021;1(3):035006. http://dx.doi.org/10.1088/2634-4505/ac3321.

[16] Larsen T. Implementing ESG in private real estate portfolios: The case of US and pan-europe core fund managers. J Sustain Real Estate 2010;2(1):249–67. http://dx.doi.org/10.1080/10835547.2010.12091806.

[17] Streicher KN, Mennel S, Chambers J, Parra D, Patel MK. Cost-effectiveness of large-scale deep energy retrofit packages for residential buildings under different economic assessment approaches. Energy Build 2020;215:109870. http://dx.doi.org/10.1016/j.enbuild.2020.109870.

[18] Deb C, Schlueter A. Review of data-driven energy modelling techniques for building retrofit. Renew Sustain Energy Rev 2021;144:110990. http://dx.doi.org/10.1016/J.RSER.2021.110990.

[19] Christensen PH, Robinson SJ, Simons RA. The influence of energy considerations on decision making by institutional real estate owners in the U.S.. Renew Sustain Energy Rev 2018;94:275–84. http://dx.doi.org/10.1016/j.rser.2018.05.061.

[20] Nielsen AN, Jensen RL, Larsen TS, Nissen SB. Early stage decision support for sustainable building renovation - a review. Build Environ 2016;103:165–81. http://dx.doi.org/10.1016/j.buildenv.2016.04.009.

[21] Gulotta TM, Cellura M, Guarino F, Longo S. A bottom-up harmonized energy-environmental models for europe (BOHEEME): A case study on the thermal insulation of the EU-28 building stock. Energy Build 2021;231:110584. http://dx.doi.org/10.1016/J.ENBUILD.2020.110584.

[22] Streicher KN, Berger M, Panos E, Narula K, Soini MC, Patel MK. Optimal building retrofit pathways considering stock dynamics and climate change impacts. Energy Policy 2021;152:112220. http://dx.doi.org/10.1016/J.ENPOL.2021.112220.

[23] Sandberg NH, Næss JS, Brattebø H, Andresen I, Gustavsen A. Large potentials for energy saving and greenhouse gas emission reductions from large-scale deployment of zero emission building technologies in a national building stock. Energy Policy 2021;152:112114. http://dx.doi.org/10.1016/j.enpol.2020.112114.

[24] Nägeli C, Jakob M, Catenazzi G, Ostermeyer Y. Policies to decarbonize the swiss residential building stock: An agent-based building stock modeling assessment. Energy Policy 2020;146:111814. http://dx.doi.org/10.1016/j.enpol.2020.111814.

[25] Ma Z, Cooper P, Daly D, Ledo L. Existing building retrofits: Methodology and state-of-the-art. Energy Build 2012;55:889–902. http://dx.doi.org/10.1016/j.enbuild.2012.08.018.

[26] Abdul Hamid A, Farsäter K, Wahlström Å, Wallentén P. Literature review on renovation of multifamily buildings in temperate climate conditions. Energy Build 2018;172:414–31. http://dx.doi.org/10.1016/j.enbuild.2018.04.032.

[27] Ascione F, Bianco N, De Stasio C, Mauro GM, Vanoli GP. Multi-stage and multi-objective optimization for energy retrofitting a developed hospital reference building: A new approach to assess cost-optimality. Appl Energy 2016;174:37–68. http://dx.doi.org/10.1016/j.apenergy.2016.04.078.

[28] Guariso G, Sangiorgio M. Multi-objective planning of building stock renovation. Energy Policy 2019;130:101–10. http://dx.doi.org/10.1016/j.enpol.2019.03.053.

[29] Iturriaga E, Aldasoro U, Terés-Zubiaga J, Campos-Celador A. Optimal renovation of buildings towards the nearly zero energy building standard. Energy 2018;160:1101–14. http://dx.doi.org/10.1016/j.energy.2018.07.023.

[30] Shen P, Braham W, Yi Y. The feasibility and importance of considering climate change impacts in building retrofit analysis. Appl Energy 2019;233–234:254–70. http://dx.doi.org/10.1016/J.APENERGY.2018.10.041.

[31] Richarz J, Henn S, Osterhage T, Müller D. Optimal scheduling of modernization measures for typical non-residential buildings. Energy 2021;238:121871. http://dx.doi.org/10.1016/j.energy.2021.121871.

[32] Schütz T, Schiffer L, Harb H, Fuchs M, Müller D. Optimal design of energy conversion units and envelopes for residential building retrofits using a comprehensive MILP model. Appl Energy 2017;185:1–15. http://dx.doi.org/10.1016/J.APENERGY.2016.10.049.

[33] Jafari A, Valentin V. An optimization framework for building energy retrofits decision-making. Build Environ 2017;115:118–29. http://dx.doi.org/10.1016/j.buildenv.2017.01.020.

[34] Stadler M, Groissböck M, Cardoso G, Marnay C. Optimizing distributed energy resources and building retrofits with the strategic DER-camodel. Appl Energy 2014;132:557–67. http://dx.doi.org/10.1016/j.apenergy.2014.07.041.

[35] Passer A, Ouellet-Plamondon C, Kenneally P, John V, Habert G. The impact of future scenarios on building refurbishment strategies towards plus energy buildings. Energy Build 2016;124:153–63. http://dx.doi.org/10.1016/j.enbuild.2016.04.008.

[36] Galimshina A, Moustapha M, Hollberg A, Padey P, Lasvaux S, Sudret B, Habert G. What is the optimal robust environmental and cost-effective solution for building renovation? Not the usual one. Energy Build 2021;251:111329. http://dx.doi.org/10.1016/J.ENBUILD.2021.111329.

[37] Ayoub AN, Gaigneux A, Le Brun N, Acha S, Shah N. The development of a low-carbon roadmap investment strategy to reach science based targets for commercial organisations with multi-site properties. Build Environ 2020;186:107311. http://dx.doi.org/10.1016/j.buildenv.2020.107311.

[38] Guardigli L, Bragadin MA, Della Fornace F, Mazzoli C, Prati D. Energy retrofit alternatives and cost-optimal analysis for large public housing stocks. Energy Build 2018;166:48–59. http://dx.doi.org/10.1016/J.ENBUILD.2018.02.003.

[39] Jennings M, Fisk D, Shah N. Modelling and optimization of retrofitting residential energy systems at the urban scale. Energy 2014;64:220–33. http://dx.doi.org/10.1016/J.ENERGY.2013.10.076.

[40] Gabrielli L, Ruggeri AG. Developing a model for energy retrofit in large building portfolios: Energy assessment, optimization and uncertainty. Energy Build 2019;202:109356. http://dx.doi.org/10.1016/j.enbuild.2019.109356.

[41] He Y, Liao N, Bi J, Guo L. Investment decision-making optimization of energy efficiency retrofit measures in multiple buildings under financing budgetary restraint. J Cleaner Prod 2019;215:1078–94. http://dx.doi.org/10.1016/J.JCLEPRO.2019.01.119.

[42] McArthur JJ, Jofeh CG. Portfolio retrofit evaluation: A methodology for optimizing a large number of building retrofits to achieve triple-bottom-line objectives. Sustainable Cities Soc 2016;27:263–74. http://dx.doi.org/10.1016/j.scs.2016.03.011.

[43] Wu R, Mavromatidis G, Orehounig K, Carmeliet J. Multiobjective optimisation of energy systems and building envelope retrofit in a residential community. Appl Energy 2017;190:634–49. http://dx.doi.org/10.1016/j.apenergy.2016.12.161.

[44] Zheng D, Yu L, Wang L. A techno-economic-risk decision-making methodology for large-scale building energy efficiency retrofit using Monte Carlo simulation. Energy 2019;189:116169. http://dx.doi.org/10.1016/j.energy.2019.116169.

[45] Antipova E, Boer D, Guillén-Gosálbez G, Cabeza LF, Jiménez L. Multi-objective optimization coupled with life cycle assessment for retrofitting buildings. Energy Build 2014;82:92–9. http://dx.doi.org/10.1016/j.enbuild.2014.07.001.

[46] Hosseinian S, Choi K, Asce M, Bae J. IRIER: A Decision-support model for optimal energy retrofit investments. J Constr Eng Manage 2017;143(9):05017016. http://dx.doi.org/10.1061/(ASCE)CO.1943-7862.000136.

[47] Zhang H, Hewage K, Prabatha T, Sadiq R. Life cycle thinking-based energy retrofits evaluation framework for Canadian residences: A Pareto optimization approach. Build Environ 2021;204:108115. http://dx.doi.org/10.1016/J.BUILDENV.2021.108115.

[48] Murray P, Marquant J, Niffeler M, Mavromatidis G, Orehounig K. Optimal transformation strategies for buildings, neighbourhoods and districts to reach CO2 emission reduction targets. Energy Build 2019;207:109569. http://dx.doi.org/10.1016/j.enbuild.2019.109569.

[49] Pannier ML, Recht T, Robillart M, Schalbart P, Peuportier B, Mora L. Identifying optimal renovation schedules for building portfolios: Application in a social housing context under multi-year funding constraints. Energy Build 2021;250:111290. http://dx.doi.org/10.1016/J.ENBUILD.2021.111290.

[50] Mavromatidis G, Petkov I. MANGO: A Novel optimization model for the long-term, multi-stage planning of decentralized multi-energy systems. Appl Energy 2021;288:116585. http://dx.doi.org/10.1016/j.apenergy.2021.116585.

[51] Mavromatidis G, Orehounig K, Bollinger LA, Hohmann M, Marquant JF, Miglani S, Morvaj B, Murray P, Waibel C, Wang D, Carmeliet J. Ten questions concerning modeling of distributed multi-energy systems. Build Environ 2019;165:106372. http://dx.doi.org/10.1016/j.buildenv.2019.106372.

[52] Petkov I, Gabrielli P. Power-to-hydrogen as seasonal energy storage: an uncertainty analysis for optimal design of low-carbon multi-energy systems. Appl Energy 2020;274:115197. http://dx.doi.org/10.1016/j.apenergy.2020.115197.

[53] Pecenak ZK, Stadler M, Fahy K. Efficient multi-year economic energy planning in microgrids. Appl Energy 2019;255:113771. http://dx.doi.org/10.1016/j.apenergy.2019.113771.

[54] Dalton B, Fuerst F. The 'green value' proposition in real estate. In: Routledge handbook of sustainable real estate. 1st ed.. 2015, p. 177–200. http://dx.doi.org/10.1201/9781315622750-12.

[55] Fuerst F, McAllister P. Green noise or green value? Measuring the effects of environmental certification on office values. Real Estate Econ 2011;39(1):45–69. http://dx.doi.org/10.1111/j.1540-6229.2010.00286.x.

[56] Institute RM. How to calculate and present deep retrofit value. Tech. Rep. April, 2015, p. 105, URL http://www.rmi.org/retrofit_epot_deepretrofitvalue.

[57] Ferreira J, Pinheiro MD, de Brito J. Refurbishment decision support tools review - energy and life cycle as key aspects to sustainable refurbishment projects. Energy Policy 2013;62:1453–60. http://dx.doi.org/10.1016/j.enpol.2013.06.082.

[58] Österbring M, Camarasa C, Nägeli C, Thuvander L, Wallbaum H. Prioritizing deep renovation for housing portfolios. Energy Build 2019;202:109361. http://dx.doi.org/10.1016/j.enbuild.2019.109361.

[59] Gade AN, Jensen RL, Larsen TS, Nissen SrB, Andresen I. Value-based decision making in the pre-design stage of sustainable building renovation projects–exploring two methods for weighting criteria. Int J Comput Math 2019;21(6):648–63. http://dx.doi.org/10.1080/15623599.2019.1578913.

[60] Friege J, Chappin E. Modelling decisions on energy-efficient renovations: A review. Renew Sustain Energy Rev 2014;39:196–208. http://dx.doi.org/10.1016/j.rser.2014.07.091.

[61] Ruggeri AG, Calzolari M, Scarpa M, Gabrielli L, Davoli P. Planning energy retrofit on historic building stocks: A score-driven decision support system. Energy Build 2020;224:110066. http://dx.doi.org/10.1016/J.ENBUILD.2020.110066.

[62] Gade AN, Larsen TS, Nissen SrB, Jensen RL. REDIS: A Value-based decision support tool for renovation of building portfolios. Build Environ 2018;142:107–18. http://dx.doi.org/10.1016/j.buildenv.2018.06.016.

[63] Serrano-Jiménez A, Femenías P, Thuvander L, Barrios-Padura A. A multi-criteria decision support method towards selecting feasible and sustainable housing renovation strategies. J Cleaner Prod 2021;278:123588. http://dx.doi.org/10.1016/j.jclepro.2020.123588.

[64] Hirsch J, Spanner M, Bienert S. The carbon risk real estate monitor - developing a framework for science-based decarbonizing and reducing stranding risks within the commercial real estate sector. J Sustain Real Estate 2019;11(1):174–90. http://dx.doi.org/10.22300/1949-8276.11.1.174.

[65] Gliedt T, Hoicka CE. Energy upgrades as financial or strategic investment? Energy star property owners and managers improving building energy performance. Appl Energy 2015;147:430–43. http://dx.doi.org/10.1016/j.apenergy.2015.02.028.

[66] Menassa CC, Baer B. A framework to assess the role of stakeholders in sustainable building retrofit decisions. Sustainable Cities Soc 2014;10:207–21. http://dx.doi.org/10.1016/j.scs.2013.09.002.

[67] Almeida M, Ferreira M. Ten questions concerning cost-effective energy and carbon emissions optimization in building renovation. Build Environ 2018;143:15–23. http://dx.doi.org/10.1016/j.buildenv.2018.06.036.

[68] Iturriaga E, Campos-Celador A, Terés-Zubiaga J, Aldasoro U, Álvarez-Sanz M. A MILP optimization method for energy renovation of residential urban areas: Towards zero energy districts. Sustainable Cities Soc 2021;68:102787. http://dx.doi.org/10.1016/j.scs.2021.102787.

[69] Bynum ML, Hackebeil GA, Hart WE, Laird CD, Nicholson BL, Siirola JD, Watson J-P, Woodruff DL. Pyomo–optimization modeling in python, Vol. 67. 3rd ed.. Springer Science & Business Media; 2021, http://dx.doi.org/10.1007/978-3-030-68928-5.

[70] Hart WE, Watson J-P, Woodruff DL. Pyomo: modeling and solving mathematical programs in python. Math Program Comput 2011;3:219–60. http://dx.doi.org/10.1007/s12532-011-0026-8.

[71] Gurobi Optimization, LLC. Gurobi optimizer reference manual. 2020.

[72] Gelaro R, McCarty W, Suárez MJ, Todling R, Molod A, Takacs L, Randles CA, Darmenov A, Bosilovich MG, Reichle R, Wargan K, Coy L, Cullather R, Draper C, Akella S, Buchard V, Conaty A, da Silva AM, Gu W, Kim GK, Koster R, Lucchesi R, Merkova D, Nielsen JE, Partyka G, Pawson S, Putman W, Rienecker M, Schubert SD, Sienkiewicz M, Zhao B. The modern-era retrospective analysis for research and applications, version 2 (MERRA-2). J Clim 2017;30(14):5419–54. http://dx.doi.org/10.1175/JCLI-D-16-0758.1.

[73] Pfenninger S, Staffell I. Long-term patterns of European PV output using 30 years of validated hourly reanalysis and satellite data. Energy 2016;114:1251–65. http://dx.doi.org/10.1016/j.energy.2016.08.060.

[74] Staffell I, Pfenninger S. Using bias-corrected reanalysis to simulate current and future wind power output. Energy 2016;114:1224–39. http://dx.doi.org/10.1016/j.energy.2016.08.068.

[75] Mavrotas G. Effective implementation of the ϵ-constraint method in multi-objective mathematical programming problems. Appl Math Comput 2009;213(2):455–65. http://dx.doi.org/10.1016/j.amc.2009.03.037.

[76] Maia I, Kranzl L, Müller A. New step-by-step retrofitting model for delivering optimum timing. Appl Energy 2021;290:116714. http://dx.doi.org/10.1016/j.apenergy.2021.116714.

[77] Christen M, Adey BT, Wallbaum H. On the usefulness of a cost-performance indicator curve at the strategic level for consideration of energy efficiency measures for building portfolios. Energy Build 2016;119:267–82. http://dx.doi.org/10.1016/j.enbuild.2016.02.056.

[78] Schroeder J. Zustandsbewertung grosser gebäudebestände (condition assessment of large building stocks). Schweiz Ing Archit (Swiss Eng Archit) 1989;17(27):449–59. http://dx.doi.org/10.5169/seals-77093.

[79] Christen M, Schroeder J, Wallbaum H. Evaluation of strategic building maintenance and refurbishment budgeting method schroeder. Int J Strateg Prop Manag 2014;18(4):393–406. http://dx.doi.org/10.3846/1648715X.2014.971917.

[80] Hosseini M, Bigtashi A, Lee B. Generating future weather files under climate change scenarios to support building energy simulation – a machine learning approach. Energy Build 2021;230:110543. http://dx.doi.org/10.1016/j.enbuild.2020.110543.

[81] Dipasquale C, Fedrizzi R, Bellini A, Gustafsson M, Ochs F, Bales C. Database of energy, environmental and economic indicators of renovation packages for European residential buildings. Energy Build 2019;203:109427. http://dx.doi.org/10.1016/j.enbuild.2019.109427.

[82] Federal Statistical Office of Switzerland (Bundesamt für Statistik). Eidgenössische gebäude- und wohnungsregister GWR (federal register of buildings and dwellings). 2021.

[83] Federal Statistical Office of Switzerland (Bundesamt für Statistik). Statistik der unternehmensstruktur STATENT (company structure statistics). 2021.

[84] OpenStreetMap Foundation. Openstreetmap. 2021.

[85] Wang D, Landolt J, Mavromatidis G, Orehounig K, Carmeliet J. CESAR: A Bottom-up building stock modelling tool for Switzerland to address sustainable energy transformation strategies. Energy Build 2018;169:9–26. http://dx.doi.org/10.1016/j.enbuild.2018.03.020.

[86] EnergyPlus. Energyplus simulation software. U.S. Department of Energy; 2019, URL https://energyplus.net/.

[87] Berger M, Worlitschek J. The link between climate and thermal energy demand on national level: A case study on Switzerland. Energy Build 2019;202:109372. http://dx.doi.org/10.1016/j.enbuild.2019.109372.

[88] Domínguez-Muñoz F, Cejudo-López JM, Carrillo-Andrés A, Gallardo-Salazar M. Selection of typical demand days for CHP optimization. Energy Build 2011;43(11):3036–43. http://dx.doi.org/10.1016/J.ENBUILD.2011.07.024.

[89] Swiss Federal Customs Administration (Eidgenössische Zollverwaltung). Steering tax on CO_2 (Lenkungsabgabe auf CO_2). Tech. rep., 2018, p. 1–2, URL https://www.ezv.admin.ch/ezv/de/home/information-firmen/steuern-und-abgaben/einfuhr-in-die-schweiz/lenkungsabgabe-auf-co.html.

[90] SIA. Energy efficiency path. Tech. rep., Swiss Society of Engineers and Architects (Schweizerische Ingenieur- und Architektenverein); 2011, p. 1–4, URL https://www.sia.ch/fileadmin/content/download/sia-norm/kommissionen/SIA_Faltblatt_Effizienzpfad_A4.pdf.

[91] Bohlayer M, Bürger A, Fleschutz M, Braun M, Zöttl G. Multi-period investment pathways - modeling approaches to design distributed energy systems under uncertainty. Appl Energy 2021;285:116368. http://dx.doi.org/10.1016/J.APENERGY.2020.116368.

[92] Shadram F, Bhattacharjee S, Lidelöw S, Mukkavaara J, Olofsson T. Exploring the trade-off in life cycle energy of building retrofit through optimization. Appl Energy 2020;269:115083. http://dx.doi.org/10.1016/J.APENERGY.2020.115083.

[93] Marsh E, Orr J, Ibell T. Quantification of uncertainty in product stage embodied carbon calculations for buildings. Energy Build 2021;251:111340. http://dx.doi.org/10.1016/J.ENBUILD.2021.111340.

[94] Schweizerischer Bundesrat (Swiss Federal Council). Verordnung über die miete und Pacht von wohn- und geschäftsräumen - VMWG (ordinance on the rent and lease of residential and commercial premises). 2020.

[95] Mieterinnen- und Mieterverband (Swiss Tenants' Association), Anfangsmietzins (Initial Rent).

[96] Mieterinnen- und Mieterverband (Swiss Tenants' Association). Umbauten, renovationen, totalsanierungen. 2018.

[97] Nie H, Kemp R, Xu JH, Vasseur V, Fan Y. Split incentive effects on the adoption of technical and behavioral energy-saving measures in the household sector in western europe. Energy Policy 2020;140:111424. http://dx.doi.org/10.1016/j.enpol.2020.111424.

[98] Copiello S, Gabrielli L, Bonifaci P. Evaluation of energy retrofit in buildings under conditions of uncertainty: The prominence of the discount rate. Energy 2017;137:104–17. http://dx.doi.org/10.1016/J.ENERGY.2017.06.159.

[99] Patt A, van Vliet O, Lilliestam J, Pfenninger S. Will policies to promote energy efficiency help or hinder achieving a 1.5° c climate target? Energy Efficiency 2018;12:551—565. http://dx.doi.org/10.1007/s12053-018-9715-8.

[100] Strachan N, Fais B, Daly H. Reinventing the energy modelling–policy interface. Nat. Energy 2016;1(3):1–3. http://dx.doi.org/10.1038/nenergy.2016.12.

[101] Wouters C, Fraga ES, James AM. A policy-based multi-objective optimisation framework for residential distributed energy system design. Renew Energy Environ Sustain 2017;2(5):1–6. http://dx.doi.org/10.1051/REES/2017011.

[102] Zhu Q, Leibowicz BD, Busby JW, Shidore S, Adelman DE, Olmstead SM. Enhancing policy realism in energy system optimization models: Politically feasible decarbonization pathways for the United States. Energy Policy 2022;161:112754. http://dx.doi.org/10.1016/j.enpol.2021.112754.

[103] Loulou R, Lehtilä A, Kanudia A, Remme U, Goldstein G. Documentation for the TIMES model part II. Tech. rep., February, Energy Technology Systems Analysis Programme (ETSAP); 2021, p. 1–408, URL https://iea-etsap.org/docs/Documentation_for_the_TIMES_Model-PartII.pdf.

[104] Bisschop J. Optimization modeling AIMMS. Tech. rep., 2021, p. 1–306, URL https://documentation.aimms.com/_downloads/AIMMS_modeling.pdf.

[105] Farahani A, Wallbaum H, Dalenbäck J-O. Optimized maintenance and renovation scheduling in multifamily buildings – a systematic approach based on condition state and life cycle cost of building components. Constr Manag Econ 2019;37(3):139–55. http://dx.doi.org/10.1080/01446193.2018.1512750.

[106] Femenías P, Mjörnell K, Thuvander L. Rethinking deep renovation: The perspective of rental housing in Sweden. J Cleaner Prod 2018;195:1457–67. http://dx.doi.org/10.1016/j.jclepro.2017.12.282.

[107] Fawcett W, Hughes M, Krieg H, Albrecht S, Vennström A. Flexible strategies for long-term sustainability under uncertainty. Build Res Inf 2012;40(5):545–57. http://dx.doi.org/10.1080/09613218.2012.702565.

[108] Cho K, Yoon Y. Decision support model for determining cost-effective renovation time. J Manage Eng 2016;32(3):1–9. http://dx.doi.org/10.1061/(ASCE)ME.1943-5479.0000418.

[109] Ben H, Steemers K. Modelling energy retrofit using household archetypes. Energy Build 2020;224:110224. http://dx.doi.org/10.1016/J.ENBUILD.2020.110224.

[110] Gholami M, Torreggiani D, Tassinari P, Barbaresi A. Narrowing uncertainties in forecasting urban building energy demand through an optimal archetyping method. Renew Sustain Energy Rev 2021;148:111312. http://dx.doi.org/10.1016/j.rser.2021.111312.

[111] Ben H, Steemers K. Modelling energy retrofit using household archetypes. Energy Build 2020;224:110224. http://dx.doi.org/10.1016/j.enbuild.2020.110224.

[112] Murray P, Mavromatidis G, Marquant J, Orehounig K. EnTeR – project report wp3 – measures and synthesis. Tech. rep., 2019.

[113] KBOB. Ökobilanzdaten im baubereich 2009/1:2016. Tech. rep., Koordinationskonferenz der Bau- und Liegenschaftsorgane der öffentlichen Bauherren (Coordination Conference of the Construction and Real Estate Bodies of public Developers); 2016, p. 1–19, URL https://www.kbob.admin.ch/kbob/de/home/publikationen/nachhaltiges-bauen/oekobilanzdaten_bauhereich.html.

[114] SFOE. Tech. rep., Swiss Federal Office of Energy (SFOE); 2019, URL https://www.bfe.admin.ch/bfe/en/home/supply/statistics-and-geodata/energy-statistics/overall-energy-statistics.html.

[115] Prognos AG. Die energieperspektiven fur die schweiz bis 2050 (the energy outlook for Switzerland until 2050). Tech. rep., Swiss Federal Office of Energy (SFOE); 2012, URL https://www.bfe.admin.ch/bfe/en/home/policy/energy-strategy-2050/documentation/energy-perspectives-2050.html.

[116] BFE, EnDK and EnFK. Harmonisiertes fördermodell der kantone hfm 2015 (harmonized support model of the cantons 2015). Tech. rep., Bundesamt für Energie BFE (Swiss Federal Office of Energy), Konferenz Kantonaler Energiedirektoren EnDK (Conference of Cantonal Energy Directors), Energiefachstellenkonferenz EnFK (Energy Specialist Conference); 2015, URL https://www.endk.ch/de/dokumentation/harmonisiertes-foerdermodell-der-kantone-hfm.

[117] Mavromatidis G, Orehounig K, Carmeliet J. Uncertainty and global sensitivity analysis for the optimal design of distributed energy systems. Appl Energy 2018;214:219–38. http://dx.doi.org/10.1016/j.apenergy.2018.01.062.

[118] Danish Energy Agency and Energinet. Technology data for individual heating 2016. Tech. rep., 2018, p. 1–167, URL https://ens.dk/en/our-services/projections-and-models/technology-data/technology-data-individual-heating-plants.

[119] ELCO Solutions.

[120] David A, Mathiesen BV, Averfalk H, Werner S, Lund H. Heat roadmap europe: large-scale electric heat pumps in district heating systems. Energies 2017;10(4):578. http://dx.doi.org/10.3390/en10040578.

[121] Coujard C, Peirano E, Sanchis G, Betraoui B. e-HIGHWAY 2050: Modular development plan of the pan-european transmission system 2050. Tech. rep., European Union; 2013, p. 1–16, URL https://docs.entsoe.eu/baltic-conf/bites/www.e-highway2050.eu/fileadmin/documents/Results/D3/report_heat_pumps.pdf.

[122] Sandvall AF, Ahlgren EO, Ekvall T. Cost-efficiency of urban heating strategies – modelling scale effects of low-energy building heat supply. Energy Strateg Rev 2017;18:212–23. http://dx.doi.org/10.1016/j.esr.2017.10.003.

[123] HSLU. Heizkostenvergleichsrechner hochschule luzern (HSLU). 2019, Available from: https://www.hslu.ch/de-ch/technik-architektur/forschung/kompetenzzentren/zig/software-tools/.

[124] SCCER JASM. Energy conversion technologies in STEM. 2020, Available from: https://data.sccer-jasm.ch/energy-conversion-technologies-stem/2020-03-05/.

[125] Murray P, Orehounig K, Grosspietsch D, Carmeliet J. A comparison of storage systems in neighbourhood decentralized energy system applications from 2015 to 2050. Appl Energy 2018;231:1285–306. http://dx.doi.org/10.1016/j.apenergy.2018.08.106.

[126] Polman A, Knight M, Garnett EC, Ehrler B, Sinke WC. Photovoltaic materials: present efficiencies and future challenges. Science 2016;352(6283). http://dx.doi.org/10.1126/science.aad4424.

[127] Grosspietsch D, Thömmes P, Girod B, Hoffmann VH. How, when, and where? assessing renewable energy self-sufficiency at the neighborhood level. Environ Sci Technol 2018;52(4):2339–48. http://dx.doi.org/10.1021/acs.est.7b02686.

[128] Nykvist B, Nilsson M. Rapidly falling costs of battery packs for electric vehicles. Nature Clim Change 2015;5(4):329–32. http://dx.doi.org/10.1038/nclimate2564.

[129] IRENA. Electricity storage and renewables: Costs and markets to 2030. Tech. rep., International Renewable Energy Agency (IRENA); 2017, p. 1–132, URL http://www.climateaction.org/images/uploads/documents/IRENA_Electricity_Storage_Costs_2017.pdf.

[130] Hoval. Hoval catalog 2021. 2021.

[131] Di Somma M, Yan B, Bianco N, Graditi G, Luh PB, Mongibello L, Naso V. Multi-objective design optimization of distributed energy systems through cost and exergy assessments. Appl Energy 2017;204:1299–316. http://dx.doi.org/10.1016/j.apenergy.2017.03.105.

[132] Kurtz S. Reliability and durability of PV modules. In: Photovoltaic solar energy. Chichester, UK: John Wiley & Sons, Ltd; 2017, p. 491–501. http://dx.doi.org/10.1002/9781118927496.ch44.

[133] Yazdanie M, Densing M, Wokaun A. Cost optimal urban energy systems planning in the context of national energy policies: A case study for the city of basel. Energy Policy 2017;110:176–90. http://dx.doi.org/10.1016/j.enpol.2017.08.009.

[134] Gabrielli P, Gazzani M, Martelli E, Mazzotti M. Optimal design of multi-energy systems with seasonal storage. Appl Energy 2018;219:408–24. http://dx.doi.org/10.1016/j.apenergy.2017.07.142.

[135] Gabrielli P, Fürer F, Mavromatidis G, Mazzotti M. Robust and optimal design of multi-energy systems with seasonal storage through uncertainty analysis. Appl Energy 2019;238:1192–210. http://dx.doi.org/10.1016/j.apenergy.2019.01.064.

[136] EASE. Thermal hot water storage. Tech. rep., European Association for Storage of Energy (EASE); 2016, URL http://ease-storage.eu/wp-content/uploads/2016/03/EASE_TD_HotWater.pdf.

[137] Stroe D-I, Knap V, Swierczynski M, Stroe A-I, Teodorescu R. Operation of a grid-connected lithium-ion battery energy storage system for primary frequency regulation: a battery lifetime perspective. IEEE Trans Ind Appl 2017;53(1):430–8. http://dx.doi.org/10.1109/TIA.2016.2616319.

[138] Swierczynski M, Stroe DI, Laerke R, Stan AI, Kjaer PC, Teodorescu R, Kaer SK. Field experience from li-ion BESS delivering primary frequency regulation in the danish energy market. ECS Trans 2014;61(37):1–14. http://dx.doi.org/10.1149/06137.0001ecst.

[139] Schütz T, Schraven MH, Fuchs M, Remmen P, Müller D. Comparison of clustering algorithms for the selection of typical demand days for energy system synthesis. Renew Energy 2018;129:570–82. http://dx.doi.org/10.1016/j.renene.2018.06.028.

[140] Ohlsson KA, Olofsson T. Benchmarking the practice of validation and uncertainty analysis of building energy models. Renew Sustain Energy Rev 2021;142:110842. http://dx.doi.org/10.1016/j.rser.2021.110842.

[141] Tian W, Heo Y, de Wilde P, Li Z, Yan D, Park CS, Feng X, Augenbroe G. A review of uncertainty analysis in building energy assessment. Renew Sustain Energy Rev 2018;93:285–301. http://dx.doi.org/10.1016/j.rser.2018.05.029.

[142] Zou PX, Xu X, Sanjayan J, Wang J. Review of 10 years research on building energy performance gap: Life-cycle and stakeholder perspectives. Energy Build 2018;178:165–81. http://dx.doi.org/10.1016/J.ENBUILD.2018.08.040.

[143] Shen P, Braham W, Yi Y, Eaton E. Rapid multi-objective optimization with multi-year future weather condition and decision-making support for building retrofit. Energy 2019;172:892–912. http://dx.doi.org/10.1016/J.ENERGY.2019.01.164.

[144] Heo Y, Choudhary R, Augenbroe GA. Calibration of building energy models for retrofit analysis under uncertainty. Energy Build 2012;47:550–60. http://dx.doi.org/10.1016/j.enbuild.2011.12.029.

[145] Larsen MA, Petrović S, Radoszynski AM, McKenna R, Balyk O. Climate change impacts on trends and extremes in future heating and cooling demands over europe. Energy Build 2020;226:110397. http://dx.doi.org/10.1016/j.enbuild.2020.110397.

[146] Celik D, Meral ME, Waseem M. Restrictions and driving forces for renewable energy production development and electrical energy demand in general and during COVID-19. In: 12th international symposium on advanced topics in electrical engineering, ATEE 2021. Institute of Electrical and Electronics Engineers; 2021, http://dx.doi.org/10.1109/ATEE52255.2021.9425216.

[147] Narula K, Chambers J, Streicher KN, Patel MK. Strategies for decarbonising the swiss heating system. Energy 2019;169:1119–31. http://dx.doi.org/10.1016/J.ENERGY.2018.12.082.

[148] Streicher KN, Padey P, Parra D, Bürer MC, Patel MK. Assessment of the current thermal performance level of the swiss residential building stock: Statistical analysis of energy performance certificates. Energy Build 2018;178:360–78. http://dx.doi.org/10.1016/J.ENBUILD.2018.08.032.

[149] Streicher KN, Padey P, Parra D, Bürer MC, Schneider S, Patel MK. Analysis of space heating demand in the swiss residential building stock: Element-based bottom-up model of archetype buildings. Energy Build 2019;184:300–22. http://dx.doi.org/10.1016/J.ENBUILD.2018.12.011.

[150] Bhadbhade N, Yilmaz S, Zuberi JS, Eichhammer W, Patel MK. The evolution of energy efficiency in Switzerland in the period 2000–2016. Energy 2019;191:116526. http://dx.doi.org/10.1016/j.energy.2019.116526.

[151] Li X, Chambers J, Yilmaz S, Patel MK. A Monte Carlo building stock model of space cooling demand in the swiss service sector under climate change. Energy Build 2021;233:110662. http://dx.doi.org/10.1016/j.enbuild.2020.110662.

[152] Mutschler R, Rüdisüli M, Heer P, Eggimann S. Benchmarking cooling and heating energy demands considering climate change, population growth and cooling device uptake. Appl Energy 2021;288:116636. http://dx.doi.org/10.1016/j.apenergy.2021.116636.

[153] Energie-Cluster and EnWI. gebäudesanierung – wirtschaftlichkeit der co2-abgabe (building renovation - economic efficiency of the co2 tax). Tech. rep., Bundesamt für Umwelt BAFU (Swiss Federal Office of the Environment SFOE); 2019, p. 1–55, URL https://www.aramis.admin.ch/Texte/?ProjectID=44296.

[154] BBSR. Nutzungsdauern von bauteilen für lebenszyklusanalysen nach bewertungssystem nachhaltiges bauen bnb (useful lives of building components for life cycle analyses according to the sustainable building assessment system). Tech. rep., Federal Institute for Research on Building, Urban Affairs and Spatial Development (BBSR); 2017, p. 1–17, URL https://www.nachhaltigesbauen.de/fileadmin/pdf/Nutzungsdauer_Bauteile/BNB_Nutzungsdauern_von_Bauteilen_2011-11-03.pdf.

[155] Wiprächtiger M, Haupt M, Heeren N, Waser E, Hellweg S. A framework for sustainable and circular system design: Development and application on thermal insulation materials. Resour Conserv Recy 2020;154:104631. http://dx.doi.org/10.1016/j.resconrec.2019.104631.